

Susitna-Watana Hydroelectric Project Document

ARLIS Uniform Cover Page

Title: Site-specific seismic hazard study plan Section 16.6, Study Completion Report. Attachment 11. Preliminary reservoir triggered seismicity		SuWa 289
Author(s) – Personal: Dina Hunt, Roland LaForge, Dean Ostenna		
Author(s) – Corporate: MWH		
AEA-identified category, if specified: November 2015; Study Completion and 2014/2015 Implementation Reports		
AEA-identified series, if specified: NTP ; 11 Technical memorandum ; no. 10		
Series (ARLIS-assigned report number): Susitna-Watana Hydroelectric Project document number 289		Existing numbers on document: AEA11-022 TM-11-0010-030113
Published by: [Anchorage : Alaska Energy Authority, 2015]		Date published: March 29, 2013
Published for: Alaska Energy Authority		Date or date range of report:
Volume and/or Part numbers: Study plan Section 16.6		Final or Draft status, as indicated: v3.0
Document type:		Pagination: iv, 2, 53 pages + [31] pages of plates
Related works(s):		Pages added/changed by ARLIS:
Notes: All other parts of Section 16.6 (the main report and Attachments 1-10) are in separate electronic files due to large file sizes.		

All reports in the Susitna-Watana Hydroelectric Project Document series include an ARLIS-produced cover page and an ARLIS-assigned number for uniformity and citability. All reports are posted online at <http://www.arlis.org/resources/susitna-watana/>

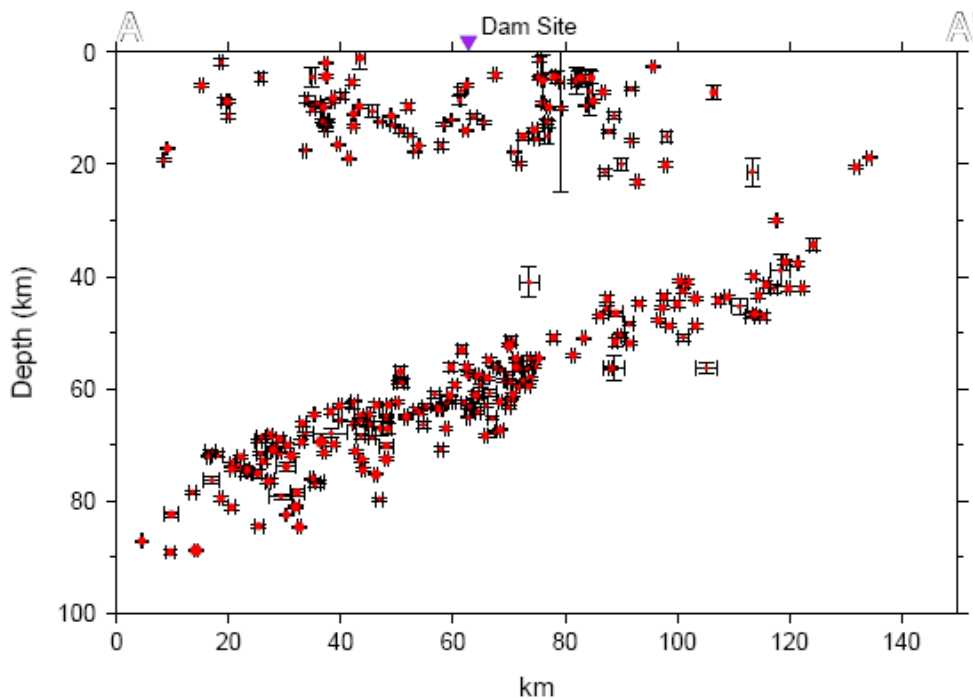


ATTACHMENT 11: PRELIMINARY RESERVOIR TRIGGERED
SEISMICITY

NTP 11
Technical Memorandum No. 10
v3.0

Preliminary Reservoir Triggered Seismicity

AEA11-022



Prepared for:
Alaska Energy Authority
813 West Northern Lights Blvd.
Anchorage, AK 99503

Prepared by:
MWH
2353 130th Avenue NE, Suite 200
Bellevue, WA 98005

March 29, 2013

The following individuals have been directly responsible for the preparation, review and approval of this Report.

Prepared by: Dina Hunt, Roland LaForge and Dean Ostenna

Reviewed by: Peter Dickson, Sandy Lawson, Mike Bruen, Justin Pearce and Dan O'Connell

Approved by:



Michael Bruen, Geology, Geotechnical, Seismic Lead

Approved by:



Brian Sadden, Project Manager

Disclaimer

This document was prepared for the exclusive use of AEA and MWH as part of the engineering studies for the Susitna-Watana Hydroelectric Project, FERC Project No. 14241, and contains information from MWH which may be confidential or proprietary. Any unauthorized use of the information contained herein is strictly prohibited and MWH shall not be liable for any use outside the intended and approved purpose.

TABLE OF CONTENTS

EXECUTIVE SUMMARY	ES-1
1.0 INTRODUCTION.....	1
1.1 Background of Project.....	1
1.2 Purpose of Study	1
2.0 PREVIOUS STUDIES	2
2.1 Terminology	2
2.2 Prefeasibility Studies.....	2
2.2.1 Input Parameters	3
2.2.2 Previous Study Results.....	4
2.3 Current Knowledge of Reservoir Triggered Seismicity.....	5
2.3.1 Causes of Reservoir Triggered Seismicity.....	5
2.3.2 Characteristics of Reservoir Triggered Seismicity.....	6
2.3.3 Current Understanding and Cases of Reservoir Triggered Seismicity.....	6
2.3.4 Physical Mechanisms of Reservoir Triggered Seismicity and Selected Cases	7
2.3.4.1 Introduction	7
2.3.4.2 Physical Mechanisms.....	8
2.3.4.3 Analysis Techniques and Case studies.....	10
2.3.4.3.1 Nurek Dam and Reservoir, Tajikistan.....	11
2.3.4.3.2 Zipingou Reservoir, Sichuan, China	12
2.3.5 State of the Practice for Determining the Potential for Reservoir Triggered Seismicity.....	13
2.3.6 Database of Reservoir Triggered Seismicity	14
3.0 GEOLOGIC AND TECTONIC SETTING OF THE RESERVOIR	16
3.1 Regional Geology and Tectonics	17
3.2 Reservoir Geology.....	19
3.2.1 Detailed Geologic Data from the Watana Dam Site.....	20
3.2.2 Quaternary Fault Evaluations and Lineament Mapping in the Project Area.....	21
3.3 Seismicity in the Reservoir Area.....	21
3.3.1 Watana Seismic Network	22
3.3.2 Seismicity in the Watana Region	22
4.0 RESERVOIR TRIGGERED SEISMICITY FACTORS.....	23
4.1 General Reservoir Parameters (Depth and Volume).....	23
4.2 Geologic Parameters.....	24
4.3 Stress Regime	25
4.4 Faulting Parameters	25
4.5 Hydrologic Parameters	25
4.5.1 Rock Mass Permeability	25

4.5.2	Fracture Orientation and Density	26
4.5.3	Proposed Reservoir Inflows/Outflows	26
5.0	POTENTIAL FOR RTS	27
5.1	Empirical Approach	27
5.1.1	Calculation of Likelihood of Occurrence	31
5.1.1.1	Single Attribute Analysis.....	32
5.1.1.2	Multi-Attribute Analysis.....	35
5.1.2	Independent Discrete Results	38
5.1.3	Dependent Discrete Results.....	38
5.1.4	Dependent Mixed Results	38
5.2	Empirical Approach Results.....	38
6.0	RECOMMENDATIONS FOR ADDITIONAL STUDIES	39
6.1	Seismic Monitoring and Seismological Analysis.....	40
6.2	Coulomb Stress Modeling.....	40
6.3	Local Geologic Field Investigations.....	41
6.4	Estimation of Maximum Magnitude of a RTS Event.....	41
6.5	Empirically-based Analysis.....	42
6.6	Deterministic Comparisons to the Largest non-RTS Earthquake	42
7.0	SUMMARY AND CONCLUSIONS.....	42
8.0	REFERENCES	44

List of Tables

Table 1	Previously Proposed Reservoir Parameters (WCC, 1982).....	3
Table 2	Proposed Watana Reservoir Parameters	28
Table 3	Dams with Reported Reservoir Triggered Seismicity that have Similar Water Depths and Reservoir Volumes	29
Table 4	Definitions for Reservoir Attribute States.....	32
Table 5	Single Attribute Analysis – Conditional Probability of RTS Given Only One Attribute	34
Table 6	Data Bins for Deep or Very Deep Dataset – Current Study.....	34
Table 7	Summary of RTS and Non-RTS Data for each State.....	34
Table 8	Revised Single Attribute Analysis – Conditional Probability of RTS Given Only One Attribute - Current Study	34
Table 9a	Comparison of Previous and Current Probabilities of RTS using a Multi-attribute Analysis – Independent and Dependent Discrete –Currently Proposed Configuration	36

List of Figures

Figure 1	Temporal variations in seismicity within the reservoir area and daily water level at Nurek
Figure 2	Simulated change in effective Coulomb stress due to Zipingpu Reservoir (Ge et al., 2009)
Figure 3	Simulated change in effective Coulomb stress due to Zipingpu Reservoir (Zhou and Deng, 2011)
Figure 4	Relationship between depth and volume and reported cases of RTS
Figure 5	Major physiographic provinces
Figure 6	Tectonic overview of central interior Alaska
Figure 7	Tectonostratigraphic terrain map of the Talkeetna block
Figure 8A	Site region geology
Figure 8B	Site region geology legend

Figure 9	Simplified geologic map and cross section – Fog Lakes Graben
Figure 10	Site geology
Figure 11	Map and cross section of seismicity in south central Alaska
Figure 12	Watana Seismic Network
Figure 13	Seismicity in the Watana region
Figure 14	Seismicity of all magnitudes near Watana dam site
Figure 15	Seismicity in site area, 2010 – November 15, 2012
Figure 16	NW-SE cross-section, seismicity 2010 – November 15, 2012
Figure 17	Seismicity in site area, November 16, 2012 – February 28, 2013
Figure 18	NW-SE cross-section, November 16, 2012 – February 28, 2013
Figure 19	Summary of crustal stress field in south-central Alaska
Figure 20	Summary of permeability values from Watana site boreholes
Figure 21	Summary of permeability values from Devil Canyon site boreholes
Figure 22	Frequency of earthquakes and water heights versus time for Almendra Dam

Appendix

Appendix A Database of Reservoir Triggered Seismicity

Acronyms and Abbreviations

°	degrees
2-D	two-dimensional
Acres	Acres American Incorporated
AEA	Alaska Energy Authority
AEIC	Alaska Earthquake Information Center

atm	atmosphere, unit of pressure
cm/sec	centimeters per second
El.	elevation in feet
FCL	Fugro Consultants, Inc.
FERC	Federal Energy Regulatory Commission
ft/s	feet per second
ft ²	square feet
ft ³	cubic feet
ft ³ /s	cubic feet per second
H:V	horizontal, vertical
ICOLD	International Committee on Large Dams
in/sec	inches per second
INSAR	Interferometric Synthetic Aperture Radar
IRIS	Incorporated Research Intuitions for Seismology
km	kilometers
ks	seismogenic permeability as defined by Talwani et al. (2007)
LiDAR	Light Detection and Ranging
M	magnitude, is assumed equivalent to Mw
M	million
Mw	moment magnitude
m ²	square meters
m ³	cubic meters
m ³ /s	cubic meters per second

Ma	million years from the present
MatSu	Matanuska-Susitna Borough
meters	meters
mi	miles
Mpa	megapascals
psi	pound-force per square inch
RCC	roller-compacted concrete
RTS	Reservoir Triggered Seismicity
SAB	Southern Alaska Block
TM	Technical Memorandum
WCC	Woodward-Clyde Consultants

Executive Summary

The purpose of this report is to provide a preliminary assessment of the potential for reservoir triggered seismicity (RTS) in the vicinity of the proposed Susitna-Watana reservoir, and to provide recommendations for studies designed to improve current estimations of potential RTS probability and the maximum RTS magnitude. Relevant large impoundment case studies are discussed and compared to the planned facility. Regional tectonics and geology in the planned reservoir and dam site area are also summarized based on previous studies at the project site and vicinity. The recently-installed seismic network is discussed, and initial pre and post network seismicity cross sections of the subducting slab and interface are presented.

The term reservoir triggered seismicity (RTS) is now the accepted term used to describe the phenomena of earthquakes occurring in the vicinity of man-made water reservoirs. This report builds on and updates studies performed in the 1980s, with the difference that the 1980s studies were completed for a planned two-impoundment system in contrast to the envisioned single Watana structure. Because it is a relatively large-volume and very deep reservoir, Watana reservoir has a higher RTS potential than shallower, lower-volume ones.

Several case studies are examined to update the historic RTS catalog from the 1980s, as well as incorporate more recent research into the phenomenon of RTS. Case studies, while useful, generally provide an empirical dataset that may not necessarily predict the magnitude and distribution of RTS for other sites. Key insights from case studies include the timing of RTS occurrence (i.e., generally within 10 years following impoundment) and the influence of reservoir filling and operational water level fluctuations on observed seismicity.

The two principal triggers of RTS are added weight stresses and pore pressure propagation. Physical theories of stress changes due to reservoir loading and the percolation of water into the upper crust are sound, but make many simplifying assumptions. The most important of these assumptions is that the physical properties of the upper crust are isotropic. This memorandum summarily reviews the physical triggers of RTS, as well as some quantitative frameworks for assessing potential RTS based on physical state changes (e.g., stress, rock permeability). However, numerical theory may not necessarily agree with, or predict, case study history in all instances.

Analyses within this memorandum include updated statistical calculations, updated seismicity maps and seismicity cross sections, as well as synthesis of recent research and computational advances. An update to the previous empirically-based probability analysis found the probability of RTS for the proposed Watana reservoir ranges from 16 to 46 percent; this is much lower than the previously proposed project configuration that was about 160 feet higher and more than twice the reservoir volume (probabilities range from 30 to 95 percent).

The location and magnitude of any future RTS event associated with the Watana Reservoir are highly uncertain. Empirical data suggest that most RTS events will have relatively small magnitudes and would most likely occur within 10 years of initial filling. From these types of observations, ICOLD (2011) and Allen (1982) suggest that maximum RTS magnitudes may be on the order of 6.3 and 6.5, respectively. Other investigators (e.g., Klose, 2011; Ge et al., 2009) have proposed that the Mw 7.9 Wenchuan earthquake should be considered an RTS event, which would increase the magnitude estimates from empirical data. In contrast, other investigators (e.g., Zhou et al., 2010; Galahut and Galahut, 2010) have argued that this event could not have been triggered by the reservoir. The status of the Wenchuan earthquake as an RTS event is controversial, and future research on it will continue to be monitored.

Mapping of existing faults and discontinuities (e.g., fractures) within and near the reservoir, regional hydraulic conductivity surrounding these faults, and regional tectonic stress provide the physical constraints which determine potential RTS locations and the physical limits for earthquake magnitudes. From existing seismic hazard studies, a possible maximum can be Mw 7.3, which was judged by the USGS to be the largest crustal event that could randomly occur in the region. This is a conservative estimate, made in consideration of no prior knowledge of seismogenic crustal thickness, hydraulic properties of rocks beneath the reservoir area, orientation of the local tectonic stress field, and the possible existence of local faults in the vicinity of the reservoir that may be favorably oriented to the local stress field.

A significant aspect of the RTS record from case studies is the fact that of the verified RTS cases large enough to be potentially damaging, only four events have exceeded magnitude M 6, and only 13 events were in the range M 5.0 to M 5.9 (USCOLD, 1997; Yeats et al, 1997). The largest reported RTS earthquake was the 1967, magnitude M 6.5, Koyna, India event. These observations contrast with the presumption that maximum RTS would not exceed maximum earthquake magnitudes from existing fault sources (i.e. “naturally occurring” sources), which in most reported cases of RTS has not been consistently evaluated. Thus, the emphasis of further recommended evaluations of RTS for the Watana site is focused on improving the understanding of the local geologic and tectonic characteristics that are significant to RTS assessment.

1.0 INTRODUCTION

The proposed Susitna-Watana dam and reservoir are part of a hydroelectric power development project planned to be constructed on the upper Susitna River. The proposed hydroelectric plan for the Watana site is a 735 feet (224 m) high roller-compacted concrete (RCC) dam and surface powerhouse, with a reservoir elevation of 2050 feet and a depth of about 595 feet (182 m). The total volume of the reservoir is planned to be 5.2 million acre feet (6.4 billion cubic meters).

1.1 Background of Project

The feasibility of an earlier configuration of the Susitna-Watana Dam site was studied in the early 1980's by Woodward Clyde Consultants. The initial design of the Susitna Hydroelectric project included impoundment of two reservoirs, one at the Devil Canyon site and another at the upstream Watana site; both located on the Susitna River. The combined reservoir parameters were a depth of approximately 725 feet and a reservoir volume of 10.67 million acre feet. In early 2011, MWH was retained by Alaska Energy Authority (AEA) – Alaska Railbelt Large Hydro Engineering Services to perform geological and geotechnical engineering studies in support of Engineering Studies of the Watana Dam to more fully define the Project for the Federal Energy Regulatory Commission (FERC) License Application, and to support the License Application. Under subcontract to MWH, Fugro Consultants, Inc.(FCL) assisted in the preparation of this report including text, tables and graphics.

1.2 Purpose of Study

The purpose of this study is to provide a preliminary assessment of the potential for reservoir triggered seismicity (RTS) in the vicinity of the proposed dam and reservoir. It does not alter the seismic hazard results as presented in Fugro Consultants, Inc. (FCL) (2012). An RTS earthquake is likely to be treated as deterministic in nature, and as such will need to be incorporated as a separate element in the seismic hazard analysis. This study will build upon the initial geologic and seismic studies completed by Acres American Incorporated (Acres), Woodward-Clyde Consultants (WCC), Harza-Ebasco, and MWH in support of conceptual dam design studies. A literature review, discussion of case studies, a statistical analysis of accepted RTS cases, and discussion of physical theories of RTS and recent modeling studies are included in this report. This comprises an important expansion and update to the previously published assessment (WCC, 1982). The objectives of this study include:

- Literature review of RTS cases worldwide
- Comparison with other large reservoirs with similar geologic conditions, tectonic setting, and having or suspected of having RTS events
- Identify and assess characteristics of the proposed dam and reservoir, and the geologic and geophysical environment that indicate a potential for RTS

- Review research into the physical mechanisms of RTS, and discuss representative cases of both empirical analysis and modeling of RTS using finite-element techniques.
- Provide recommendations for further RTS analysis activities.

2.0 PREVIOUS STUDIES

This section will discuss current terminology, previous RTS studies completed for the project, regulatory guidelines, current knowledge, and new approaches for assessing RTS.

2.1 Terminology

The term reservoir triggered seismicity (RTS) is now the accepted term used to describe the phenomena of earthquakes occurring in the vicinity of artificial water reservoirs. McGarr and Simpson (1977) deliberated on the terms “induced” versus “triggered”. They proposed that the term “triggered” be used to describe earthquakes that occur due to a small fraction of the stress change causing the event, whereas “induced” be used to describe earthquakes that are mostly caused by human-caused stress changes. Examples of induced events would include those that closely associate with hydraulic fracturing at a site with no known faults or seismicity, as compared to triggered events, which would be an event that occurred on a known fault near a reservoir after a significant change in water depth. The International Committee on Large Dams (ICOLD, 2011), in their draft “Reservoirs and Seismicity – State of Knowledge” accept reservoir triggered seismicity as the most adequate term. Therefore, for this report the term reservoir triggered seismicity (RTS) will be used.

2.2 Prefeasibility Studies

During initial prefeasibility studies in the early 1980s for the Susitna-Watana Hydroelectric project Woodward-Clyde Consultants (WCC, 1980) completed an assessment of RTS. The scope of this study is summarized below:

- A comparison of the depth, volume, regional stress, geologic setting, and faulting at the Devil Canyon and Watana sites with the same parameters at comparable reservoirs worldwide
- Assessment of the likelihood of RTS at the sites based on the above comparison
- A review of the relationship between reservoir filling and the length of time to the onset of induced events and the length of time to the maximum earthquake
- An evaluation of the significance of these time periods for the sites
- The development of a model to assess the impact of RTS and method of reservoir filling

Data compilation of RTS events began in the early 1940's with a study completed at Hoover Dam (Carder, 1945). Several studies were completed over the next 30 years that gained recognition of RTS as a real phenomenon; the Packer et al. (1979) study which was first published in 1977 for Auburn Dam significantly contributed to the increase in awareness. The study completed for Susitna in 1982 by WCC includes empirical data with calculations of likelihood of occurrence and mean number of RTS events. This study was based on the work by Packer et al. (1979) and Perman et al. (1981).

At the time the study was completed for Susitna, there were 68 cases that were classified as RTS. The studies showed that RTS is influenced by the depth and volume of the reservoir, the state of tectonic stresses in the shallow crust beneath the reservoir, and the existing pore pressures and permeability of the rock under the reservoir. The WCC (1980) report presents probability calculations based on empirical knowledge related to the depth and volume of the reservoir.

2.2.1 Input Parameters

The initial design of the Susitna Hydroelectric project included impoundment of two reservoirs, one at the Devil Canyon site and another at the Watana site. The study completed by WCC treated both reservoirs as one, but a separate RTS analysis was performed for each site. In other words, the input parameters for the reservoir were the same but the potential sources and distances were analyzed independently of each other. The parameters for the two sites are summarized in **Table 1** below. It should be noted that the previous configuration had a maximum reservoir at El. 2185, whereas the current proposed configuration has a maximum reservoir at El. 2050.

Table 1 Previously Proposed Reservoir Parameters (WCC, 1982)

Parameter	Devil Canyon	Watana	Combined
Maximum Water Depth	551 feet (168 meters)	725 (221)	725 (221)
Maximum Reservoir Elevation		2185	N/A
Maximum Water Volume	1.05 million acre feet (1,296 million cubic meters)	9.62 million acre feet (11,876 million cubic meters)	10.67 million acre feet (13,172 million cubic meters)
Stress Regime	Compressional	Compressional	Compressional
Bedrock	Metamorphic	Igneous	Igneous

2.2.2 Previous Study Results

The results of the RTS analysis were summarized into three categories; with the first category having 4 sub-categories:

- Empirical Analysis
 - Calculation of likelihood of occurrence of RTS event
 - Calculation of mean number of RTS events
 - Distribution of mean number of RTS events
 - Use of RTS events in Seismic Exposure Analysis
- RTS and Method of Reservoir Filling Analysis
- Potential for Landslides in the Reservoir Area resulting from RTS

The empirical analyses used two different models to determine the likelihood of RTS occurrence. In the first model, depth and volume are treated as discrete variables; in the second model, depth and volume are treated as continuous dependent variables. For the combined Devil Canyon-Watana reservoir the first model produced an expected likelihood of 0.37 for a RTS event of any magnitude with a standard deviation of 0.13. The second model produced an expected likelihood of 0.46 with a standard deviation of 0.22.

The mean number plus one standard deviation (84th percentile) of RTS events greater than or equal to magnitude 4 was calculated to be 1.14 and for those events greater than or equal to magnitude 5 was calculated to be 0.93. It was assumed that these events would occur within 10 years of impoundment and subsequently only naturally occurring seismicity would occur.

WCC also estimated that the distribution of events would occur within the three-dimensional rectangular space, 37 mile length, 37 mile width, and a depth of 19 miles (60 km x 60 km x 30 km) surrounding each of the reservoirs.

The method of reservoir filling that should cause the least amount of RTS was recommended by WCC to be a controlled smooth filling curve, with no sudden changes or fluctuations in filling rate.

The likelihood of a large landslide in the proposed reservoir during a RTS event was judged to be low; however it was recommended that the landside potential should be reviewed during final design.

The previous study presented evidence that moderate to large RTS events are only expected to occur along faults with recent displacement. Up until the 1980s, only 10 cases of RTS had magnitudes of greater than or equal to magnitude 5. Therefore, at the time this study was completed field reconnaissance and information available in the literature indicated that Quaternary or late Cenozoic

surface fault rupture (i.e., rupture on faults with recent displacement) occurred within the hydrologic regime of eight of these ten reservoirs (Packer and others, 1979). On this basis WCC (1982) concluded that because there were no faults with recent displacement within the hydrologic regime of the proposed reservoir that the maximum magnitude that could be triggered by the proposed reservoir was judged to be 6. Magnitude 6 also corresponded to the maximum magnitude of the detection level earthquake developed for that study.

2.3 Current Knowledge of Reservoir Triggered Seismicity

RTS has been studied since the first documented case at Hoover Dam due to the impoundment of Lake Mead in 1935. The phenomenon has always been controversial, but the idea that earthquakes can in fact be triggered started to gain acceptance in the late 1960's. As the number of dams increased so did the cases of RTS. Improvements in seismic monitoring and installation of instruments prior to impoundment also helped verify that RTS was a real phenomenon. Triggered seismicity was recognized as a physical response of a crustal region to reservoir impounding when a causative fault is near failure. The two triggers of RTS are added weight stresses and pore pressure propagation. There are also empirical characteristics of RTS events and theoretical ways to judge if an event was triggered. This section will describe the characteristics and causes of RTS.

2.3.1 Causes of Reservoir Triggered Seismicity

Several factors are linked to RTS: a seismically active environment, presence of a causative fault, added weight, pore pressure propagation from the reservoir, and changes in water level after impoundment.

Triggered seismicity requires the presence of a causative fault. It is thought that no earthquake can be triggered by a reservoir with a magnitude higher than that of the naturally occurring earthquake. The seismic triggering parameters of impounding are the added weight of the reservoir and the pore pressure effects from the reservoir. The added weight causes stress changes in the crust immediately while pore pressure build up or propagation may take some time and may even recur. For example, triggered events at Monticello reservoir were largely attributable to changes in pore pressure due to diffusion. Diffusion through different rock types helps explain why the reservoir experienced renewed RTS after about 6 years of no triggered events (Chen and Talwani, 2001b). Annual fluctuations in reservoir level after impoundment can also have an effect on RTS (Roeloffs, 1988).

Proposed physical mechanisms of RTS and two selected case histories which illustrate them are discussed in detail in **Section 2.3.4**.

2.3.2 Characteristics of Reservoir Triggered Seismicity

RTS events tend to be clustered around the reservoir. Gupta et al., (1972) speculate that the b-value in the Gutenberg-Richter recurrence equation increases from the normal pre-impoundment value. Several foreshocks gradually increase in magnitude until a main shock occurs, which is followed by aftershocks that cease after some time (Gupta et al., 1972). If the RTS event is the result of an increase in pore pressure then there is normally a lag between the height of water in the reservoir and increases seismic activity, due to the time it takes for water to infiltrate through the bedrock beneath the reservoir.

Klose (2012) published regression analyses in an attempt to correlate reservoir and tectonic characteristics with RTS. His catalog of 92 events judged to be RTS includes those due to all human activities (including mining, and oil and gas extraction as well as reservoir impoundment). The major conclusions of the study were:

- The magnitude of the maximum RTS event is correlated with the mass change of the activity (i.e., the greater the reservoir volume, the larger the maximum RTS magnitude; e.g., McGarr, 1976).
- There is a correlation between distance from the “operation point” (for reservoirs defined as the area of maximum reservoir depth) and the maximum RTS magnitude. For the Watana case this would mean that the farther the distance from the area of maximum reservoir depth, the larger the magnitude. All cases of RTS from human activities occurred less than 19 miles (30 km) from the “operation point”.
- The great majority of maximum RTS events due to reservoir impoundment occurred within 10 years after initial impoundment (20 of 27).
- There is a strong correlation of RTS with compressive stress regimes, in contrast to weak correlations with strike-slip and normal faulting stress regimes. This is contrary to previous studies which presented evidence that compressive regimes tend to inhibit RTS (e.g., Jacob et al., 1979; Gupta and Rajendran, 1986).
- The great majority of reservoir-caused RTS cases occur at depths between 0.6 miles and 6 miles (1 and 10 km).

2.3.3 Current Understanding and Cases of Reservoir Triggered Seismicity

Throughout the world, several thousand dams have been constructed and are impounding reservoirs which are operating without any observed RTS. Compared to the large number of operating large reservoirs, there are only a very few instances of possible RTS cases. Out of some 11,000 worldwide “large” dams, only a small number have triggered known seismic activity (USCOLD, 1997). A large dam according to the ICOLD definition is one more than 33 feet (15 m) high or one between 33 and 49 feet (10 and 15 m) high satisfies one of the following criteria:

- more than 1640 feet (500 m) long;
- reservoir capacity exceeding 811 acre-feet (1 Mm^3 , or $1 \times 10^6 \text{ m}^3$); or
- spillway capacity exceeding $70,629 \text{ ft}^3/\text{s}$ ($2,000 \text{ m}^3/\text{s}$)

Gupta (2002) reports that, over 90 sites have been globally identified where earthquakes have been triggered by filling of water reservoirs. Although it is uncommon for a reservoir to experience RTS (0.08%, based on 11,000 reservoirs of which 90 experienced RTS) it cannot be precluded from occurring at the planned Susitna-Watana site.

At those reservoirs where RTS has been suspected, the maximum reported earthquake magnitudes for RTS events are primarily much less than M 6.0 (M is assumed equivalent to M_w), and typically in the micro earthquake, or small macro earthquake range (i.e., $< M 4.0$). These are nearly all below the range felt by humans and are only detectable by local seismographs.

The most significant aspect of the RTS record is the fact that of the verified RTS cases large enough to be potentially damaging, only four events have exceeded magnitude M 6 and only 13 events were in the range M 5.0 to M 5.9 (USCOLD, 1997; Yeats et al, 1997). The largest reported RTS earthquake was the 1967, magnitude M 6.5, Koyna, India event. The other three events were: Hsinfengkang (China, 1962) M 6.1; Kariba (Zambia, 1963) M 6.0; and Kremasta (Greece, 1966) M 6.3. It is still disputed whether the May 12, 2008 $M_w 7.9$ Wenchuan earthquake in China was influenced by the impoundment of nearby Zipingpu Dam (see section 2.3.4.3).

The state of the practice on understanding and being able to predict RTS is quite primitive, and likely to remain so for the near future. Physical theories of stress changes due to reservoir loading and the percolation of water into the upper crust are sound, but make many simplifying assumptions. The most important assumption is that the physical properties of the upper crust are isotropic. This is nearly always not the case, and the determination of these properties in the volume of crust affected by reservoir impoundment is usually not practically possible, not financially possible, or both. A fault plane can be modeled with properties that deviate from the isotropic case, but the location of the fault and its properties are usually impossible to determine with the required accuracy.

2.3.4 Physical Mechanisms of Reservoir Triggered Seismicity and Selected Cases

2.3.4.1 Introduction

Early studies of RTS for the most part focused on documenting the phenomenon and compiling empirical data on its occurrence. These observations consisted of parameters such as reservoir depth, volume and filling history, and tectonic parameters such as geology of the region, historic seismicity, crustal stress state and direction, and presence or absence of faults, active or not, in the vicinity of the reservoir. These observations were then treated in a statistical manner to obtain probabilities of future

RTS occurrence. The earlier analysis of RTS for the Watana site (WCC, 1980) relies completely on such an empirically-based statistical approach.

Because RTS is a physical process, the ideal method of forecasting RTS behavior would be to accurately model and calculate the stress changes in the volume of upper crust beneath the reservoir and determine whether these changes exceed the failure strength of faults that exist in the volume. However, because very little is known about the detailed physical, mechanical, and hydraulic properties of the rocks beneath the planned reservoir, as well as the existence of faults and their properties, this method will not be possible, in most cases, for the foreseeable future.

In spite of these practical difficulties, it has been recognized that the production of earthquakes from stress changes due to reservoir impoundment has two causes: the weight of water on the crust (reservoir loading), and pore pressure changes on fault surfaces due to downward diffusion of water (e.g., Simpson et al., 1988).

The following discussions of reservoir loading and pore pressure changes highlight representative studies and conclusions, but are not an exhaustive review of the literature.

2.3.4.2 Physical Mechanisms

Carder (1945) was one of the first studies relating reservoir loading to enhanced seismicity. Coincident with the filling of Lake Mead behind Hoover Dam in the late 1930's, local seismograph stations documented increases in seismicity correlated with reservoir level. A prominent spike in activity rate was observed about 6 months after the reservoir reached maximum height. He applied the Richter (1958) formula relating magnitude of all observed earthquakes to energy

$$\text{Log } E = 11.3 + 1.8 * M \quad (1)$$

Where E is energy in ergs, and M is magnitude, and then calculated the depression of the crust due to weight of the water by dividing the energy from the earthquakes by the reservoir load (12×10^9 tons). He arrived at a "settlement" of the crust of about 10 inches. Later geodetic studies (Lara and Sanders, 1970) found the maximum settlement to be about 8 inches, a reasonable agreement.

Gough and Gough (1970) proposed that RTS is caused by either 1) the direct increase of shear stress on a fault caused by the added surface load, 2) the indirect effect of the added stress in triggering the release of stress on an already stressed fault, or 3) the increase in pore pressure due to the water load and its downward diffusion. Bell and Nur (1978) ruled out 1) as an independent mechanism since at 1 bar/10 m water depth, a deep (200 m) reservoir would provide a stress of only about 20 bars, insufficient to cause fault rupture, and also rule out 2), since water load alone leads to fault strengthening. Simpson (1976) also rules out 2) based on Mohr circle analysis, showing that increased normal stress on either normal, thrust, or strike-slip faults moves the stress state away from failure.

A number of publications describe the technical details of 3) above. The discussion below is abstracted or paraphrased from Snow (1972), Bell and Nur (1978), Simpson (1976), Simpson et al. (1988), Roeloffs (1988), Kisslinger (1976), Scholz (1990), Talwani (1997), and Ge et al. (2009).

As discussed above, RTS has been ascribed to two mechanisms: 1) the direct effect of reservoir loading, through increased elastic shear stress; and (2) the effect of increased pore pressure, through decreased effective normal stress across a fault. Increased pore pressure at depth can either be due to the volumetric strain component of the elastic field producing a decrease in pore volume, or result from diffusion of pore pressure from the reservoir at the surface.

These effects can be expressed by the change in effective Coulomb stress ΔS_e :

$$\Delta S_e = \Delta \tau - \mu(\Delta \sigma + \Delta P) \quad (2)$$

where μ is the coefficient of friction on the fault, τ is shear stress in the fault slip direction, σ is normal stress perpendicular to the fault, and P is pore pressure (Ge et al., 2009). Hence positive change in ΔS_e promotes failure, and negative change inhibits failure. Coulomb stress increases of ≥ 1.45 pounds per square inch (psi) (0.01 MPa) have been shown to be associated with seismicity rate increase and in many cases triggering earthquakes (Reasenber and Simpson, 1992; Stein, 1999).

The fluid diffusion term, ΔP , in equation (2) accounts for two effects: 1) the instantaneous pore pressure response to the volumetric stress resulting from the static load of the reservoir pool, known as the “undrained” response, and 2) the time-dependent pore pressure diffusion due to the permanent presence of water pressure at the bottom of the reservoir (Roeloffs, 1988). “Undrained” means that the water does not have time to migrate away from the fault. The magnitude of the undrained pressure change depends on rock compressibility and is proportional to the mean stress, is largest upon initial loading, and decays through time due to pore pressure diffusion. The rate of pore pressure change depends on the hydraulic diffusivity of the rocks.

Thus there are two fundamental physical mechanisms of RTS, both of which are time-dependent. The first begins almost immediately following the first filling of the reservoir. In the second, increases in seismicity are not observed until a number of seasonal filling cycles have passed. These differences in response may correspond to two fundamental mechanisms by which a reservoir can modify the strength of the crust - one related to rapid increases in elastic stress due to the load of the reservoir, and the other to the more gradual diffusion of water from the reservoir to hypocentral depths. Decreased strength can arise from changes in either elastic stress (decreased normal stress or increased shear stress) or from decreased normal stress due to increased pore pressure. Pore pressure at hypocentral depths can rise rapidly, from a coupled elastic response due to compaction of pore space, or more slowly, with the diffusion of water from the surface. Talwani (1997) refers to this as a coupled response.

There are substantial differences in the temporal and spatial characteristics of the response of the crust to these processes and it should be possible to identify the dominant mechanism, through a comparison of changes in seismicity with water level in the reservoir.

Talwani et al. (2007) concluded that hydraulic parameters could be directly related to RTS. The hydrologic property controlling pore pressure diffusion is hydraulic diffusivity c , which is directly related to intrinsic permeability k . By analyzing more than 90 case histories of induced seismicity, they determined the hydraulic diffusivity value of fractures associated with seismicity to lie between $1.1 \text{ ft}^2/\text{s}$ and $108 \text{ ft}^2/\text{s}$ (0.1 and $10 \text{ m}^2/\text{s}$). This range of values of c corresponds to a range of intrinsic permeability values between 5×10^{-15} and $5 \times 10^{-13} \text{ ft}^2$ (5×10^{-16} and $5 \times 10^{-14} \text{ m}^2$). They call this range the seismogenic permeability k_s . Fractures with permeability less than k_s were aseismic, as the pore pressure increase was negligible.

Schaeffer (1991) published observations relating joint intensity to RTS at Lake Keowee, South Carolina. He found a negative correlation between joint intensity (measured as joint surface area per unit rock volume at surface exposures) and location of RTS. His explanation is that low joint density implies low permeability, inhibiting fluid flow and thus increasing pore pressure which in turn promotes RTS. Borehole data showed that the fracture density did not change significantly through depths up to 350 m. It has been shown in other studies (e.g., Rice and Cleary, 1976) that fracture characteristics are the primary controlling factor in fluid flow through the crust.

Saxena et al. (1988), through modeling studies involving changes in effective stress (equation 2), *in situ* stress, and water level variations, concluded that high permeability is associated with high RTS activity during initial filling, but low activity after reservoir level stabilizes. In contrast, they found that low permeability is associated with low initial RTS but continuous RTS afterward.

In summary, this section discusses a limited number of representative studies that have presented RTS physical theory and relate hydraulic parameters and rock fracture characteristics to its occurrence. While the theory and mechanisms have a sound basis and correlate with well-documented RTS cases, it must be emphasized that for the purposes of this report they have little predictive value. This is because they are forensic in nature, and present hydraulic parameters and physical conditions in the top few kilometers of crust that are not practically possible to measure through conventional sampling methods. For example, the Talwani et al. (2007) k_s parameter can only be determined after the time-dependent behavior of RTS has been observed.

2.3.4.3 Analysis Techniques and Case studies

While most case studies of RTS have consisted of attempts to explain observations in light of the above mechanisms, recent studies, particularly of the Mw 7.9 Wenchuan, Sichuan, China earthquake, have been analyzed with dynamic 2-D finite element techniques. While these methods have been unable to

definitively state whether the earthquake was a case of RTS, they represent a new technique with which future RTS cases will be analyzed. These modeling efforts are used in conjunction with traditional observational and statistical techniques.

Below, two cases are discussed in detail to give a sense of how similar analyses for the Watana site might be conducted. The first is for Nurek Dam and reservoir, Tajikistan (Simpson and Negmatullaev; 1981). This dam and reservoir have important similarities to the proposed Watana dam: it is 1033 feet (315 m) high, 2624 feet (800 m) long, with a maximum reservoir depth of 984 feet (300 m). The reservoir contains 8.5×10^6 acre-feet ($10.5 \times 10^9 \text{ m}^3$) of water, and extends 25 miles (40 km) upstream with a maximum width of 4 miles (6 km). In comparison, the proposed Watana dam will be 735 feet (224 m) high and 1640 feet (500 m) long, with a maximum reservoir depth of 595 feet (183 m). The reservoir will contain 5.2×10^6 acre-feet ($6.4 \times 10^9 \text{ m}^3$) of water, extend 44 miles (70 km) upstream, with a maximum width of 1.2 miles (2 km). Both lie within seismically active, compressive tectonic environments. The region surrounding Nurek Dam had adequate seismic monitoring before and after initial filling, as will be the case for Watana Dam.

The second is the case of Zipingu reservoir, Sichuan, China. With a volume 811,000 acre-feet ($1 \times 10^9 \text{ m}^3$) this reservoir has less capacity than Nurek or Watana, is not as deep at 426 feet (130 m), but also lies within a seismically active, compressive tectonic environment. The Mw 7.9 earthquake occurred 2 ½ years after initial impoundment on a previously identified fault. Though the epicenter was only 12 miles (20 km) from the reservoir, the rupture initiation depth was 12 miles (20 km), deeper than that usually attributed to RTS. The magnitude is significantly greater than that (~ 6.5) associated with RTS historically (Allen, 1982).

2.3.4.3.1 Nurek Dam and Reservoir, Tajikistan

In the Nurek area more than 1800 earthquakes with magnitude less than 4.6 were recorded in the 9 years after initial filling in 1971, which was four times the pre-impoundment rate. Increased seismicity coinciding with initial filling was located 6-9 miles (10-15 km) away from the reservoir, but migrated to beneath the reservoir and upstream, as the reservoir area increased with time. An important observation was that bursts of seismicity (including the largest events) coincided with changes in filling and drawdown rates. These changes (in terms of reservoir elevation) were as small as 0.66 ft/day (0.2 m/day), and seismicity response times were short, on the order of 1-4 days.

As shown in **Figure 1** (from Simpson and Negmatullaev, 1981), the initial filling of the reservoir was accompanied by increased seismicity and again four years later when the water depth was raised over 200 m.

Simpson and Negmatullaev (1981) attributed these observations to the physical mechanisms described above operating dynamically as follows:

“Raising the water level immediately increases the vertical stress which opposes the natural horizontal compression and stabilizes faults. The diffusion of increasing pore pressure into fault zones gradually decreases the effective stress, weakening the faults. As long as the water level continues to rise and the load effect exceeds the pore pressure, the net effect is one of increased stability. If the water level decreases rapidly, however, the stabilizing effect of the increased vertical stress is removed immediately, whereas high pore pressure persists until it can diffuse away. Thus, rapid decreases in water level can lead to immediate instability (Simpson, 1976). Lateral variations in permeability (e.g., along faults) can produce zones of increased pore pressure where net weakening can occur (Bell and Nur, 1978).

The opposing nature of the effects of load and pore pressure in regions of maximum horizontal compression can explain the relationship between loading rate and seismicity at Nurek. As the water level rises, the load effect initially dominates causing lower seismicity. When the filling rate decreases, rising pore pressure exceeds the load effect, resulting in increased seismicity as a peak in water level is reached. If the water level remains constant, pore pressure and load equilibrate and seismicity decreases. When the water level drops, the load is removed before pore pressure can disperse and activity increases with little or no time delay. If changes in the rate of filling take place slowly compared to the diffusion time constant, the effect is small. When they occur rapidly the effect on seismicity is much greater.”

2.3.4.3.2 Zipingou Reservoir, Sichuan, China

The epicenter of Mw 7.9 Wenchuan earthquake that occurred after filling of the reservoir was located 12 miles (20 km) from the reservoir, but is postulated to have occurred on the Yinxiu-Beichuan fault, part of a belt of northwest-dipping thrust faults which forms the edge of the Tibetan Plateau.

Ge et al. (2009) constructed a 2-D finite-element model across the fault and reservoir, in order to dynamically model the physical mechanisms described above. The results are shown in **Figure 2**. Parameters in the model include fault geometry, coefficient of friction on the fault (μ), diffusivity (**D**), Skempton’s constant (**B**) (which relates pore pressure to mean stress; see Roeloffs; 1988), and Poisson’s ratio (ν) (an rock elasticity parameter, e.g., Jaeger and Cook, 2007). Panel (a) shows the stress changes due only to the static reservoir load, (b) shows the stress changes due to diffusion of pore pressure, and (c) shows the combined effects of (a) and (b) at the time of the Mw 7.9 earthquake. The blue areas are where stresses are increased, therefore inhibiting slip, and red areas are where stresses are decreased, thus promoting slip. Because the earthquake location is within the region of decreased stress, Ge et al. proposed that the earthquake can be attributed to the influence of Zipingou reservoir, which elevated the Coulomb stress (equation 2) by 1.45 -7.25 psi (0.01 – 0.05 Mpa [megapascals]).

A similar analysis was published by Klose (2011), who supported the hypothesis that the earthquake was most likely triggered by lithostatic and poroelastic stress changes on the fault plane.

Lei (2011) studied both local seismicity and Coulomb stress changes, and while concluding that microseismicity in the vicinity was caused by reservoir effects, reserved judgment on whether the Mw 7.9 event was directly caused by reservoir operations.

Similar analyses by Deng et al. (2010), Zhou et al. (2010), and Galahaut and Galahaut (2010) came to the opposite conclusion; that it is unlikely that the reservoir played a role in the Mw 7.9 earthquake.

All of these studies applied the same physical theory described in **Section 2.3.4.2**. A comment and reply between Ge and Zhou and Deng (Ge, 2011; Zhou and Deng, 2011) provided a debate regarding their conclusions and details of the modeling technique and analyses. **Figure 3**, from Zhou and Deng (2011) provides an alternative analysis, and a conclusion contrary to that of Ge et al. (2009).

A recent inversion for rupture history using teleseismic body waves, strong motion data, and geodetic observations by Hartzell et al. (2013) resulted in a complex, interacting faulting model on three spatially separated fault planes; a more complicated geometry than was assumed in the Coulomb stress models. The hypocentral depth and fault dip angles he used were also different, due to the availability of more recent geophysical data.

A primary cause of the discrepancy in the conclusions of the various studies is the uncertainty in the location of the fault plane at depth, and in the hypocentral location of the earthquake. As seen in **Figure 2**, the dashed fault plane location implies that it is an estimate, and the two hypocentral positions, in addition to discussion by Zhou et al. (2010) indicates that the uncertainty in the earthquake location may be on the order of several kilometers.

These analyses of the Wenchuan earthquake reveal the strengths and weaknesses of Coulomb stress change modeling. While long-accepted and confirmed formulations of stress changes due to reservoir impoundment and finite element computer codes allow for numerical modeling of the phenomenon in both 2-D and 3-D, the conclusions are inescapably sensitive to knowledge of hydraulic parameters, and detailed knowledge of the existence of and geometry of faults beneath the reservoir.

Due to its size, the massive destruction it caused, the quantity of geological and geophysical data collected before and after the earthquake, and its status as a suggested RTS event, the Wenchuan earthquake has been, and will continue to be, the subject of further research. The purpose of this discussion is not to judge whether or not it can be classified as an RTS event, but to illustrate current modeling techniques and sources of associated uncertainties.

2.3.5 State of the Practice for Determining the Potential for Reservoir Triggered Seismicity

To assess the potential and monitor RTS, especially for dams of greater height, ICOLD recommends that the following sets of data be evaluated:

- tectonic conditions and data on structural geology, supported by study of aerial photographs
- macroseismic data pertinent for the reservoir under study
- detailed information on active faults in a wider region especially all available data on recent fault activity in the dam and reservoir region
- assessment of the seismic capability of all known faults in the dam and reservoir region
- the regimes of underground water

Based on the current state of the practice and in consideration of ICOLD's recommendations on assessing the potential and monitoring RTS the following recommendations are made for this project: 1) statistical comparisons to cases of accepted RTS, 2) measurement of hydraulic properties of rocks beneath the reservoir, 3) measurement of joint density and orientation of rocks at the dam site and deeper parts of the reservoir, 4) numerical modeling of stress changes due to loading and pore pressure changes due to downward diffusion of water, 5) monitoring and analysis of pre- and post-impoundment seismicity, and 6) identification of faults favorably oriented to the current stress field as potential locations of RTS.

2.3.6 Database of Reservoir Triggered Seismicity

A database was compiled of all the reported RTS cases worldwide. This database, included in Appendix A, was completed by combining the following studies:

- Appendix A and Appendix B from the Woodward Clyde Consultants (WCC 1977) study for Auburn Dam. Appendix A consists of summaries of the reservoir impoundment data and information regarding the geology and seismicity that were compiled during this study for the 55 reported cases of RTS. Appendix B consists of summaries of the data compiled regarding reservoir impoundment and geologic conditions at the very deep reservoirs of the world. For the purposes of this study, a very deep reservoir was defined as being 492 feet (150 m) deep or more.
- The International Commission on Large Dams (ICOLD or CIGB) list of dams was sorted as follows:
 - ICOLD-CIGB 2012 database was obtained and all dams with a height of 328 feet (100 m) were selected. (see calculation for water depth based on dam height below)
 - Dams that were under construction or abandoned were removed
 - All dams classified as "Secondary" were removed.
 - Database was sorted by reservoir name and those reservoirs with more than the main dam listed were removed.

- Database was sorted by reservoir capacity and those reservoirs with more than the main dam listed were removed (after cross checking for similar locations).
- Database was sorted by reservoir area and those reservoirs with more than the main dam listed were removed (after checking for similar locations).
- Dams built after 2002 were not included in the study, which gives approximately 10 years for a RTS event to occur and be reported.

This database from ICOLD was presented as a listing of dams, because several dams exist for a single reservoir every effort was made to remove duplicate reservoirs.

- This database was also compared to Table 10-1 in the WCC (1980) Study for Susitna and additional Reported Cases of RTS were added. The classification of RTS was also edited.
- A literature review was completed and the database was updated with references as needed. A report by Gupta (2002), titled “A review of recent studies of triggered earthquakes by artificial water reservoirs with special emphasis on earthquakes in Koyna, India”, was used extensively.
- A list of RTS published by International Rivers (internationalrivers.com) was compared to the existing list. Dams that were not already included in the database were investigated to evaluate the validity of the reported RTS.
- A final review of ICOLD’s document was performed and cases that were not RTS were edited

It should be noted that no determination was made whether a case was accepted, questionable, or reported, other than removing non-RTS events as clarified by the ICOLD (2011). In addition, the height of the dam was used to estimate the maximum water depth because water depth is directly related to the stress imposed by a reservoir. The depth was estimated from dam height and type as done by Packer et al. (1977). The following formulas were used:

- Concrete dams greater than 492 feet (150 meters) in height, 98 feet (30 meters) was subtracted from the dam height
- Concrete dams between 328-492 feet (100-150 meters) in height, 59 feet (18 meters) was subtracted from the dam height
- Concrete dams less than 328 feet (100 meters) in height, the height was multiplied by 0.9
- Earth or rock dams greater than or equal to 328 feet (100 meters) in height, the dam height was multiplied by 0.95
- Earth or rock dams less than 328 feet (100 meters) in height, the dam height was multiplied by 0.90.

Based on this research a total of 109 dams were classified as having reported RTS. The following references were used to classify a case as RTS:

- Anglin, F. M., & Buchbinder, G. G. (1985). Induced seismicity at the LG3 Reservoir, James Bay, Quebec, Canada. *Bulletin of the Seismological Society of America*, 75(4), 1067-1076.
- Chen, L., & Talwani, P. (1998). Reservoir-induced Seismicity in China. *Pure and Applied Geophysics*, 133-149.
- Gupta, H. K. (2002). A review of recent studies of triggered earthquakes by artificial water reservoirs with special emphasis on earthquakes in Koyna, India. *Earth-Science Reviews*.
- ICOLD Committee on Seismic Aspects of Dam Design. (2011). *Reservoirs and Seismicity - State of Knowledge- Bulletin 137*. Bulletin 137.
- Leblanc, G., & Anglin, F. (1978, October). Induced seismicity at the Manic 3 reservoir, Quebec. *Bulletin of the Seismological Society of America*, 68, 1469-1485.
- Lei, X. (2011). Possible Roles of the Zipingpu Reservoir in triggering the 2008 Wenchuan earthquake. *Journal of Asian Earth Sciences*, 844-854.
- Packer, D. R., Cluff, L. S., Knuepfer, P. L., & Withers, R. J. (1979). Study of Reservoir Induced Seismicity. San Francisco: Woodward-Clyde Consultants. WCC Auburn Report Appendix A:
- Plotnikova, L. M., Makhmudova, V. I., & Sigalova, O. B. (1992). Seismicity Associated with the Charvak Reservoir, Uzbekistan. *PAGEOPH, Vol. 139, No. 3/4*.
- Woodward-Clyde Consultants. (1977). Reservoir Induced Seismicity- Auburn Dam. San Francisco.

ICOLD (2011) states that the range is likely between 40 and 100. However, for conservatism reported or questionable cases were used in the statistical analysis and only those as determined non-RTS were removed from this list. **Figure 4**, is a plot showing all of the dams with water depths greater than 300 feet (92 m)) and reservoir volumes greater than 8.1×10^5 acre-feet ($1 \times 10^9 \text{ m}^3$) used in this study.

3.0 GEOLOGIC AND TECTONIC SETTING OF THE RESERVOIR

TM-4 (Fugro Consultants, 2012) provided an updated summary of the geologic and tectonic setting of the project for use in the seismic hazard evaluation. Discussions of geology and tectonics that follow in this section are largely abstracted from that report. South-central Alaska experiences rapid rates of tectonic deformation driven by the obliquely convergent northwestward motion of the Pacific plate relative to the North American plate. In southern and south-eastern Alaska the convergent and oblique relative plate motion is caused by subduction of the Pacific Plate at the Alaska-Aleutian megathrust and dextral (right-lateral) transform faulting along the Queen Charlotte and Fairweather fault zones. The transition from subduction to transform tectonics is complicated by the Yakutat microplate which is colliding with southern Alaska along the eastern edge of the subducting slab. The collision of the

Yakutat microplate is considered to have substantial influence on the deformation and counter-clockwise rotation in the interior of south-central Alaska (Haeussler, 2008). In the interior of south-central Alaska, transpressional deformation primarily is accommodated by dextral slip along the Denali and Castle Mountain faults, as well as by horizontal crustal shortening to the north of the Denali Fault. The crustal stress data in the site region, south of the Denali fault and north of the Castle Mountain fault, is heterogeneous and appears to rotate in orientation from west to east, but largely seems to be consistent with a transpressional tectonic setting and dominantly reverse and dextral strike-slip faulting (**Figures 5 and 6**).

3.1 Regional Geology and Tectonics

The Susitna-Watana dam site is located within a distinct crustal and geologic domain referred to in this report as the Talkeetna block. The Talkeetna block is bounded by the Denali fault system to the north, the Castle Mountain fault to the south, the Wrangell Mountains to the east and the northern Aleutians and Tordrillo Mountains volcanic ranges to the west (**Figure 5**). The Talkeetna block encompasses the north-central portion of the Southern Alaska Block (SAB) of Haeussler (2008) (**Figure 6**). Major strain release occurs on northern and southern block boundaries (i.e., Denali and Castle Mountains bounding faults), but mechanisms of strain accommodation are less well defined to the east and west. There is a relative absence of large historical earthquakes within the Talkeetna block, as well as a lack of mapped faults with documented Quaternary displacement within the Talkeetna block (Fugro Consultants, 2012, TM-4).

The Talkeetna block is comprised of three principal physiographic provinces: the Susitna basin, Talkeetna Mountains, and the Copper River basin (**Figure 5**). The Susitna-Watana dam site is located within the Talkeetna Mountains province. The Copper River basin is an intermontane basin surrounded by the Alaska, Talkeetna, Chugach and Wrangell mountains. The basin is characterized by flat lying to hummocky topography and is overlain by extensive glacial, glacio-fluvial, and glacial-lacustrine deposits. The Susitna basin is a somewhat north south trending basin and is the principal depocenter for alluvium transported by numerous major river systems which originate in the surrounding mountains. The Talkeetna Mountains are an elevated block which lies between the Copper River and Susitna basins, with glaciated peaks between 6560 feet and 9840 feet (2000 m and 3000 m) elevation. The Susitna River heads in the ranges north of the Copper River basin and flows westward through the northern Copper River basin and through the Talkeetna Range following a deeply incised canyon. Downstream, sediments from the river contribute to alluvial deposition in the Susitna Basin.

The Talkeetna Mountains consist of an assemblage of northeast trending tectonostratigraphic terranes including the North Talkeetna Flysch Basin, the Wrangellia Terrane, and the Peninsular Terrane (Glen et al., 2007b). The Wrangellia and Peninsular Terranes are comprised of largely late-Paleozoic to early Mesozoic metavolcanic and metasedimentary rocks that originated well south of their current position

(~30° latitude), and likely were sutured together in the Late Jurassic (Csejtey, et al. 1982). The terranes were accreted onto North America in the mid- to late-Cretaceous and translated northward to approximately their current location via strike-slip faults on the continental margin (i.e. Fairweather fault) (Ridgway et al., 2002). The North Talkeetna Flysch Basin contains part of the Kahiltina assemblage, which consists of argillaceous strata deposited in an oceanic basin between the Wrangellia Terrane and North America prior to and during the early stages of accretion. The North Talkeetna flysch basin consists of sediments shed to the northwest from the Wrangellia Terrane (Glen et al., 2007a). Following deposition, the basin sediments were obducted on to the continent during Wrangellia emplacement. The north-east striking Talkeetna thrust fault is the principal terrane-bounding structure in the dam site region, separating the North Talkeetna flysch basin in the northwest from the Wrangellia Terrane in the southeast (**Figures 7 and 8**). In addition to the three principal tectonostratigraphic terranes, numerous narrow, fault bounded terranes are tectonically intermixed within the Kahiltina Assemblage between the Denali fault and the Talkeetna thrust fault (i.e. Chulitna Terrane) (Nokleberg et al., 1994). Late Cretaceous through Tertiary intrusive and extrusive volcanic rocks are found throughout the Talkeetna Mountains, and often intrude or overlie the Cretaceous accretionary structures.

Early tectonic studies of the Talkeetna Mountains described the Talkeetna thrust fault as a southeast dipping thrust that accommodated the middle to late Cretaceous emplacement of the Wrangellia Terrane (Csejtey, et al., 1982; Nokleberg et al., 1994). The fault trace is recognized by the juxtaposition of the Triassic and Permian metavolcanic and metasedimentary Wrangellia terrain rocks on the south and Late Jurassic through Cretaceous sedimentary rocks of the Kahiltina Assemblage on the north. The approximate fault trace follows a broad topographic trend striking northeast across the Talkeetna Mountains (**Figure 8**). On older maps, the southwestern margin of the fault is mapped as overlain or terminated by Tertiary intrusive and volcanic rocks (Csejtey and others, 1978); to the northeast the fault is interpreted to terminate or merge against the younger, north-dipping Broxson Gulch fault (Nokleberg et al., 1994).

Mapping by O'Neill et al. (2003a) along the northeastern reaches of the Talkeetna thrust fault found little evidence for penetrative deformation adjacent to the fault and stratigraphic relationships which suggest limited displacement along the fault. Based on these observations they concluded that major contractional displacement has not occurred along the Talkeetna thrust fault. O'Neill et al. (2003a) further propose that the principal suture zone is located to the northwest near Broad Pass where miniterranes of uplifted Wrangellia terrane basement rocks are exposed. They characterize the Talkeetna thrust fault as a deep crustal structure bounding the northwestern edge of the Wrangellia Terrane, overlain by a wide zone (0.5-12 mi [1-20 km]) of Tertiary or younger faults. Glen et al. (2007b) use tectonic analysis of gravity and magnetic data to propose replacement of the term Talkeetna thrust fault with the Talkeetna suture zone. Glen et al. (2007b) and O'Neill et al. (2003b) propose that the surface fault structures may have been reactivated in the late Tertiary as a broad dextral shear zone associated with movement along the Denali fault. As depicted on **Figure 9**, these interpretations likely

imply that near-surface structures of the Talkeetna suture zone, termed the Fog Lakes Graben by Glen et al. (2007b) would have much different shallow geometries than the southeastern-dipping thrust fault implied from earlier mapping.

3.2 Reservoir Geology

The topography of the Watana Reservoir and adjacent slopes is characterized by a narrow, V-shaped, stream-cut valley superimposed on a broad, glaciated basin. Late Quaternary glacial deposits overlie bedrock throughout much of the area, such that bedrock units are only intermittently exposed along the lower canyon walls and the upper elevations of the reservoir will overlie or onlap the Quaternary glacial deposits (**Figures 8 and 10**).

Generally, the upper slopes of the reservoir, and the broad flats adjacent to the Susitna River are covered by a stratified sequence of glacial till, outwash, and lacustrine deposits. These deposits were investigated extensively in the 1980's near the dam site and along the southern reservoir rim to assess the water holding capabilities of the reservoir and as potential borrow sources (Acres, 1982; Harza-Ebasco, 1984). Two main types of till have been identified in this area: ablation and basal tills. The basal till is predominately overconsolidated, with a fine grain matrix (more silt and clay) and low permeability. The ablation till has fewer fines and a somewhat higher permeability. Outwash units consist of gravels, and sands, with higher permeabilities. Lacustrine deposits consist primarily of poorly graded fine grained sands and silts, with lesser amounts of gravel and clay, and exhibit a crude stratification.

The deepest portions of the planned reservoir, from just upstream of the dam site to Watana Creek (**Figure 10**) are mostly underlain by bedrock units comprised of a sequence of Cretaceous shales (regionally altered to argillite) and lithic greywacke sandstone of the Kahiltna assemblage (Csejtey et al., 1978). The Kahiltna assemblage is regionally intruded by small bodies of Paleocene granite units with interfingering migmatite and pelitic schists, and granodiorites with minor diorite (Csejtey et al., 1978). The intrusive rocks are part of a large suite of igneous (largely granitic and granodioritic) rocks which intruded between 53.2 Ma to 64 Ma during the late stages of accretionary tectonics. At the planned damsite, and for a short distance upstream within the reservoir extent, diorite and quartz diorite bedrock which is likely part of this regional intrusive suite underlies the reservoir (Acres, 1982). Other rock units, present as relatively small areas in the deeper portions of the reservoir include Paleocene to Miocene subaerial volcanic rocks and related shallow intrusives that may be related to the Paleocene plutons (WCC, 1980). At the dam site, these young volcanic rocks include andesite porphyry and numerous felsic through mafic dikes (Acres, 1982). Basalt flows outcropping in Deadman Creek, to the east of the dam site have an early-mid Eocene age (approximately 48 Ma, based on Argon isotope analyses AR40/39) (Schmidt et al., 2002).

The main structural feature known within the Watana Reservoir is the Talkeetna thrust, which trends northeast-southwest and crosses the Susitna River approximately 8 miles (13 km) upstream from the Watana dam site (**Figures 8 and 10**). The Talkeetna thrust fault is a major terrane bounding structure associated with continental accretion in the Late-Cretaceous and Early Tertiary. The extension of this feature northeast of the reservoir is along Watana Creek. A sequence of folded and faulted Tertiary sediments is exposed along Watana Creek, elongated along the presumed trend of the Talkeetna thrust fault. These Tertiary sediments are in turn overlain by Quaternary glacial deposits and widespread landslides and slumps. To the southwest, prior site investigations (Acres, 1982; Harza-Ebasco, 1984) defined a buried channel of the Susitna River, filled with Quaternary glacial sediment that generally follows the trend of the Talkeetna thrust fault to the southwest towards Fog Creek (**Figure 10**).

Upstream of Watana Creek and the Talkeetna thrust fault, there is little detailed mapping information on the bedrock units or structures that would underlie the reservoir. Regional mapping (**Figure 8**) depicts these rocks as folded and deformed Paleozoic age shales, and limestones which are part of the Wrangellia Terrain (**Figure 7**). Older intrusive rocks may also underlie the shallow, upper reaches of the reservoir.

3.2.1 Detailed Geologic Data from the Watana Dam Site

The Watana dam site is primarily underlain by an intrusive dioritic body which varies in composition from diorite to granodiorite to quartz diorite (**Figure 10**). These intrusive rocks are part of a large suite of igneous rocks which intruded between 53 Ma to 64 Ma. These intrusive rocks are massive and they are generally hard, competent, and fresh except within locally developed fractured, sheared, and altered zones. These rocks have been subsequently intruded by mafic and felsic dikes which are generally only a few feet wide. The rock contacts are healed and competent. Bedrock immediately downstream and south of the dam site is Tertiary volcanic rocks that locally is a volcanic flow, an andesite porphyry but varies in composition to include dacite and basalt. The andesite is similar in chemical composition to the diorite. The andesite is generally slightly weathered, strong to very strong, competent and in places contains inclusions of the diorite. The nature of the contact zone of the andesite with the diorite is poorly understood. However, where mapped or drilled through, the contact zone is generally weathered and fractured over an interval of up to 10 to 15 feet. Detailed discussion of the andesite porphyry/diorite contact is presented in the Acres (1982) report.

In a number of boreholes, alteration zones were penetrated, zones where hydrothermal solutions have caused the chemical breakdown of the feldspars and mafic minerals in the host rock. The degree of alteration encountered is highly variable across the site. These zones are rarely seen in outcrop as where alteration is moderate to severe, bedrock is easily eroded into gullies, but were encountered in many of the boreholes. The transition between fresh and altered rock is gradational. The thickness of these zones in boreholes range up to 20 feet but are usually less than 5 feet and are often associated with close

fracturing, fracture zones, or shear zones. The degree and character of rock fractures and joints farther upstream of the dam site is not known.

The two most prominent structural geologic features are located upstream and downstream of the Watana dam site (GF1 and GF7 on **Figure 8**). A detailed discussion of the significant upstream and downstream geologic features is presented in the Harza-Ebasco (1984) report along with permeability and hydraulic conductivity testing information from site drilling.

3.2.2 Quaternary Fault Evaluations and Lineament Mapping in the Project Area

Regional mapping is being performed by Fugro Consultants, Inc. for MWH using recently-acquired, detailed, topographic data (i.e., INSAR and LiDAR). Results of these evaluations are being documented as separate technical memorandum. As of February 2013, no new features which are strongly suggestive of Quaternary faulting have been identified, however additional field evaluations are planned to further evaluate several features within the region, including those that may lie within the planned reservoir. These evaluations are expected to include additional mapping and characterization of bedrock faults within the reservoir area, including along the Talkeetna thrust fault near Watana Creek. Additional analyses will be required to further evaluate the mapped lineaments, at which time the RTS study will also need to be updated.

3.3 Seismicity in the Reservoir Area

The Watana Dam site lies in a seismically active area associated with the Pacific-North American plate boundary. **Figure 11** shows a map and cross section of seismicity in south central Alaska. The seismicity clearly outlines the location and geometry of the subducting Pacific plate. The zone of contact between the two plates, termed the interface, is marked by an almost flat plane at a depth of 19 miles (30 km). About 37 miles (60 km) southeast of the site the plate starts to dip more steeply as the Pacific plate loses contact with the North American plate and begins its descent into the upper mantle. While interface earthquakes have thrust mechanisms reflecting underthrusting of the Pacific plate, earthquakes in the downgoing plate (termed intraslab) are largely due to the dynamic forces of gravitational pull and push from the spreading ridge that generates the Pacific plate. From the cross-section, the downgoing plate lies about 31 miles (50 km) beneath the site. This plate collision system comprises the primary seismic hazard at the site. The 1964 Mw 9.2 Alaska earthquake occurred on the plate interface.

In addition to these primary plate interactions, crustal faults have formed in response to stresses are transmitted to the crust above and landward of the plate interface. The oblique angle at which the Pacific plate intersects the North American plate has given rise to a transpressional environment in the crust, in effect causing the movement of south central Alaska to the southwest. The major expression of this environment is the Denali fault, which lies 43 miles (70 km) north of the site. The fault exhibits a slip

rate of about 1 cm/year, and a Mw 7.9 earthquake occurred on it in 2002. The Castle Mountain fault is a similar but lower slip rate feature that lies 62 miles (100 km) to the south of the site. Although these are the most active and easily identified crustal faults, geomorphic evidence shows that less active, but potentially hazardous faults may exist in the vicinity of the dam and reservoir. These are the subject of ongoing investigations.

3.3.1 Watana Seismic Network

The Alaska Earthquake Information Center (AEIC), part of the Geophysical Institute of University of Alaska Fairbanks, has operated a seismic network in the state of Alaska since the 1970's. During the planning phases for the Watana Dam project, it was recognized that increased seismograph station density would be required to adequately locate and analyze pre and post impoundment seismicity in the reservoir area. To that end, a four-station microseismic network was installed in late 2012 (August 12-November 16) by AEIC. The four stations are WAT1, WAT2, WAT3, WAT4. WAT1 is a 6-component, broadband-and-strong-motion station located near the proposed Watana Dam site. WAT2 and WAT3 are 3-component broadband stations located about 10 miles to the north and south of WAT1, respectively. WAT4 is a broadband station about 20 miles east of WAT1, on the north side of the proposed Watana Reservoir (**Figure 12**).

The data from the Watana network are integrated into the Alaska regional seismic network. Waveform data can be accessed via Incorporated Research Intuitions for Seismology (IRIS, www.iris.edu). Hypocenter data for a region around the site will be accessible on a monthly basis via an ftp site. With a station separation on the order of 16 km, this sub-network (in addition to surrounding AEIC stations) has greatly improved earthquake detection and location precision. One of the reasons this network was set up prior to dam construction was to monitor microseismicity in the area, as recommended by ICOLD (2011).

3.3.2 Seismicity in the Watana Region

Figure 13 shows all seismicity of magnitude greater than or equal to 3 from 1898 through 2010 from the AEIC catalog. There are about 4000 earthquakes on this figure, many of them being aftershocks of the Mw 7.9 Denali fault event. Another magnitude 7 event occurred in 1912, seen in the northeast part of the figure. There are five magnitude 6 events, and about 50 of magnitude 5.

Figure 14 shows local seismicity of all magnitudes from the AEIC catalog in an area within about 19 miles (30 km) of the dam and reservoir within the "RTS Zone" as defined in **Section 4.1** below. There are 2716 earthquakes with magnitudes of 1 through 6. There are six magnitude 5 earthquakes in this data set. The pattern shows that the site lies within a relatively dense zone that abruptly decreases in intensity about 12 miles (20 km) east of the site.

Figure 15 shows local seismicity from 2010 through November 16, 2012, the date the WAT stations in **Figure 12** were integrated into the AEIC routine location process. Hypocenters with depth greater than 19 miles (30 km) are plotted in blue, those shallower in red. **Figure 16** shows a cross-section through the A – A' line on **Figure 15**, replicating the section shown in **Figure 11**, but local to the site area. The delineation between crustal seismicity and seismicity occurring within the downgoing North American plate is distinct.

Figures 17 and 18 show similar plots, but for the 3 ½ month period after deployment of the Watana sub-network. Comparing **Figures 14, 15, and 17**, the epicentral pattern appears stable over the 3 ½ year period. Comparing **Figure 16** to **Figure 18**, the limit of crustal seismicity at about a 12 mile (20 km) depth, and the linear nature of intraslab seismicity appear better defined after deployment of the Watana sub-network. The cluster of crustal seismicity seen about 6 miles (10 km) northeast of the site in **Figure 15** appears to be a persistent feature.

4.0 RESERVOIR TRIGGERED SEISMICITY FACTORS

Several parameters can be useful when looking at the potential for RTS. These parameters are the depth, volume, stress state, geology, and fault activity (Baecher and Keeney, 1982). Empirical procedures for determining RTS will be presented in this report. However based on current research it is now believed that hydrology plays a more important role in determining a site's susceptibility to RTS (Talwani et al., 2007)

4.1 General Reservoir Parameters (Depth and Volume)

In the vicinity of the proposed Watana Dam site, the Susitna River has incised a narrow, steep-walled, east-west valley up to 800-feet deep into the broad Fog Lakes upland formed by repeated glaciations and surrounded by mountains of 3,000 to 6,300 feet in elevation. On the right bank (north) the valley rises at about a 2:1 slope from river level at El. 1,450 for approximately 600 feet, then flattens to a maximum elevation of 2,350 feet. Conversely, the left bank (south) rises more steeply from the river for about 450 feet at a slope of 1.4H:1V, then flattens to a 3H:1V or less to approximately El. 2,600 feet.

The proposed reservoir has a depth of about 600 feet (183 m). The total volume of the reservoir is planned to be 5.2 million acre feet (6 billion cubic meters). In comparison, the previously proposed reservoirs had a total volume of 10.7 million acre feet (13 billion cubic meters). The proposed reservoir's dimensions would be approximately 41 miles (70 km) long and 2 miles (3 km) wide, following the general topography of a narrow steep-walled valley.

The previous study performed by WCC in 1982 used 3 times the reservoir width as the radius of the bottom of half-pipe in three-dimensional space (Withers, 1977). Then this was converted into rectangular three-dimensional space, with a length and width of 37 miles by 37 miles (60 km x60 km)

and a depth of 19 miles (30 km). This rectangular space was centered about each site, such that the distance from the site to the edge of the space in all three dimensions was 19 miles (30 km). It was also assumed that the effects of ground motion from a RTS event outside of the 19 miles (30 km) would be negligible, based on their maximum RTS event and ground motion attenuation relations available at the time.

It is envisioned that the currently proposed configuration of the Watana Reservoir could experience RTS in a rectangular space defined as regions at least 30 km of the shoreline of the maximum reservoir level (**Figure 14**), with dimensions 75 miles (118 km) east to west and 54 miles (85 km) north. The 30 km distance is based on the Klose (2012) observation that all RTS cases occurred within 30 km of the “operation point”. The “operation point” is conservatively defined as the reservoir shoreline at maximum height. The fact that the WCC (1982) rectangle was also defined as points 30 km from the reservoir is coincidental.

This rectangle is shown as the “RTS Zone” in **Figures 14, 15 and 17**. The depth of the volume will be restricted to that defined by crustal seismicity, exclusive of subduction zone seismicity. From the cross sections in **Figures 16 and 18** this depth appears to be about 20 km, but will be refined as more accurate hypocenters are developed. It is assumed that any RTS processes will be confined to the upper crust and mechanically decoupled from subduction zone processes.

4.2 Geologic Parameters

The Watana Reservoir will straddle the Talkeetna thrust fault, a major terrane boundary in central Alaska (**Section 3.1; Figures 7 through 10**). Bedrock beneath the reservoir is dominantly metamorphic sediments, although the Watana dam site is in igneous and shallow volcanic rocks (**Figures 7 through 10**). The reservoir topography is long and narrow, with only relatively small arms along Deadman and Watana Creeks. Through most of the reservoir, the higher reservoir elevations will be in Quaternary glacial deposits which overlie the bedrock units in the lower and deeper sections of the reservoir.

Major known bedrock structures include the Talkeetna thrust fault which traverses the reservoir along Watana Creek, and where a folded and deformed trough of Tertiary sedimentary deposits is elongated to the northeast along the zone (**Figure 10**). Existing mapping of these features are primarily reconnaissance in nature and the detailed characteristics of this zone of bedrock fractures are unknown. Based on the more extensive geotechnical investigations near the Watana dam site some local structures have been mapped and described in intrusive rocks (**Section 3.2.1**). Some detailed descriptions of fractures and hydraulic parameters are available for these features; however, the applicability of these measurements to the non-igneous rocks and fracture systems within the proposed reservoir area is uncertain. Elsewhere in the proposed reservoir extent, existing mapping is primarily regional in nature, and additional bedrock faults are likely present, but not depicted on existing maps.

4.3 Stress Regime

RTS analysis requires knowledge of the local crustal stress field, because the larger earthquakes associated with reservoir operations have occurred on faults with a favorable orientation for re-activation. **Figure 19**, adapted from Ruppert (2008), summarizes an interpretation of the crustal stress field in south-central Alaska from earthquake focal mechanisms. Because this region is dominantly a compressive tectonic environment, the direction of maximum compressive stress, (σ_1), is the important parameter in the azimuthal diagrams. The figure shows five polygons, selected on the basis of consistent stress directions indicated by the individual earthquakes in each polygon. Stresses in the three easterly polygons show a consistent counterclockwise rotation of σ_1 from northeast-southwest to east-west. The “South of Denali” zone, which contains the Watana site, shows east-west compression in the southern Talkeetna Mountains, but rotates to northwest – southeast azimuth in the northern Talkeetna Mountains. This suggests that northeast-trending compressional structures may be favorably oriented for RTS. Variations in the least compressive stress, σ_3 , appear to imply a mix of strike-slip and thrust faulting. This zone covers a fairly large region, and it is not known if this pattern can be spatially discriminated on a finer scale within the zone. Additional seismograph stations installed in the region, including those specifically for the Watana Project, should be useful for this task, since the Ruppert (2008)-type of analysis will provide the ability to obtain finer resolution of the patterns of shallow crustal stress in the reservoir region. Preliminary data for one crustal M 2.0 earthquake located about 15 km southwest of the Watana site appears to support the northwest – southeast orientation of compressive stress in the reservoir region (AEIC, 2013).

4.4 Faulting Parameters

Studies to date have not identified evidence of Quaternary faults near the proposed reservoir with evidence of Quaternary faulting nor any existing zones of ongoing seismicity that define potentially active structural features (FCL, 2012). Additional detailed mapping of lineaments, faults, and evaluations of seismicity are part of ongoing efforts to confirm and further characterize the existence and potential for seismically active structures in the reservoir region, generally shown as the “RTS zone” area on **Figure 14**, at which time the RTS study will also need to be updated.

Potentially undiscovered faults in the region are most likely to have either low slip rates or long return periods between events. However, it is very important to identify these faults with low slip rates or long return periods that fall within the dam or reservoir area, to correctly define the design earthquake.

4.5 Hydrologic Parameters

4.5.1 Rock Mass Permeability

Rock mass permeability, the transmissibility of water through the bedrock, does not vary significantly within the site area, and is generally characterized as low to very low permeability, ranging between 0 to

50 lugeons or 6.6×10^{-4} ft/sec to 8.7×10^{-6} ft/sec, but appears to be generally less than 15 lugeons. Transmissibility is controlled by a degree of fractures within the rock, with the higher rock mass permeability occurring in the more sheared and fractured zone (e.g., 30 – 50 lugeons. Rock mass permeability tends to decrease with depth. However, with the potential for frozen ground and ice-filled discontinuities, the low to very low rock mass permeability determined on the left (south) abutment may be influenced by ground temperature below freezing.

Earlier drilling programs at the Watana site, and also the Devil Canyon sites (30 km downstream of the Watana site) (Acres America; 1981; Harza-Ebasco; 1984) performed permeability tests in a number of boreholes. **Figure 20** taken from Acres America (1981) for the Watana site shows average permeabilities of 2×10^{-6} to 1×10^{-5} in/sec (5×10^{-6} to 3×10^{-5} cm/sec) at bedrock depths of 200 – 800 ft. At the Devil Canyon site the values are more variable, ranging from 1×10^{-6} to 2×10^{-5} inches/sec (3×10^{-6} to 5×10^{-5} cm/sec) over the same depth range (**Figure 21**). The greater variability at Devil Canyon may reflect differences the argillite-graywacke rock properties compared to the metamorphosed igneous diorite at the Watana site.

4.5.2 Fracture Orientation and Density

The Acres America (1981) report summarized fracture orientations at the two sites. At Watana “...The prominent jointing and shearing direction is northwest trending with steep dips. Many fractures have thin clay gouge seams and slickensides”. At the Devil Canyon site “...Three joint sets were defined with the master set striking approximately 335° and dip 80° to vertical...Joint spacing ranges about 4 to 5 feet apart.” These were based on surface observations.

In the borehole summary logs for both sites the number of joints per 10 feet of core is highly variable from hole to hole, but generally varies between 5 and 25.

In summary, at both sites the dominant fracture and joint pattern appears to be northwest trending. The fact that this pattern is observed in two different rock types 30 km apart suggests that it may be a conceptual framework for jointing and fracturing over a larger regional area (i.e., the proposed reservoir). However, the continuation of this fracture pattern to rocks that underlie the reservoir area needs to be confirmed.

4.5.3 Proposed Reservoir Inflows/Outflows

The proposed reservoir inflows and outflows are cyclic; the water is stored from May through October and then released November through April. A significant portion of the inflows from May through October (5,340,000 acre-feet average inflow) are stored to be released during the months of November through April, when the inflows are at the lowest level (510,000 acre-feet average inflow). The total active storage or reservoir storage in acre-feet between the maximum normal pool level and the minimum power pool level is 3,500,000 acre-feet. The proposed maximum normal pool level is El

2050, with a water depth of 595 feet (183 meters) and the power pool level would be El. 1850, which means there is 200 feet of annual drawdown..

5.0 POTENTIAL FOR RTS

5.1 Empirical Approach

An empirical approach was developed similar to that previously performed for the project by WCC in 1982. The empirical RTS approach includes a comparison of reservoirs that have experienced RTS with comparable depths, volumes and bedrock. A statistical analysis is also presented that is a revision of the work completed by WCC (1982). The statistical analysis will look at probabilities of RTS for the previous and current proposed reservoir configurations using the statistical analysis developed by Baecher and Keeney (1982). However, the database used in the statistical analysis by Bacher and Keeney (1982) is approximately 31 years old and with any statistical analysis, the results depend on the current understanding of the historical record. Therefore, this analysis included additional data on RTS, gathered to date and focused on updating two of the reservoir parameters that are the most discriminating in determining the probability of RTS, depth and volume. Appendix A, presents the database.

The empirical approach is presented to serve as basis for communication and to better understand the phenomenon of RTS, not a substitute for professional judgment or a physically based approach. As it is generally agreed in the scientific community, the occurrence of RTS is also affected by the filling history of the reservoir, existing pore pressures and permeability of the rock beneath the reservoir.

It should also be noted that the previous configuration had a maximum reservoir at El. 2185, whereas the current proposed configuration has a maximum reservoir at El. 2050. General Reservoir Parameters that are significant to RTS

Table 2 summarizes the maximum water depth, maximum water volume, stress regime, bedrock and fault activity located at the proposed Watana Reservoir.

Table 2 Proposed Watana Reservoir Parameters

Maximum Water Depth	595 feet (182 meters)
Maximum Water Volume	5.2×10^6 acre-feet ($6,377 \times 10^6 \text{ m}^3$)
Maximum Water Elevation	2050
Stress Regime (Stress State ¹)	Compressional
Bedrock (Geology ¹)	Igneous\Metamorphic
Fault Activity	Active\Not Considered

Notes: 1. Equivalent terminology used by Baecher and Keeney (1982)

Watana Reservoir in its proposed configuration is classified as a very deep and large reservoir. A classification of reservoirs presented by Packer and others (1977) is as follows: a deep reservoir is 300 feet (92 meters) or deeper, a very deep reservoir is 492 feet (150 meters) deep or deeper; a large reservoir has a maximum water volume greater than 1×10^6 acre feet ($12 \times 10^8 \text{ m}^3$) and a very large reservoir has a volume greater than 8.1×10^6 acre feet ($100 \times 10^8 \text{ m}^3$). **Table 3** presents a comparison of the proposed Watana Reservoir to other reservoirs with accepted, reported or questionable RTS that have similar water depths, reservoir volumes, stress regimes, or bedrock.

Table 3 Dams with Reported Reservoir Triggered Seismicity that have Similar Water Depths and Reservoir Volumes

Case Number	Dam Name	Reservoir Name	Water Depth		Reservoir Volume		Stress State	Bedrock	Main Reference
			feet	meters	10x6 acre-feet	10x6 cubic meters			
1	ALMENDRA	Tormes	594	181	2.15	2649	Not Obtained	Not Obtained	1,2
2	CHARVAK		525	160	1.62	2000	Not Obtained	Not Obtained	7
3	DONGJIANG		489	149	7.42	9148	Not Obtained	Not Obtained	5,6
4	EUCUMBENE	Lake Eucumbene	348	106	3.89	4798	Compressional	Not Obtained	1,2
5	FIERZE		522	159	2.19	2700	Not Obtained	Not Obtained	4,6
6	GEHEYAN		469	143	2.79	3440	Not Obtained	Not Obtained	5,6
7	GRANCAREVO	Bileca	318	97	1.04	1280	Compressional	Sedimentary	1,2
8	HOA BINH		400	122	7.66	9450	Not Obtained	Not Obtained	4,6
9	HUNANZHEN		404	123	1.67	2060	Not Obtained	Not Obtained	4,6
10	IDUKKI		518	158	1.18	1460	Not Obtained	Not Obtained	3,4
11	JOCASSEE	Lake Jocassee	364	111	1.29	1588	Extensional/Shear	Metamorphic	1,2
12	KATSE		577	176	1.58	1950	Not Obtained	Not Obtained	4
13	Komani		407	124	1.3	1600	Not Obtained	Not Obtained	4
14	KOYNA	Shivaji Sagar Lake	328	100	2.27	2797	Shear	Igneous	1,2
15	OROVILLE	Lake Oroville	669	204	3.54	4367	Extensional	Metamorphic	1,2
16	ROI PAUL	Lake Kremasta	394	120	3.85	4750	Compressional	Sedimentary	1,2
17	SHASTA	Lake Shasta	453	138	4.66	5750	Compressional	Sedimentary	1,2
18	SRISAILAM		417	127	7.07	8722	Not Obtained	Not Obtained	4,6
19	WARRAGAMBA	Lake Burragorang	407	124	1.67	2057	Not Obtained	Sedimentary	1,6
20	WUJIANGDU		443	135	1.86	2300	Not Obtained	Not Obtained	4,6
21	HOA BINH		400	122	7.66	9450	Not Obtained	Not Obtained	4,6

Sources Key:1: Packer et al, 1979, 2: WCC Auburn Report Appendix A, 3: WCC Auburn Report Appendix B, 4: Gupta, 2002, 5: Chen and Talwani, 1998,6: ICOLD-CIGB, 2012,7: Plotnikova et al. 1992

A total of 120 reservoirs located around the world have deep or very deep water depths 300 feet deep or deeper, and have a large reservoir but not a very large reservoir (between 1×10^6 acre-feet and 8.1×10^6 acre-feet)(ICOLD-CIGB, 2012). Of these 120 reservoirs 21 cases have reported, accepted or questionable RTS. The determination of acceptable or questionable RTS was based on the classification by Packer et al 1979 and Gupta, 2002 and reservoir and depth dimensions were given by ICOLD-CIGB, 2012. Because the classification of RTS can change overtime as more data is acquired the ICOLD-CIGB report was used as the final reference. These 21 cases are presented in **Table 3**. Of those 21 cases only four are located in a compressional stress regime and one case has igneous bedrock. Therefore no cases exactly match all four reservoir parameters, as shown in **Table 2**, of the proposed Watana reservoir. However, based on the data compiled it can be gathered that the frequency of RTS is 18 percent (or 21/120) based on the depth and volume of the reservoir.

As shown in **Table 3**, Lake Shasta has the closest reservoir capacity and depth to the proposed Watana Reservoir and also lies in a compressional tectonic regime. The bedrock or geology for Lake Shasta is sedimentary whereas the bedrock at the proposed Watana Reservoir is igneous. The classification of RTS for Lake Shasta was reported as questionable in the WCC Auburn Report due to the ambiguity of the reporting of the maximum size event (reported as 3.0, Simpson, 1976). The next closest reservoir with a similar stress state would be Lake Eucumbene with a reservoir depth of approximately 348 feet (106 meters) and a reservoir volume of 4,000 acre-feet ($4,798 \times 10^6 \text{ m}^3$). The reservoir was completed in 1958, and in May of 1959 a magnitude 5 event occurred within 6 km of the reservoir. Aftershocks occurred within 12 miles (20 km) of the main event and focal depths ranged from 8 to 17 miles (12 to 27 km). The classification of RTS was reported as questionable in the WCC Auburn Report due to poor accuracy of epicenters and the correlation between impoundment and activity as not being clear.

The best match with an accepted case of RTS was observed at Tomes reservoir (Almendra Dam) in western Spain approximately 10 km from the Portuguese border. The reservoir depth is 594 feet (181 meter) which is almost an exact match to the proposed Watana reservoir (595 feet or 182 meters). The reservoir volume of Tomes, 2.15 million acre-feet, is less than half of Watana's proposed volume, 5 million acre-feet. Nonetheless, it is still an important case history with a similar depth. Almendra's Dam construction was completed in 1970 and in January of 1972 a magnitude 2.0 event was recorded (Packer et al., 1979), a magnitude of 3.2 was later reported by USSD in 1997 as referenced in ICOLD, 2011. The Tomes reservoir (Almendra Dam) is located in an area characterized by low historical seismicity (Bufo and Udias, 1979). The region is described as being seismically quiet with no tectonic movements since Miocene; from 1800 to 1970 only 6 earthquakes greater than magnitude 5 occurred within a 62 mile (100 km) radius of the dam. The dam was fitted with three seismometers and seismic monitoring was recorded between November 1971 (first filling) and March 1973. Over that time frame 181 events were recorded. During rapid filling early in 1972, microearthquake activity increased (a total of 56 events were recorded), reaching a peak 45 days after the water level peaked (**Figure 22**). The

magnitude of largest event is 3.2; the rest of them have very small magnitudes ($M < 3$) (Bufo and Udias, 1979). As the reservoir water level decreased, microseismic activity also lessened. All events were within 16 miles (25 km) of the dam and most were adjacent to or under the reservoir and had very shallow focal depths. Although the period of microearthquake monitoring is limited, the study by Bufo and Udias (1979) indicates a strong correlation between the impoundment of the Almendra (Tomes) reservoir and microearthquake activity.

Case histories can give a general idea of what types of events happened after impoundment of similar reservoir depths and volumes, however if RTS were to occur at the proposed reservoir, it cannot be assumed the results would be comparable.

5.1.1 Calculation of Likelihood of Occurrence

The likelihood of occurrence performed in the WCC (1982) study looked at four parameters or reservoir attribute states to statistically calculate the probability of RTS. This work was based on the methodology developed by Baecher and Keeney (1982). Baecher and Keeney (1982) completed a statistical examination on deep, very deep, and very large reservoirs, and considering those reservoirs with RTS. In order to complete their study, the authors gathered information on all dams that fell within the deep, very deep, or very large reservoir (234 in total) and each of the five reservoir attributes were recorded. This compilation performed by Baecher and Keeney (1982) took several person years of effort to complete. Four of the five parameters were used in the WCC (1982) study: depth, volume, stress state and geology, as shown in **Table 1**. Two data sets were evaluated: 1) a data set that included reservoirs that were deep, very deep or very large, and 2) a data set that included reservoirs that were deep or very deep. The second subset (deep or very deep reservoirs) of data was chosen for the study presented herein because the proposed reservoir is not very large. The same approach was used for the evaluation performed by Baecher and Keeney (1982) for Auburn dam which had similar dimensions as the new proposed Watana reservoir. The definitions for reservoir attribute states from Baecher and Keeney (1982) are presented in **Table 4** below.

Table 4 Definitions for Reservoir Attribute States

Attribute	State			
	1	2	3	4
Depth	d ₁ very deep(over 150m [492 feet])	d ₂ deep(92 to 150m [302 to 492 feet])	d ₃ shallow(less than 92m [302 feet])	d ₄ not known
Volume	v ₁ very large(over 100 x 10 ⁸ m ³ [8.11x10 ⁶ acre-feet])	v ₂ large(12 to 100 x 10 ⁸ m ³ [8.11 x10 ⁶ to 9.73 x 10 ⁵ acre-feet])	v ₃ small(less than 12 x 10 ⁸ m ³ [9.73 x 10 ⁵ acre-feet])	v ₄ not known
Stress State	s ₁ extensional	s ₂ compressional	s ₃ shear	s ₄ not known
Fault Activity	f ₁ active fault	f ₂ no active faults present	f ₃ not known	
Geology	g ₁ sedimentary	g ₂ metamorphic	g ₃ igneous	g ₄ not known

Source: Baecher and Keeney, 1982

Notes: The abbreviations used in the table are: d, depth; v, volume; s, stress state; f, fault activity; g, geology.

A comparison using the statistical examinations completed by Baecher and Keeney (1982) will be computed for the new proposed Watana Reservoir using the reservoir attributes of depth, volume, stress state, geology and fault activity. This will also include a comparison to the previous work performed by WCC (1982), which assumed a much larger reservoir (no longer proposed, combined Watana and Devil Canyon reservoirs, see **Table 1**). Finally, an updated assessment will be performed for the new proposed reservoir considering only two reservoirs attributes (depth and volume), Table 2 shows the current configuration . The maximum water depth of the proposed configuration was calculated using the maximum water elevation minus the elevation of the reservoir prior to filling (595 feet, El. 2050-1455). MatSu LiDAR was used to determine the elevation of the reservoir prior to filling. Computations will be based on the current compilation of RTS and newly built dams performed for this study.

Two types of statistical analyses were completed: 1) the probability of RTS was calculated considering only one attribute (single attribute), and 2) the probability of RTS was calculated using a multi-attribute analysis, where more than one attribute was considered. Due to the correlation between depth and volume of a reservoir the multi-attribute analysis included three separate models (Baecher and Keeney, 1982, Table 6). These models are as follows: independent discrete case, dependent discrete case and the dependent mixed (discrete / continuous) case. The independent discrete case considers each of the attributes are completely independent (no correlation). The dependent discrete case is based on the correlation between discrete depth and volume. The dependent mixed case is based on the correlation between continuous depth and volume and the other states (stress state, faulting and geology) are independent discrete.

5.1.1.1 Single Attribute Analysis

The single attribute analysis looks at the conditional probability of RTS given only one reservoir attribute (depth, volume, stress state, fault activity or geology). This analysis assumes that the attributes

are independent of each other. The results are presented based on the deep or very deep reservoir criteria, as used in WCC (1982). **Table 5** summarizes single attribute analysis for the previous study with data gathered up until 1982. **Table 6** shows how the data was binned into depth and volume categories for the current study. For example, five (5) reservoirs fell into the d_1 : very deep (over 492 feet or 150 m) and v_1 : very large (over 8.11×10^6 acre-feet or $100 \times 10^8 \text{ m}^3$) or the d_1v_1 bin. **Table 7** is a summary of the RTS and non-RTS date for each state. **Table 8** shows the results of the single attribute analysis for the current study with data gathered up until 2012. The calculation sheet provides additional data on the equations used to perform the calculations. The updated current study does not include the stress state, fault activity or the geology; therefore only depth and volume are shown. The results are summarized in **Tables 5** and **6** below.

Table 5 Single Attribute Analysis – Conditional Probability of RTS Given Only One Attribute

Attributes	State (correlates to reservoir state as shown in Table 4)		
	1	2	3
Depth	0.27 [0.24]	0.11 [0.10]	0.00
Volume	0.25 [0.22]	0.23 [0.21]	0.09 [0.07]
Stress State	0.11	0.14	0.17
Fault Activity	0.20	0.0	-
Geology	0.20	0.10	0.12-

Source: Baecher and Keeney, 1982. Round off errors were identified, but not revised, see brackets for reported values.

Table 6 Data Bins for Deep or Very Deep Dataset – Current Study

RTS				Non-RTS			
d1	5	6	6	d1	8	21	25
d2	10	15	11	d2	20	78	259
d3	0	0	0	d3	0	0	0
	v1	v2	v3		v1	v2	v3
d ₁ very deep(over 150m [492 feet])				v ₁ very large(over 100 x 10 ⁸ m ³ [8.11x10 ⁶ acre-feet])			
d ₂ deep(92 to 150m [302 to 492 feet])				v ₂ large(12 to 100 x 10 ⁸ m ³ [8.11 x10 ⁶ to 9.73 x 10 ⁵ acre-feet])			
d ₃ shallow(less than 92m [302 feet])				v ₃ small(less than 12 x 10 ⁸ m ³ [9.73 x 10 ⁵ acre-feet])			

Table 7 Summary of RTS and Non-RTS Data for each State

	Number of Reservoirs	State		
		1	2	3
RTS Data				
Depth	53	17	36	0
Volume	53	15	21	17
Non-RTS Data				
Depth	411	54	357	0
Volume	411	28	99	284

Source: MWH (2013) From deep or very deep dataset. Total number of reservoirs 464.

Table 8 Revised Single Attribute Analysis – Conditional Probability of RTS Given Only One Attribute - Current Study

Attributes	State (correlates to reservoir state as shown in Table 4)		
	1	2	3
Depth	0.24	0.09	-
Volume	0.35	0.18	0.06

The single attribute analysis for the proposed Watana Reservoir configuration has a Depth State of 1 (d_1) and a Volume State of 2 (v_2). This means that the conditional probability of RTS given only the depth attribute would have a probability of RTS of about 24 percent (24 percent based on previous analysis). Considering only the volume attribute would have a conditional probability of RTS of approximately 18 percent (21 percent based on previous analysis). In the previous work completed by Baecher and Keeney (1982), the depth was the most discriminating and then volume. This analysis shows that the volume is the most discriminating factor. The current analysis included a total of 464 dams, whereas the study performed by Baecher and Keeney (1982) only included 199 dams. Baecher and Keeney (1982) also noted that results depend on current understanding of the historical record and, as that understanding changes (potentially resulting in a reassignment of RTS), the results of these statistical analyses could change as more data is gathered.

5.1.1.2 Multi-Attribute Analysis

Independent discrete, dependent discrete and dependent mixed (discrete / continuous) cases were calculated using a multi-attribute analysis. The first analysis, independent discrete, calculates the probability of RTS assuming independence between the attributes. The second analysis, dependent discrete, calculates the probability of RTS based on correlations between discrete volume and depth. The third analysis, dependent mixed case, is based on the correlation between continuous depth and volume and the other states (stress state, faulting and geology) are independent discrete.

In the work completed by Baecher and Keeney (1982), the likelihood if all five attributes were to occur (depth, volume, stress state, faulting and geology) was evaluated. The analysis for the study performed by MWH (2013) only considered two of the attributes, depth and volume; the other attributes were assumed to have a probability of one. The results for the multi-attribute analyses are shown in Tables 9a and 9b and discussed in the following subsections. Table 9a is based on the currently proposed dam and reservoir configuration and Table 9b is based on the previously proposed configuration.

A sensitivity analysis was performed to gain some insight to the range of probabilities that could be expected if the geology changed from igneous to metamorphic and if the fault activity were considered to be active. Calculations were performed for each of the three cases.

Table 9a Comparison of Previous and Current Probabilities of RTS using a Multi-attribute Analysis – Independent and Dependent Discrete –Currently Proposed Configuration

Attributes Considered	Previous Work by Baecher and Keeney (1982) – Proposed Watana Reservoir			Current Work-Proposed Watana Reservoir		
	Independent	Dependent Discrete	Dependent Mixed	Independent	Dependent Discrete	Dependent Mixed
Depth = 595 feet (182 meters) Volume = 5.2 x10 ⁶ acre-feet (6,377 x10 ⁶ m ³) Stress State = Compressive Geology = Igneous Fault Activity = Not Considered	0.36	0.18	0.36	NA	NA	NA
Depth = 595 feet (182 meters) Volume = 5.2 x10 ⁶ acre-feet (6,377 x10 ⁶ m ³) Stress State = Compressive Geology = Igneous Fault Activity = Active	0.46	0.25	0.46	NA	NA	NA
Depth = 595 feet (182 meters) Volume = 5.2 x10 ⁶ acre-feet (6,377 x10 ⁶ m ³) Stress State = Compressive Geology = Metamorphic Fault Activity = Not Considered	0.33	0.16	0.33	NA	NA	NA
Depth = 595 feet (182 meters) Volume = 5.2 x10 ⁶ acre-feet (6,377 x10 ⁶ m ³) Stress State = Compressive Geology = Metamorphic Fault Activity = Active	0.42	0.23	0.43	NA	NA	NA
Depth = 595 feet (182 meters) Volume = 5.2 x10 ⁶ acre-feet (6,377 x10 ⁶ m ³)	0.41	0.21	0.41	0.34	0.22	0.37

Table 9b Comparison of Previous and Current Probabilities of RTS using a Multi-attribute Analysis – Independent and Dependent Discrete – Previously Proposed Configuration

	Previous Work by Baecher and Keeney (1982) – Old Reservoir		
Attributes Considered	Independent	Dependent Discrete	Dependent Mixed
Depth = 725 feet (221 meters) Volume = 10.67 x10 ⁶ acre-feet (13,172 x10 ⁶ m ³) Stress State = Compressive Geology = Igneous Fault Activity = Not Considered	0.37*	0.33	0.93
Depth = 725 feet (221 meters) Volume = 10.67 x10 ⁶ acre-feet (13,172 x10 ⁶ m ³) Stress State = Compressive Geology = Igneous Fault Activity = Active	0.48	0.43	0.95
Depth = 725 feet (221 meters) Volume = 10.67 x10 ⁶ acre-feet (13,172 x10 ⁶ m ³) Stress State = Compressive Geology = Metamorphic Fault Activity = Not Considered	0.35	0.30	0.92
Depth = 725 feet (221 meters) Volume = 10.67 x10 ⁶ acre-feet (13,172 x10 ⁶ m ³) Stress State = Compressive Geology = Metamorphic Fault Activity = Active	0.45	0.39	0.95
Depth = 725 feet (221 meters) Volume = 10.67 x10 ⁶ acre-feet (13,172 x10 ⁶ m ³)	0.43	0.38	0.94

* As presented in WCC, 1982. It should also be noted that the previous configuration had a maximum reservoir at elevation 2185, whereas the current proposed configuration has a maximum reservoir at elevation 2050.

5.1.2 Independent Discrete Results

The results of the previous work for Susitna (very deep and large reservoir) included the four attributes – depth, volume, stress state, and geology – and the probability for these four attributes was 37 percent (WCC, 1982). Using the previous database developed by Baecher and Keeney (1982) and the same four attributes, the newly proposed reservoir’s probability of RTS was estimated to be about 36 percent. Finally, using the new database and considering only attributes of depth and volume, the probability of RTS was calculated to be about 34 percent; this can be compared to the probability calculated using the old database for the proposed reservoir of about 41 percent.

A sensitivity analysis was performed holding the known parameters, depth, volume, stress state constant and varying the geology and fault activity. The results show that for the proposed dam the classification of geology from igneous to metamorphic would decrease the probability of RTS from 0.36 to 0.33. However, if the fault activity is considered to be active then the probabilities increase about 10 percent. The classification of geology as igneous and fault activity as active is the highest probability 46 percent, whereas the classification of geology as metamorphic and activity of faults as “not considered” would be about 33 percent.

5.1.3 Dependent Discrete Results

The dependent discrete cases for the newly proposed reservoir with the Baecher & Keeney database show that the results are about 50 percent lower than the independent discrete results. Again we see the same trend in lower probabilities for the igneous geology and when the fault activity is not considered. Using only the attributes of depth and volume, the dependent discrete results considering the old database for the proposed reservoir were estimated to have a probability of RTS of about 21 percent. This can be compared to the evaluation performed using the new database, which resulted in a probability of RTS of approximately 22 percent.

5.1.4 Dependent Mixed Results

The dependent mixed cases for the newly proposed reservoir with the Baecher & Keeney database show that the results are the same as the independent discrete analysis (41 percent). In comparison, the current work for the proposed reservoir increases about 3 percent (34 to 37 percent) when comparing the independent to the dependent mixed for the specific case only considering depth and volume.

5.2 Empirical Approach Results

Based on the newly developed database the empirical results show a decrease in the likelihood of RTS occurring at the reservoir site in two of the three models considered; this is most likely due to the increase in the amount of deep and very deep dams (greater than 92 meters but less than 150 meters

[greater than 302 feet but less than 492 feet]) without reported RTS. Overall, the probability calculations for the proposed Watana reservoir fall between 16 to 46 percent; this is explainably much lower than the previously proposed configuration that was about 160 feet higher and more than double the reservoir volume (30 to 95 percent). The lowest probability of RTS would be 16 percent from the old dataset for the dependent discrete case, where the geology was classified as metamorphic and the fault activity is not considered. The highest probability of RTS (46 percent) is also from the old database for the independent or dependent mixed cases, where the geology is classified as igneous and the fault activity is considered to be active.

Based upon an evaluation and application of the historical and current datasets for RTS and non-RTS reservoirs, it is concluded that the probability of RTS at the proposed Watana Reservoir is in the range 16 to 46 percent. These probabilities do not consider the magnitude or significance of the induced events, but only reflect a probability that some RTS may occur.

Every effort was made to insure the accuracy of the data, but errors or omissions are possible. These results should be used with caution as the likelihoods are very sensitive to changes in data classification (i.e. determination of RTS). This study varies from the previous by using all events with reported RTS in the calculations. If the classifications were changed to use only those events with accepted RTS the results could be different.

The potential maximum magnitude of an RTS event is difficult to estimate. The largest accepted event within the empirical database is 6.5 and most events are less than magnitude 4. Based on empirical data and understanding at the time, Allen (1982) suggested that a reasonable maximum event for RTS should be about magnitude 6.5. Similarly, ICOLD (2011) recommends consideration of a maximum magnitude of 6.3. However, uncertainty in a maximum magnitude estimate based on the empirical approach arises due to the differing conclusions of prior investigators on whether events such as Wenchuan may have been induced or triggered.

6.0 RECOMMENDATIONS FOR ADDITIONAL STUDIES

This section presents recommendations for additional studies to further explore and evaluate the potential range in plausible RTS. The approach recommended is to further assess the size of and potential for an RTS event by synthesizing geologic field investigations, seismological analysis, deterministic ground motion analyses of RTS vs. natural earthquakes, and stress modeling. Specifically, additional studies recommended to refine the potential for and size of an RTS event include: 1) analysis of seismological data from the recently installed Watana seismic network in order to determine the local stress field and possibly identify favorable orientations to re-active features; 2) integration with planned field studies to further define the characteristics of faults and fracture systems within the reservoir

vicinity to constrain estimates of fault geometry and hydraulic parameters; 3) preliminary Coulomb stress modeling to build and test physical models that combine loading of the crust from reservoir impoundment with pore pressure changes at depth; and 4) development of deterministic ground motions from the dominant naturally occurring earthquake to provide upper bounding ground motions to which various RTS magnitude-distance scenarios can be compared. These are described in the sections below.

6.1 Seismic Monitoring and Seismological Analysis

Seismic monitoring in the vicinity of the reservoir is a necessary task for analyzing pre and post-impoundment seismicity. An improved instrumentation program has been implemented through the University of Alaska whereby several stations in the vicinity of the dam site and reservoir area have been integrated into their larger regional network and seismicity occurring in the dam and reservoir region will be monitored and analyzed on a regular basis. Analyses will include examination of spatial and seismicity rate patterns in light of RTS cases observed worldwide. In particular, seismicity variations associated with changes in filling and drawdown rates, as was observed at Nurek, Kazakhstan will be looked at once reservoir operations begin.

High quality earthquake data will permit more advanced seismological analyses such as inversion for 3-D velocity structure to expedite more accurate hypocenter locations, focal mechanism analysis and local stress orientations, and possible identification of faults in the vicinity of the reservoir.

Specific tasks should include investigation of accurately located shallow crustal seismicity in the site and reservoir area seen in **Figures 15 and 17**. Development of single or composite focal mechanisms from this seismicity may be critical in determining the tectonic stress orientation near the site.

6.2 Coulomb Stress Modeling

It is recommended that preliminary Coulomb stress modeling be performed. Studies of this type have become an accepted technique for quantitatively analyzing stress changes, and resulting seismicity, due to reservoir operations.

Measurements of rock mechanical and hydraulic parameters obtained as part of the geotechnical data collection program will be helpful in constraining these values in a Coulomb stress model. Such measurements should include parameters such as permeability, and joint density and orientation, at locations in the reservoir area as well as at the dam site. The model can be refined in the future, when and if improved knowledge of subsurface fault structures becomes available through seismicity analysis, geologic field studies, and structural analysis of surficial geologic features.

6.3 Local Geologic Field Investigations

Because RTS events are most likely to occur on faults favorably oriented to the local stress field, it is important that 1) local faults, and 2) the local stress field, be identified to the best of our ability. Identification of local faults requires detailed field studies focused on gathering structural and kinematic data from faults, and geomorphic analyses. Evaluation of stress fields requires further analysis, similar to that shown in **Figure 19**, but focusing on the vicinity of the Watana Reservoir. Focal mechanism analysis of local earthquakes as part of the seismological analysis will play a key role in this characterizing the local stress field.

Although permeability and fracture and joint analyses have been conducted in the local Watana site area, most of the measurements were made in rock types that will underlie a small percentage of the reservoir area. No such measurements or observations have been made upstream of the site. Although such drilling activities at representative sites in the entire reservoir area may be impractical, reconnaissance field investigations can resolve questions such as what rock types exist upstream, the characteristics of significant faults, and whether the joint pattern seen at the Watana and Devil Canyon sites persists along the entire reservoir length.

6.4 Estimation of Maximum Magnitude of a RTS Event

ICOLD (2011) recommends a maximum RTS magnitude of 6.3, and Allen (1981) recommends magnitude 6.5. These were based on consideration of the largest RTS events observed worldwide from empirical data, and did not consider the potential for more recent events, such as Wenchuan to be included as potential RTS events.

FCL (2012) set the upper limit to background seismicity (i.e., that not associated with an identified fault) as Mw 7.3, based on U.S. Geological Survey estimates from Wesson et al. (2007). This value is designed to account for the fact that the shallow seismogenic crust in central Alaska can be thick (20+ km), the region is a tectonically active area, and surface or hidden faults that are capable of producing such magnitudes may not have been identified. Thus, it is a relatively high earthquake magnitude value and may not necessarily be the final maximum RTS magnitude evaluated, chiefly because the fault source and characterization studies for the dam site are not yet completed.

Physical concepts would link the occurrence and magnitude of potential RTS events to the tectonic stress and characteristics of faults in the area of reservoir influence. Thus, reservoirs transected by faults which may be subject to RTS would be considered to have maximum RTS events which reflect potential maximum events on these nearby faults or other identified seismic sources. For the Watana site, no faults have been identified in the reservoir area with Quaternary displacement from the ongoing studies, but regional seismic source models do allow for potential earthquakes much larger than magnitude 6.3 or 6.5 as suggested from empirical data by ICOLD (2011) and Allen (1982).

Refinement of the local maximum RTS event for the Watana site should include specific information on the local geologic structures and potential seismic sources that may exist in the RTS Zone (encompassing regions within 30 km of the reservoir). This would include consideration of whether geologic structures are favorably oriented to the current tectonic stress field as well as consideration of the geometry (fault location, length, and dip) with respect to the reservoir and dam site.

6.5 Empirically-based Analysis

As additional data regarding RTS cases are gathered, the inputs of the empirically-based analyses should be revised. Revisions may include stress state, geology, and fault activity. No specific recommendations on gathering this data are suggested. However, during the proposed local geological field investigations and seismological analysis the stress state, geology and fault activity will be further refined and the study should be updated to reflect this.

6.6 Deterministic Comparisons to the Largest non-RTS Earthquake

For a deterministic assessment, comparisons can be made between deterministic ground motions from RTS magnitude-distance scenarios and the dominant natural earthquake in the preliminary seismic source model. In other words, it is possible that the dam will ultimately be designed to withstand earthquake ground motions greater than those from the expected maximum RTS event. From the FCL (2012) preliminary seismic source model, this is currently a Mw 7.5 intraslab event about 31 miles (50 km) beneath the site. Deterministic response spectra from the dominant natural earthquake may be large enough to supersede all but very conservative RTS magnitude assessments. It is possible that certain RTS magnitude-distance scenarios developed under Recommendations 6.2, 6.3, and 6.4 above may be eliminated on the basis of being exceeded by ground motions from the dominant naturally occurring design earthquake.

7.0 SUMMARY AND CONCLUSIONS

RTS is a phenomenon that is accepted by the scientific community but is not well understood, and difficult to predict. Both empirical and physical modeling approaches were discussed in this document. Both approaches should be employed to further assess the potential for RTS.

An update to the previous empirically-based probability analysis computed by WCC (1982) was performed. The results show that the probability of RTS occurring at the proposed Watana reservoir, using the new proposed depth of 595 feet and volume of 5.2×10^6 acre-feet, range between 16 to 46 percent; this is lower than the previously proposed project configuration that was about 160 feet higher and more than double the reservoir volume (probabilities range from 30 to 95 percent). The lowest probability of RTS would be 16 percent from the old dataset for the dependent discrete case, where the

geology was classified as metamorphic and the fault activity is not considered. The highest probability of RTS (46 percent) is also from the old database for the independent or dependent mixed cases, where the geology is classified as igneous and the fault activity is considered to be active. Only considering the attributes of depth and volume and using an updated database from the 1980s the probability of RTS was calculated to be between 22 and 36 percent. The lowest probability is for the dependent discrete at 22 percent and the highest is for the dependent mixed case at 36 percent. These results for the currently proposed reservoir configuration are lower than previous analyses. These results may be attributed to: the somewhat shallower and lower volume of the presently proposed reservoir compared to the 1980s dual impoundment configuration; the increased number of large impounded reservoirs since the 1980s that have not experienced RTS; and improvements in the understanding of physical RTS mechanisms.

The location and magnitude of any future RTS events associated with the Watana Reservoir are highly uncertain. Most empirical data suggest that most RTS events will have relatively small magnitudes and would most likely occur within 10 years of initial filling. ICOLD (2011) and Allen (1982) suggest that maximum RTS magnitudes may be on the order of 6.3 and 6.5, respectively. Other investigators (e.g., Klose, 2011; Ge et al., 2009) have proposed that the Mw 7.9 Wenchuan earthquake should be considered as an RTS event, which would increase the magnitude estimates from empirical data. In contrast, other investigators (e.g., Zhou et al., 2010; Galahut and Galahut, 2010) have argued that this event could not have been triggered by the reservoir. Although the Wenchuan earthquake was included in the updated empirical analysis as a “questionable” case, its status as an RTS event is controversial. For conservatism “questionable” cases were chosen to be included in the RTS empirical analysis. Although in this report judgment has been withheld on its status, future research on this event will continue to be monitored.

The mapping of existing faults and fractures within and near the reservoir, regional hydraulic conductivity surrounding these faults, and regional tectonic stress provide the physical constraints which determine potential RTS locations and the physical limits for earthquake magnitudes. From existing seismic hazard studies, a possible maximum can be Mw 7.3, defined in prior hazard studies to be the largest crustal event that could randomly occur in the region. This is a conservative estimate, made in consideration of no prior knowledge of seismogenic crustal thickness, hydraulic properties of rocks beneath the reservoir, orientation of the local tectonic stress field, and the possible existence of local faults in the vicinity of the reservoir that may be favorably oriented to the local stress field. Further evaluations of these factors will provide a basis for refinement of the site-specific conclusions for the Watana site.

8.0 REFERENCES

- Acres America Inc. (1981). Susitna Hydroelectric Project, 1980-1981 Geotechnical Report, vol. 1, Final Draft.
- Acres America Inc. (1982). Susitna Hydroelectric Project, Feasibility Report.
- AEIC (2013). Susitna-Watana Seismic Monitoring Project, August-December 2012 Quarterly Report, AEIC-11-0001-022813.
- Allen, C.R. (1982), Reservoir-induced seismicity and public policy, California Geology, November, 248-250.
- Anglin, F. M., and Buchbinder, G. G. (1985). Induced seismicity at the LG3 Reservoir, James Bay, Quebec, Canada. *Bulletin of the Seismological Society of America*, 75(4), 1067-1076.
- Baecher, G. B., and Keeney, R. L. (1982). Statistical Examination of Reservoir-Induced Seismicity. *Bulletin of the Seismological Society of America*, 72(2), 553-569.
- Beck, J. L. (1976). Weight-induced stresses at the recent seismicity at Lake Oroville, California. *Bulletin of the Seismological Society of America*, 72(2), 1121-1131.
- Bell, M. L., and Nur, A. (1978). Strength changes due to reservoir-induced pore pressure and stresses an application to Lake Oroville, *Journal of Geophysical Research*, 83, 4469-4483.
- Bolt, B. A., and Cloud, W. K. (1974). Recorded strong motion on the Hsifengkiang dam, China. *Bulletin of the Seismological Society of America*, 64(4), 1337-1342.
- Bufo, E., and Udias, A. (1979). A note on induced seismicity in dams and reservoirs in Spain. *Bulletin of the Seismological Society of America*, 69(5), 1629-1623.
- Carder, D. S. (1945). Seismic Investigations in the Boulder Dam Area 1940-44 and the Influence of Reservoir Loading on Local Earthquake Activity. *Bulletin of Seismological Society America*, 35(4), 175-192.
- Chen, L., & Talwani, P. (1998). Reservoir-induced Seismicity in China. *Pure and Applied Geophysics*, 133-149.
- Chen, L., and Talwani, P. (2001a). Mechanism of initial seismicity following impoundment of the Monticello Reservoir South Carolina. *Bulletin of the Seismological Society of America*, 91(6), 1582-1594.

-
- Chen, L., and Talwani, P. (2001b). Renewed seismicity near Monticello Reservoir, South Carolina. *Bulletin of the Seismological Society of America*, 91(1), 94-101.
- Csejtey, B., Jr., Nelson, W.H., Hones, D.L., Silberling, N.J., Dean, R.M., Morris, M.S., Lanphere, M.A., Smith, J.G., and Silberman, M.L. (1978). Reconnaissance geologic map and geochronology, Talkeetna Mountains quadrangle, northern part of Anchorage quadrangle, and southwest corner of Healy quadrangle: Alaska U.S. Geological Survey, Open-File Report 78-558A, 60 p.
- Csejtey, B., D.P. Cox, R.C Evarts, G.D.Stricke , and H.L.Foster (1982). The Cenozoic Denali fault system and the Cretaceous accretionary development of southern Alaska, *Journal of Geophysical Research*, v. 87, no. B5, p. 3741–3754.
- Dahm, T. E. and 12 others (2012). Recommendation for the discrimination of human-related earthquakes. *Journal of Seismology*, DOI 10.1007/s10950-012-9295-6.
- Deng, K., S. Zhou, R. Wang, R. Robinson, C. Zhao, and W. Cheng (2010). Evidence that the 2008 Mw 7.9 Wenchuan Earthquake Could Not Have Been Induced by the Zipingpu Reservoir, *Bulletin of the Seismological Society of America*, 100(5b), 2805-2814.
- Denlinger, R. P., and C. G. Bufe (1982). Reservoir conditions related to induced seismicity at The Geysers steam reservoir, Northern California. *Bulletin of the Seismological Society of America*, 72(4), 1317-1327.
- do Nascimento, A. F., Lunn, R. J., and Cowie, P. A. (2005). Modeling the heterogenous hydraulic properties of faults using constraints from reservoir-induced seismicity. *Journal of Geophysical Research*, 110(B09201), 17.
- Ferreira, J. M., De Oliveria, R. T., Assumpcao, M., Moreira, J. A., Pearce, R. G., and Takeya, M. K. (1995). Correlation of seismicity and water level in the Acu reservoir --An example from northeast Brazil. *Bulletin of the Seismological Society of America*, 85(5), 1483-1489.
- Fletcher, J. B. (1982). A comparison between the tectonic stress measured in situ and stress parameters from induced seismicity at Monticello Reservoir, South Carolina. *Journal of Geophysical Research*, 87(B8), 6931-6944.
- Fletcher, J. B., Boatwright, J., and Joyner, W. B. (1983). Depth dependence of source parameters at Monticello, South Carolina. *Bulletin of the Seismological Society of America*, 73(6), 1735-1751.
- Fugro Consultants, Inc. (FCL) (2012). *NPT 6: Seismic Studies, Draft Technical Memorandum*.

- Galahut, K., and V.K. Galahut (2010). Effect of the Zipingpu reservoir impoundment on the occurrence of the 2008 Wenchuan earthquake and local seismicity, *Geophysical Journal International* , doi: 10.1111/j.1365-246X.2010.04715.x.
- Ge, S., M. Liu, N. Lu, J. Godt, and G. Luo (2009), Did the Zipingpu Reservoir trigger the 2008 Wenchuan earthquake?, *Geophysical Research Letters*, Vol. 36, L20315, doi:10.1029/2009GL040349.
- Ge, S. (2011). Comment on “Evidence that the 2008 Mw 7.9 Wenchuan Earthquake Could Not Have Been Induced by the Zipingpu Reservoir” by Kai Deng, Shiyong Zhou, Rui Wang, Russell Robinson, Cuiping Zhao, and Wanzheng Cheng, *Bulletin of the Seismological Society of America*, 101(6), 3117-3118.
- Glen, J.M.G., Schmidt, J., Pellerin, L., McPhee, D.K., and O’Neill, J.M. (2007a). Crustal structure of Wrangellia and adjacent terranes inferred from geophysical studies along a transect through the northern Talkeetna Mountains, in Ridgway, K.D., Trop, J.M., Glen, J.M.G., and O’Neill, J.M., eds., *Tectonic Growth of a Collisional Continental Margin: Crustal Evolution of Southern Alaska: Geological Society of America Special Paper 431*, p. 21–41.
- Glen, J.M.G., Schmidt, J., and Morin, R. (2007b). Gravity and magnetic character of southcentral Alaska: Constraints on geologic and tectonic interpretations, and implications for mineral exploration, in Ridgway, K.D., Trop, J.M., Glen, J.M.G., and O’Neill, J.M., eds., *Tectonic Growth of a Collisional Continental Margin: Crustal Evolution of Southern Alaska: Geological Society of America Special Paper 431*, p. 593–622.
- Gough, D. K. and W. I. Gough (1970). Stress and deflection in the lithosphere near Lake Kariba--1, *Geophys.J.* 21, 65-78.
- Gupta, H. K. (1983). Induced seismicity hazard mitigation through water level manipulation at Koyna, India: a suggestion. *Bulletin of the Seismological Society of America*, 73(2), 679-682.
- Gupta, H. K. (1992). Are RIS events of $M \geq 5$ preceded by a couple of foreshocks of $M \geq 4$?, *Bulletin of the Seismological Society of America*, 82(1), 517-520.
- Gupta, H. K., Rastogi, B. K., and Narain, H. (1972). Common Features of the Reservoir-Associated Seismic Activities. *Bulletin of the Seismological Society of America*, 62(2), 481-492.
- Gupta, H. K., and Iyer, H. M. (1984). Are reservoir-induced earthquakes of magnitude ≥ 5.0 at Koyna, India, preceded by pairs of earthquakes ≥ 4.0 ? *Bulletin of the Seismological Society of America*, 74(3), 863-873.

- Gupta, H. K., and Rajendran, K. (1986). Large artificial water reservoirs in the vicinity of the Himalayan foothills and reservoir-induced seismicity. *Bulletin of the Seismological Society of America*, 76(1), 205-215.
- Gupta, H. K. (2002). A review of recent studies of triggered earthquakes by artificial water reservoirs with special emphasis on earthquakes in Koyna, India. *Earth-Science Reviews*, 58 , 279–310.
- Haeussler, P.J. (2008). An overview of the neotectonics of interior Alaska—Far-field deformation from the Yakutat Microplate collision, in Freymueller, J.T., Haeussler, P.J., Wesson, R.L., and Ekstrom, Goran, eds., 2008, Active tectonics and seismic potential of Alaska: American Geophysical Union, Geophysical Monograph 179, p. 83–108.
- Hartzell, S., C Mendoza, L. Ramirez-Guzman, Y. Zeng, and W. Mooney (2013). Rupture History of the 2008 Mw 7.9 Wenchuan, China, Earthquake: Evaluation of Separate and Joint Inversions of Geodetic, Teleseismic, and Strong-Motion Data, *Bulletin of the Seismological Society of America*, 103(1), 353–370.
- Harza-Ebasco (1984), 1984 Geotechnical Exploration Program Watana Damsite, Document no. 1734, Final Report.
- Hickman, S., and M.D. Zoback (1982). In Situ Study of the Physical Mechanisms Controlling Induced Seismicity at Monticello Reservoir, South Carolina. *Journal of Geophysical Research*, 87(B8), 6959-6974.
- Houquin, C., Zeping, X., and Ming, L. (2010). The Relationships between Large Reservoirs and Seismicity. *Water Power Magazine*, 29-33.
- ICOLD (2011). Committee on Seismic Aspects of Dam Design, *Reservoirs and Seismicity - State of Knowledge- Bulletin 137*.
- ICOLD (2010). Committee on Seismic Aspects of Dam Design. *Selecting Seismic Parameters for Large Dams - Guidelines*. Bulletin 72.
- Jacob, K. H., Pennington, W. D., Ambruster, J., Seeber, L., and Farhatulla, S. (1979). Tarbela Reservoir, Pakistan: a region of compressional tectonics with reduced seismicity upon initial reservoir filling. *Bulletin of the Seismological Society of America*, 69(4), 1175-1192.
- Jaeger, J.C., and N. Cook (2007), Fundamentals of Rock Mechanics, Chapman and Hall, Ltd.
- Kalpna, & Chander, R. (1997). On some microearthquakes near Tarbela Reservoir during three low water stands. *Bulletin of the Seismological Society of America*, 8(1), 265-271.

- Keith, C. M., Simpson, D. W., and Soboleva, O. V. (1982). Induced seismicity and style of deformation at Nurek Reservoir, Tadjik SSR. *Journal of Geophysical Research*, 87(B6), 4609-4624.
- Klose, C. D. (2011). Evidence for Anthropogenic Surface Loading as Trigger Mechanism of the 2008 Wenchuan Earthquake Environmental Earth Sciences DOI 10.1007/s12665-011-1355-7.
- Klose, C. D. (2012). Mechanical and statistical evidence of the causality of human-made mass shifts on the Earth's upper crust and the occurrence of earthquakes. *Journal of Seismology*, DOI 10.1007/s10950-012-9321-8.
- Lahr, K. M., Lahr, J. C., Lindh, A. G., Bufe, C. G., & Lester, F. W. (1976). The August 1975 Oroville earthquakes. *Bulletin of the Seismological Society of America*, 66(4), 1085-1099.
- Lamontagne, M., Hammamji, Y., and Peci, V. (2008). Reservoir-triggered seismicity at the Toulmoustouc hydroelectric project, Quebec Northshore, Canada. *Bulletin of the Seismological Society of America*, 98(5), 2543-2552.
- Langston, C. A., and Franco-Spera, M. (1985). Modeling of the Koyna, India aftershock of 12 December 1967. *Bulletin of the Seismological Society of America*, 75(3), 651-660.
- Lara, J. M. and J. I. Sanders (1970). The 1963-1964 Lake Mead Survey, *Bur. Reclamation Rep. REC-OCE-70-21*, 174 pp.
- Leblanc, G., and Anglin, F. (1978). Induced seismicity at the Manic 3 reservoir, Quebec. *Bulletin of the Seismological Society of America*, 68, 1469-1485.
- Lei, X. (2008). Possible roles of the Zipingpu Reservoir in triggering the 2008 Wenchuan earthquake, *Journal of Asian Earth Sciences*, 40, 844-854.
- Liu, Y., Zhu, C., Wang, C., Lu, R., and Chen, J. (1982). Modeling focal parameters for the magnitude 5.3 earthquake of the Xingengjiang reservoir area, People's Republic of China. *Bulletin of the Seismological Society of America*, 72(4), 1085-1092.
- Mandal, P., Rastogi, B. K., and Sarma, C. S. (1998). Source Parameters of Koyna earthquakes, India. *Bulletin of the Seismological Society of America*, 88(3), 833-842.
- Marion, G. E., and Long, L. T. (1980). Microearthquakes spectra in the southeastern United States. *Bulletin of the Seismological Society of America*, 70(4), 1037-1054.
- McGarr, A. (1976). Seismic moments and volume changes. *Journal of Geophysical Research*, 81, n8, 1487-1494.

- McGarr, A., Simpson, D. (1997). Keynote lecture: A broad look at induced and triggered seismicity, “Rockbursts and seismicity in mines”. In: Gibowicz, S.J., Lasocki, S. (Eds.), Proc. of 4th Int. Symp. On Rockbursts and Seismicity in Mines, Poland, 11–14 Aug, 1997. A.A. Balkema, Rotterdam, pp. 385–396.
- Mekkawi, M., Grasso, J. R., & Schnegg, P. A. (2004). A long-lasting relaxation of seismicity at Aswan Reservoir, Egypt 1982-2001. *Bulletin of the Seismological Society of America*, 94(2), 479-492.
- MWH (2011). *Briefing Document on Reservoir Triggered Seismicity*.
- O’Neill, J.M., Ridgway, K.D., and Eastham, K.R. (2003a) Mesozoic sedimentation and deformation along the Talkeetna thrust fault, south-central Alaska: New insights and their regional tectonic significance, in Galloway, J.P., ed., Studies by the U.S. Geological Survey in Alaska, 2001: U.S. Geological Survey Professional Paper 1678, 83–92.
- Nokleberg, W.J., Plafker, George, and Wilson, F.H. (1994). Geology of south-central Alaska, in Plafker, George, and Berg, H.C., eds., The geology of Alaska, v. G–1 of The geology of North America: Boulder, Colo., Geological Society of America, p. 311–366.
- Packer, D. R., Cluff, L. S., Knuepfer, P. L., and Withers, R. J. (1979). *Study of Reservoir Induced Seismicity*. San Francisco: Woodward-Clyde Consultants.
- Packer, D. R., Lovegreen, J. R., and J.L. Born (1977). Earthquake Evaluation Studies of the Auburn Dam Area. Denver, CO, USA: U.S. Bureau of Reclamation.
- Pavlis, G. B., & Langston, C. A. (1983). Source depth determination using multi-modal Rayleigh spectral ratios and linear discriminate analysis: a study of the reservoir-induced seismicity sequence at Lake Kariba, Africa (September 1963 to August 1974). *Bulletin of the Seismological Society of America*, 73(1), 59-82.
- Perman, R. C., Packer, D. R., Coppersmith, K. J., P.L. Knuepfer (1981). *Collection of data for data bank on reservoir induced seismicity*. Report to the U.S. Geological Survey, Contract Nol 14-08-0001-19132.
- Plotnikova, L. M., V.I. Makhmudova,, and O.B. Sigalova (1992). Seismicity Associated with the Charvak Reservoir, Uzbekistan. *PAGEOPH*, 139, No. 3/4.
- Ratchkovski, N. and R. Hansen (2002). New Evidence for Segmentation of the Alaska Subduction Zone, *Bulletin of the Seismological Society of America*, 95(5), 1754–1765.

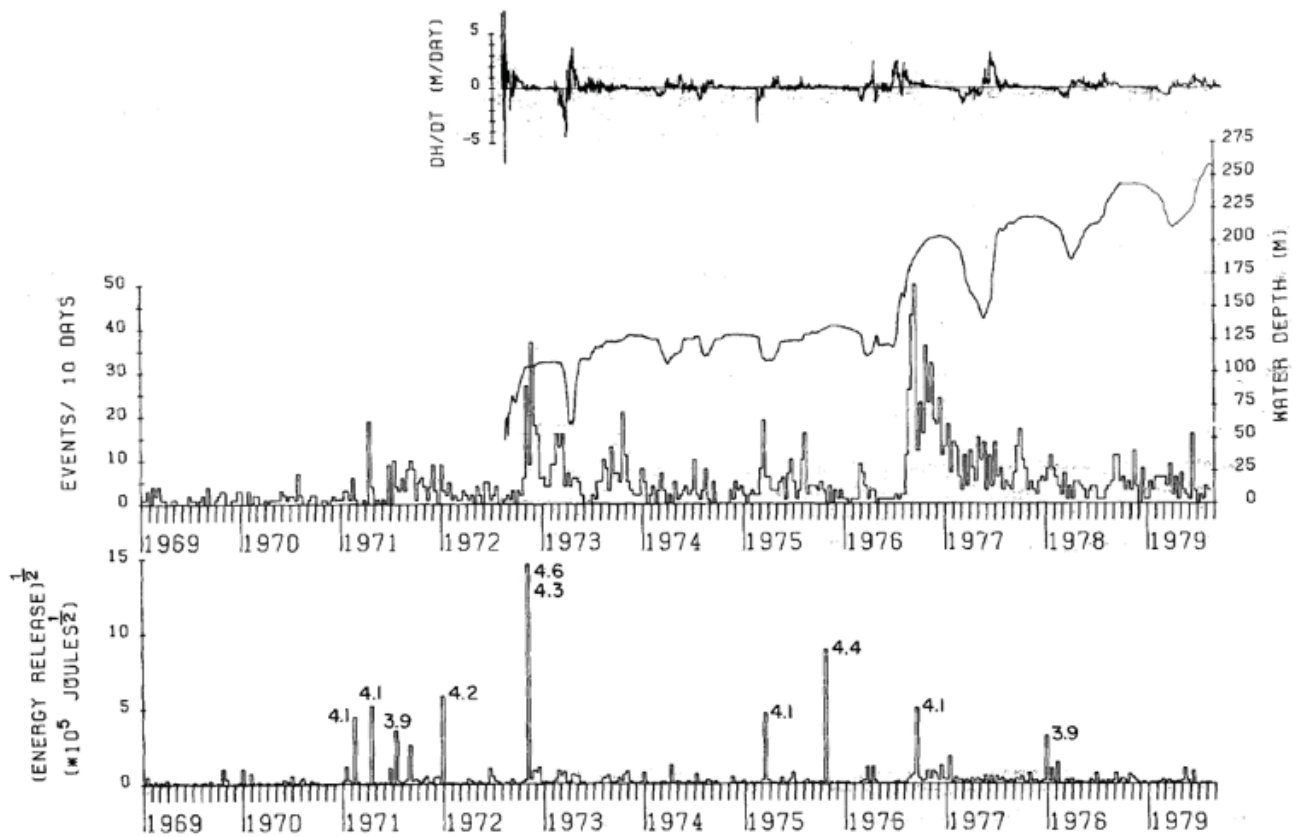
- Rajendran, K., and Talwani, P. (1992). The role of elastic, undrained, and drained responses in triggering earthquakes at Monticello Reservoir, South Carolina. *Bulletin of the Seismological Society of America*, 82, 1867-1888.
- Rastogi, B. K., and Talwani, P. (1980). Relocation of Koyna earthquakes. *Bulletin of the Seismological Society of America*, 70(5), 1849-1868.
- Rastogi, B. K., and Talwani, P. (1980). Spatial and temporal variations in ts/tp at Monticello Reservoir, South Carolina. *Geophysical Research Letters*, 7(10), 781-784.
- Rastogi, B. K., Chadha, R. K., Sarma, C. P., Mandal, P., Satyanarayana, H. S., Raju, I. P. (1997). Seismicity at Warna Reservoir (near Koyna) through 1995. *Bulletin of the Seismological Society of America*, 87(6), 1484-1494.
- Reasenburg, P., and D.W. Simpson (1992), Response of regional seismicity to the static stress change produced by the Loma Prieta earthquake, *Science*, 255, 1687-1690.
- Rice, J.R., and M.P. Cleary (1976), Some basic diffusion solutions for fluid-saturated elastic porous media with compressible constituents, *Reviews of Geophysics and Space Physics*, 14, 227-241.
- Richter, C.F. (1958). *Elementary Seismology*, W.H. Freeman and Co., 768 pp.
- Ridgway, K. D., J. M. Trop, W. J. Nokleberg, C. M. Davidson, and K. R. Eastham (2002). Mesozoic and Cenozoic tectonics of the eastern and central Alaska Range: Progressive basin development and deformation in a suture zone, *Geol. Soc. Am. Bull.*, 114, 1480-1504.
- Roeloffs, E. A. (1988). Fault stability changes beneath a reservoir with cyclic variations in water level. *Journal of Geophysical Research*, 93(B3), 2107-2124.
- Rogers, A. M., & Lee, W. K. (1976). Seismic study of earthquakes in the Lake Mead, Nevada-Arizona region. *Bulletin of the Seismological Society of America*, 1657-1681.
- Ruppert, N. (2008). Stress Map for Alaska From Earthquake Focal Mechanisms, Active Tectonics and Seismic Potential of Alaska Geophysical Monograph Series 179, 351-367.
- Saxena, S.K., A. Ger, and A. Sengupta (1988), Reservoir-induced seismicity- a new model, *International Journal for Numerical and Analytical Methods in Geomechanics*, v. 12, 263-281.
- Schaeffer, M. (1991), A relationship between joint intensity and induced seismicity at Lake Keowee, northwestern South Carolina, *Bulletin of the Association of Engineering Geologists*, vol. XXVIII, no. 1, 7-30.

- Schmidt, J.M., Oswald, P.J., and Snee, L.W. (2002). The Deadman and Clark Creek fields: Indicators of early Tertiary volcanism in an extensional tectonic setting in the northern Talkeetna Mountains, Alaska: Geological Society of America Abstracts with Programs, v. 34, no. 5, p. A-101.
- Scholz, C.H. (2002). The mechanics of earthquake faulting, Columbia University, New York, 496 pp.
- Schwartz, D. P., Joyner, W. B., Stein, R. S., Brown, R. D., McGarr, A. F., Hickman, S. H., et al. (1996). *Review of seismic - hazard issues associated with the Auburn Dam Project, Sierra Nevada*. U.S. Geological Survey Open File Report 96-0011.
- Secor, D. T., Peck, L. S., Pitcher, D. M., Simpson, D. H., Smith, W. A., & Snoke, A. W. (1982). Geology of the area of induced seismic activity at Monticello Reservoir, South Carolina. *Journal of Geophysical Research*, 87(B8), 6945-6957.
- Secor, Jr., D. T. (1981). *Geological Studies in an area of Induced Seismicity, Monticello Reservoir*. US Geological Survey.
- Seeber, L., Ambruster, J. G., and Kim, W.-Y. (2004). A fluid-injection-triggered earthquake sequence in Ashtabula, Ohio: implication for seismogenesis in stable continental regions. *Bulletin of the Seismological Society of America*, 94(1), 76-87.
- Shirley, J. E. (1980). Tasmanian seismicity -- natural and reservoir induced. *Bulletin of the Seismological Society of America*, 70(6), 2203-2220.
- Simpson, D. W. (1976). Seismicity Changes associated with reservoir loading. *Engineering Geology*, 10, 123-150.
- Simpson, D. W., & Hamburger, M. W. (1981). Tectonics and seismicity of the Toktogul reservoir region, Kirgizia, USSR. *Journal of Geophysical Research*, 86(B1), 345-358.
- Simpson, D. W., & Negmatullaev, S. K. (1981). Induced seismicity at Nurek Reservoir Tadjikistan, USSR. *Bulletin of the Seismological Society of America*, 71(5), 1561-1586.
- Simpson, D. W., & Negnatullaev, S. H. (1978). Induced Seismicity studies in Central Asia. *Earthquake Information Bulletin*, 10, 209-213.
- Simpson, D. W., Leith, W. S., and Scholz, C. H. (1988). Two types of reservoir induced seismicity. *Bulletin of the Seismological Society of America*, 78(6), 2025-2040.
- Singh, C., Bhattacharya, P. M., and Chadha, R. K. (2008). Seismicity in the Koyna-Warna reservoir site in western Indian: fractal and b-value mapping. *Bulletin of the Seismological Society of America*, 98(1), 476-482

-
- Snow, D. T. (1972). Geodynamics of seismic reservoirs, Proc. Symp. Percolation through Fissured Rock, Stuttgart: Ges. Erd- und Grundbau, T2J: 1-19.
- Stein, R.S. (1999), The role of stress transfer in earthquake occurrence, *Nature*, 402, 605-609.
- Stuart-Alexander, D. E., and Mark, R. K. (1976). *Impounded-induced seismicity associated with large reservoirs*. USGS OFR 76-770.
- Talwani, P. (1997). On the Nature of Reservoir-induced Seismicity. *Pure and Applied Geophysics*, 473-492.
- Talwani, P., Chen, L., and Gahalaut, K. (2007). Seismogenic permeability, ks. *Journal of Geophysical Research*, 112(B07309), 18.
- Talwani, P., Cobb, J. S., and Schaeffer, M. F. (1999). In situ measurements of hydraulic properties of a shear zone in northwestern South Carolina. *Journal of Geophysical Research*, 107(B7), 14,993-15,003.
- Tarr, A. C., Talwani, P., Rhea, S., Carver, D., and Amick, D. (1981). Results of recent South Carolina seismological studies. *Bulletin of the Seismological Society of America*, 71(6), 1883-1902.
- US Committee on Large Dams (USCOLD) (1997). *Reservoir Triggered Seismicity*.
- Wells, D. and K. Coppersmith. (1994). New empirical relationships among magnitude, rupture length, rupture width, rupture area and surface displacement. *Bulletin of the Seismological Society of America Vol. 84 No.4*.
- Wesson, R. L., Boyd, O. S., Mueller, C. S., Bufe, C. G., Frankel, A. D., Petersen, M. D. (2007). Revision of time-Independent probabilistic seismic hazard maps for Alaska: U.S. Geological Survey Open-File Report 2007-1043.
- Withers, R. J. (1977). *Seismicity and stress determination at manmade lakes: PhD Dissertation*. University of Alberta, Canada.
- Withers, R. J., and Nylan, E. (1978). Time evolution of stress under an artificial lake and its implication for induced seismicity. *Canadian Journal of Earth Sciences*, 15, 1526-1534.
- Woodward-Clyde Consultants (WCC) (1980). Interim Report on Seismic Studies at Susitna Hydroelectric Project: Report prepared for Acres America Inc. Orange: Woodward-Clyde Consultants.
- Woodward Clyde Consultants (WCC) (1982). *Final Report on Seismic Studies for Susitna Hydroelectric Project*.

-
- Yagi, Y., Nishimura, N., and Kasahara, A. (2012). Source process of the 12 May 2008 Wenchuan, China, earthquake determined. *Earth Planets Space*, e13-e16.
- Yeats, R. S., Sieh, K. E., and Allen, C. A. (1997). *Geology of Earthquakes*. New York, NY: Oxford University Press.
- Zhang, Y., WP Feng, LS Xu, CH Zhou, and YT Chen (2009), Spatio-temporal rupture process of the 2008 great Wenchuan earthquake, *Science in China Series D-Earth Sciences*, 52(2), 145.
- Zhou, S., K. Deng, and W. Cheng (2010), Discussion on ‘Was the 2008 Wenchuan earthquake triggered by Zipingpu Reservoir?’, *Earthquake Science*, 23, 577-581.
- Zhou, S. and K. Deng (2011). Reply to “Comment on ‘Evidence that the 2008 Mw 7.9 Wenchuan Earthquake Could Not Have Been Induced by the Zipingpu Reservoir’ by Kai Deng, Shiyong Zhou, Rui Wang, Russell Robinson, Cuiping Zhao, and Wanzheng Cheng” by Shemin Ge, *Bulletin of the Seismological Society of America*, 101(6), 3119-3120.
- Zoback, M. D., and Hickman, S. (1982). In situ study of the physical mechanisms controlling induced seismicity at Monticello Reservoir, South Carolina. *Journal of Geophysical Research*, 87(B8), 6959-6974.

FIGURES



Notes: The number of earthquakes and square root of energy release/10 days . Numbers in the lower section are the magnitudes of the larger earthquakes. Water level gradient (dH/dt) is the daily change in the water level, calculated from the water level data. Positive gradient represents filling, and negative gradient emptying, of the reservoir.

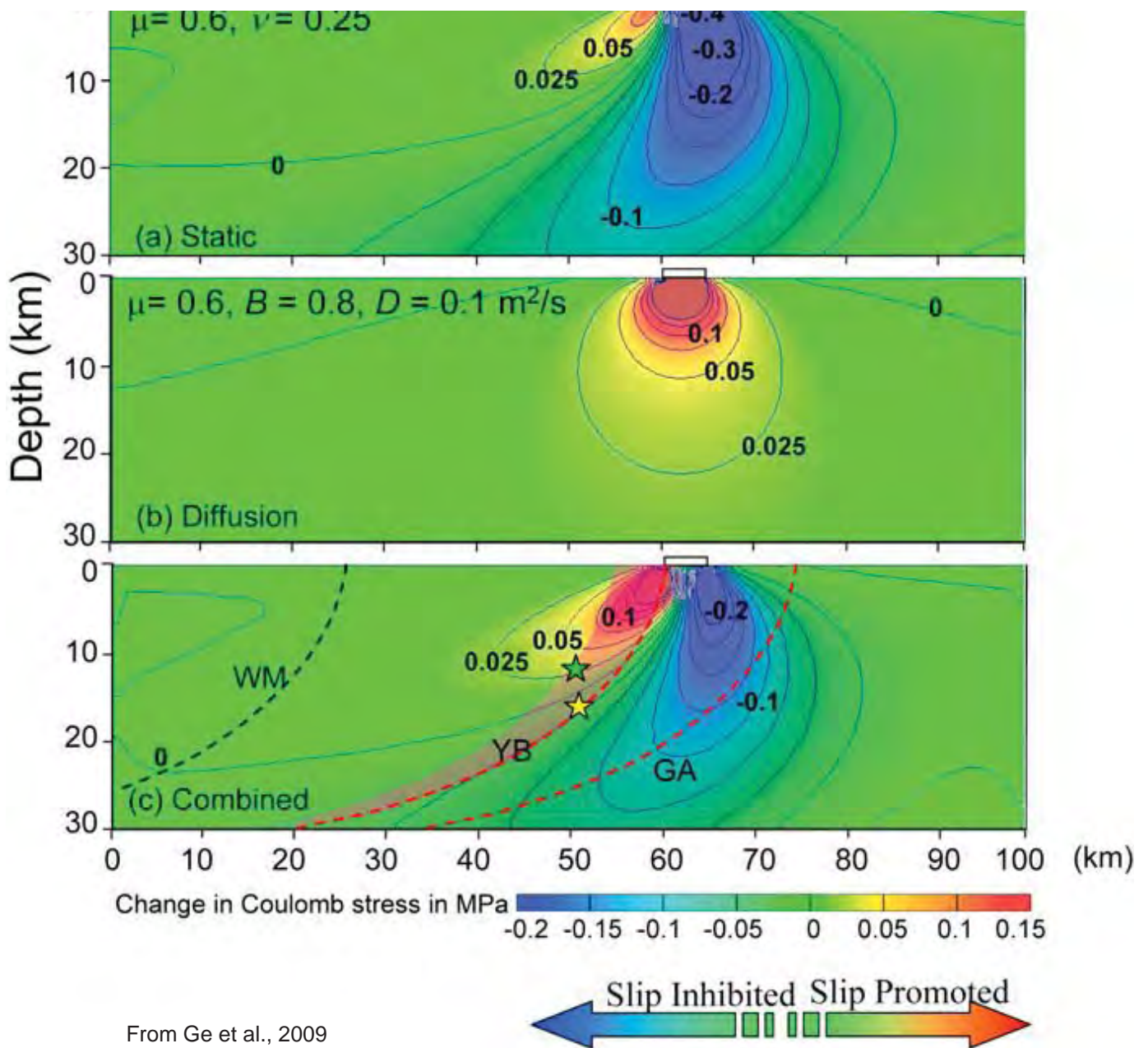


SUSITNA-WATANA HYDROELECTRIC PROJECT

TEMPORAL VARIATIONS IN SEISMICITY WITHIN THE RESERVOIR AREA AND DAILY WATER LEVEL AT NUREK

02/25/13

FIGURE 1



Notes: Simulated change in effective Coulomb stress due to the load from the Zipingpu Reservoir. (a) Coulomb stress change due to a static load of 100 m of water in the reservoir. (b) Hydrodynamic contribution to the Coulomb stress change 2.7 years after the impoundment. (c) Effective Coulomb stress change, the combined effects of static loading and hydrodynamic contribution. YB is Yinxiu-Beichuan fault. Green and yellow stars are alternative locations of the Mw 7.9 earthquake.

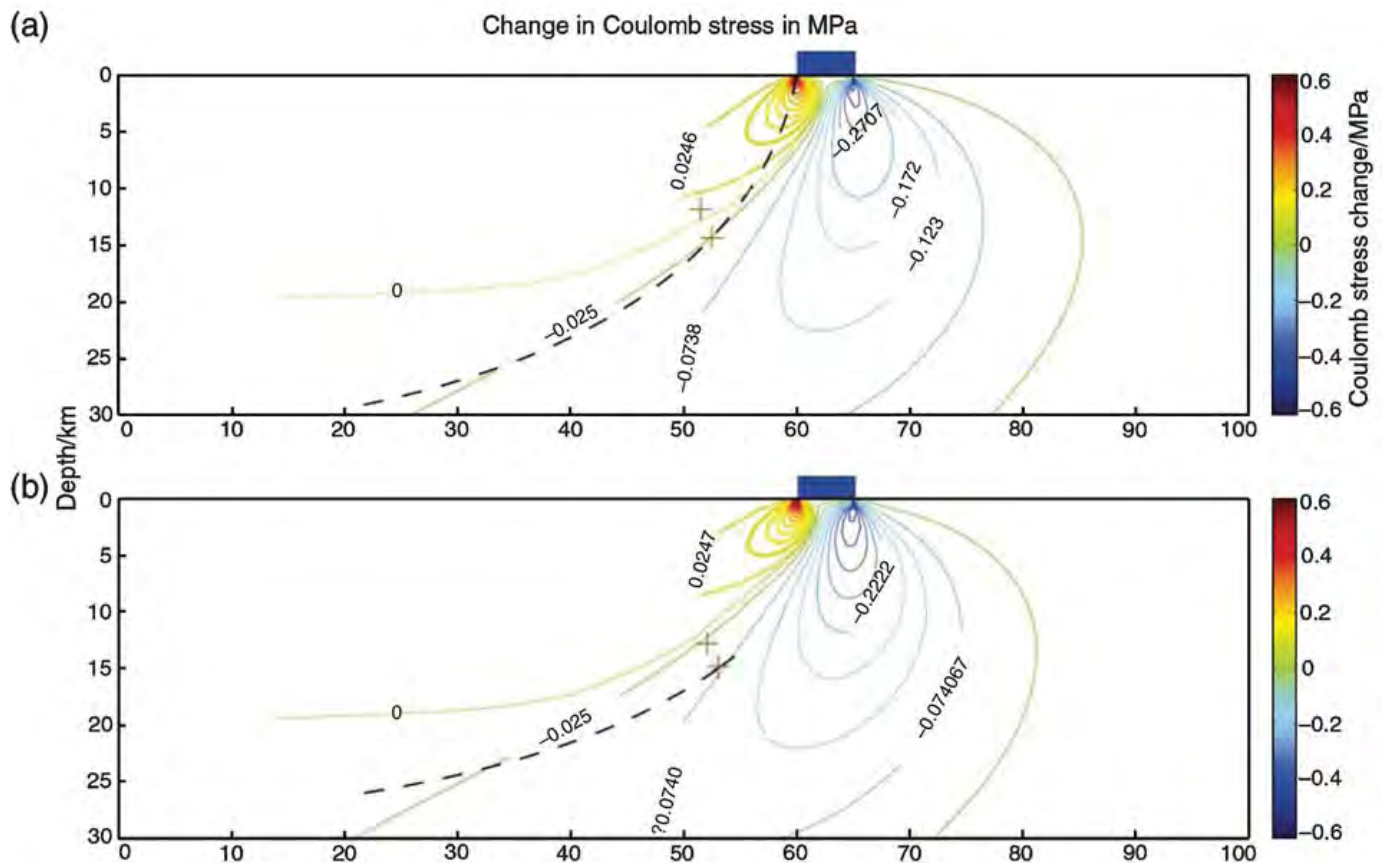


SUSITNA-WATANA HYDROELECTRIC PROJECT

**SIMULATED CHANGE
IN EFFECTIVE COULOMB STRESS
DUE TO ZIPINGPU RESERVOIR**
(Ge et al., 2009)

03/26/13

FIGURE 2



From Zhou and Deng, 2011

Notes: (a) Repeat of the model by Ge et al. (2009) with the same results as Ge et al.; (b) Model with dip decreased to 35° and with other parameters the same as Ge et al.'s calculation. The red cross indicates the hypocenter of the Wenchuan earthquake as reported by the USGS; the yellow cross indicates the hypocenter of the Wenchuan earthquake reported by CEA (China Earthquake Administration); the dashed line indicates the rupturing fault (Yingxiu–Beichuan) fault; and the blue rectangle indicates the area of Zipingpu Reservoir.

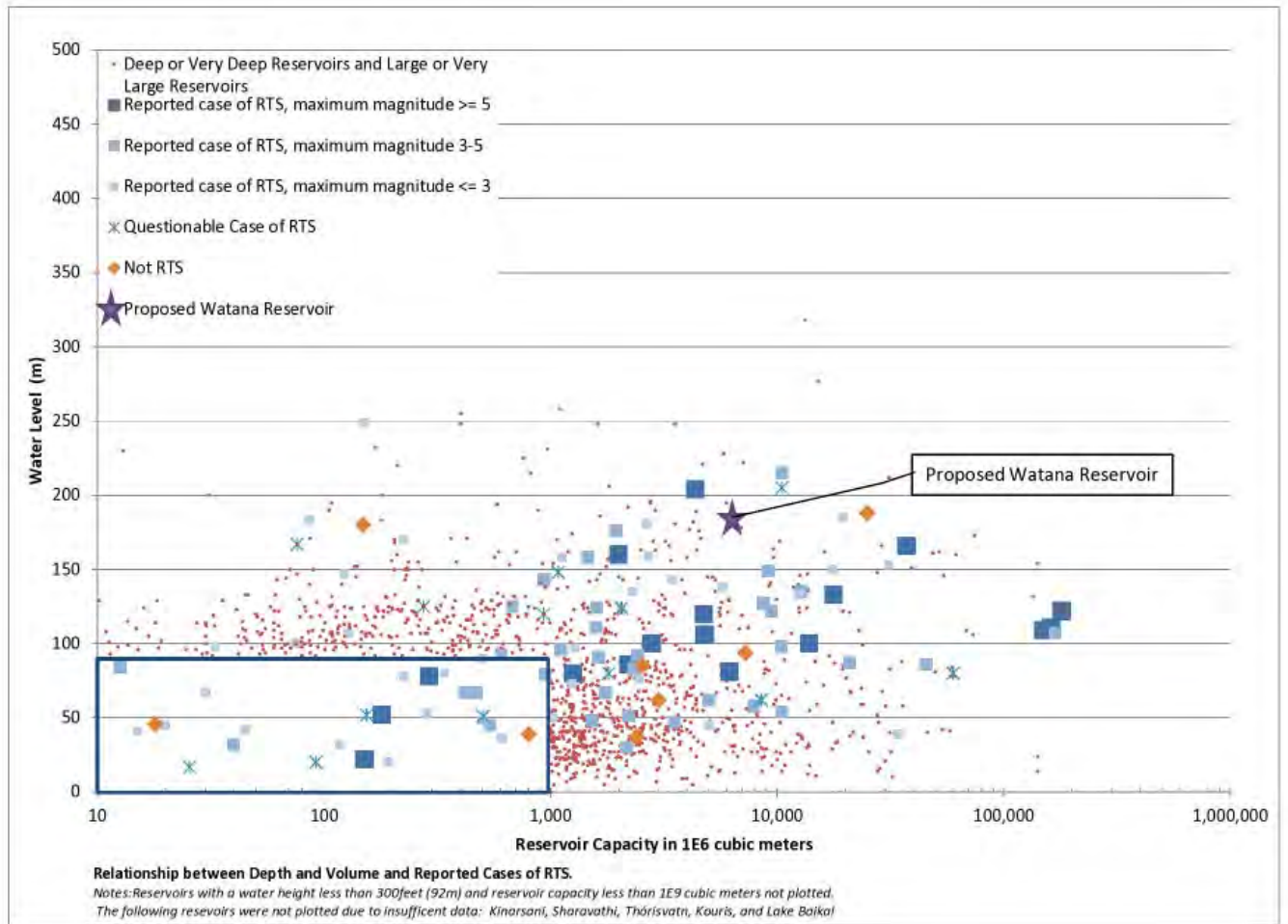


SUSITNA-WATANA HYDROELECTRIC PROJECT

**SIMULATED CHANGE
IN EFFECTIVE COULOMB STRESS
DUE TO ZIPINGPU RESERVOIR
(Zhou and Deng, 2011)**

03/26/13

FIGURE 3



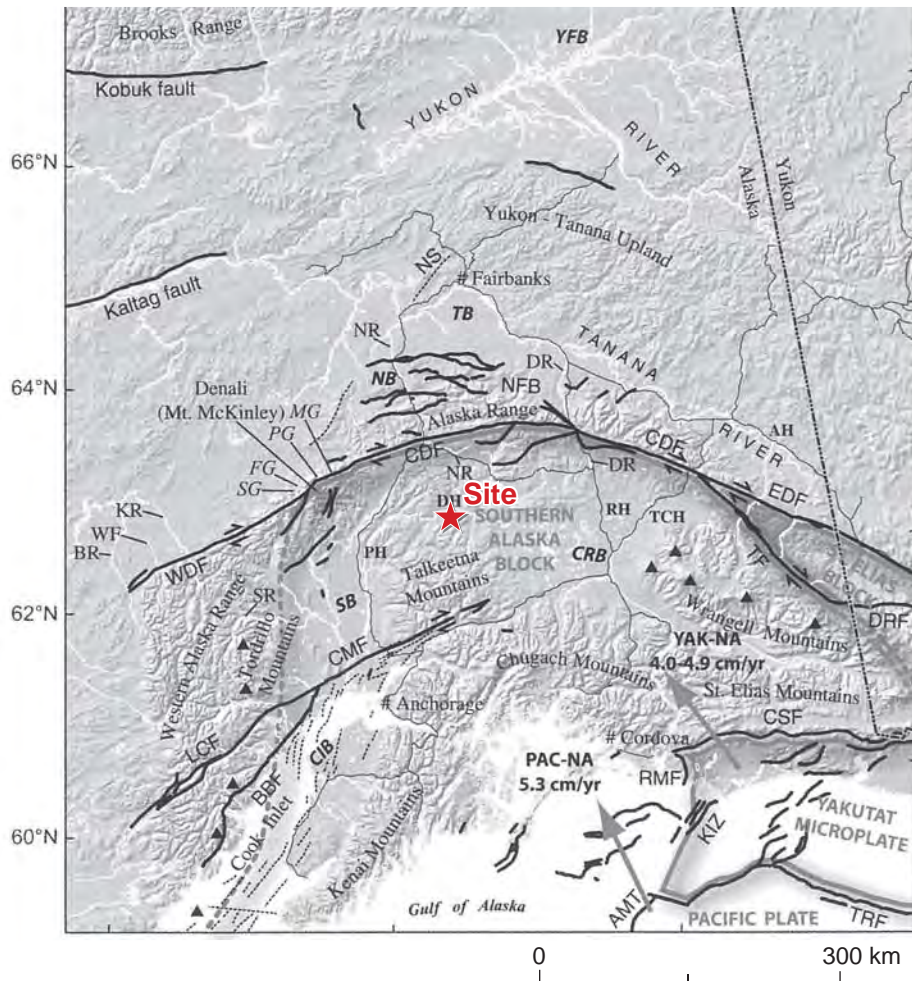


SUSITNA-WATANA HYDROELECTRIC PROJECT

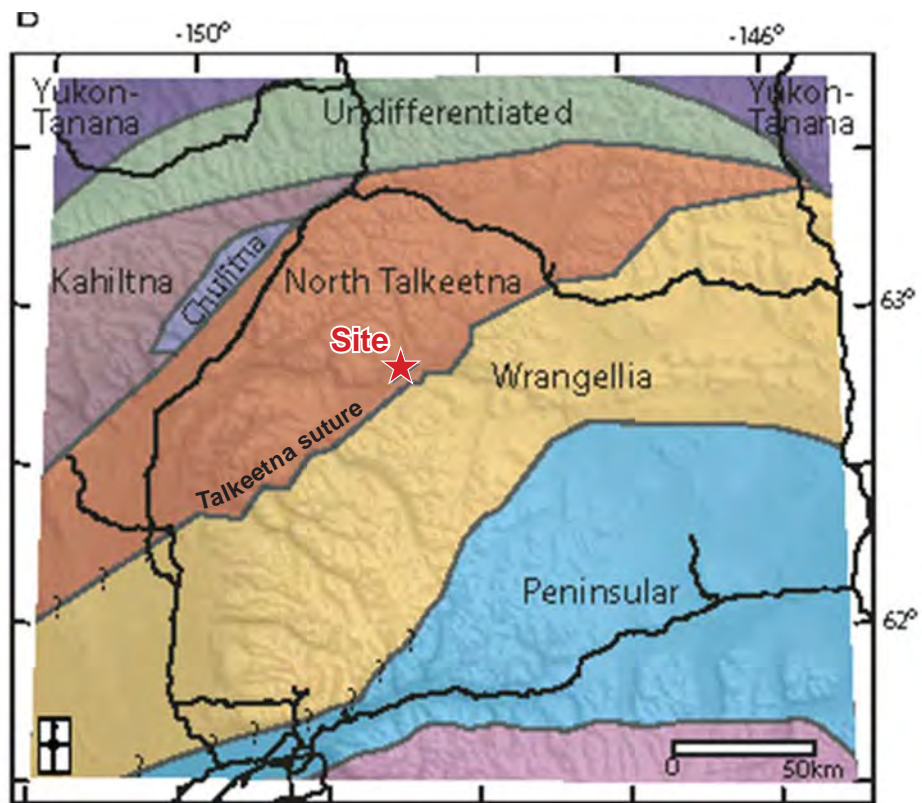
MAJOR PHYSIOGRAPHIC PROVINCES

02/22/13

FIGURE 5



Black lines are Neogene and active faults, dashed lines are anticlines. Triangles show active volcanoes. Crustal blocks are outlined in gray and are dashed where boundaries are uncertain. Faults: WDF, western Denali fault; CDF, central Denali fault; EDF, eastern Denali fault; NFB, northern foothills fold-and-thrust belt; NS, Nenana structure; TF, Totschunda fault; DRF, Duke River fault; LCF, Lake Clark fault; CMF, Castle Mountain fault; BBF, Bruin Bay fault; CSF, Chugach-St. Elias thrust fault; KIZ, Kayak Island fault zone; RMF, Ragged Mountain fault; AMT, Aleutian megathrust; TRF, Transition fault. Major roads are shown with thin black lines. AH, Alaska highway; PH, Parks highway; DH, Denali highway; RH, Richardson highway; DH, Denali highway; TCH, Tok cutoff highway. Abbreviated river names mentioned in text: NR, Nenana River, Delta River (both rivers flow north); BR, Big River; WF, Windy Fork; KR, Kuskokwim River; SR, Skwentna River. Glaciers: SG, Straightaway Glacier; FG, Foraker Glacier; PG, Peters Glacier; MG, Muldow Glacier. Sedimentary basins: cm, Cook Inlet basin; SB, Susitna basin; CRB, Copper River basin; NB, Nenana basin; TB, Tanana basin; YFB, Yukon Flats basin. From Haeussler (2008).



Map based on the geophysical character of the terranes (Glen et al., 2007b).

 Ice fields or glaciers


QUATERNARY DESPOSITS

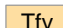
 Surfical deposits, undifferentiated

TERTIARY ROCKS
Sedimentary Rocks

 Sedimentary rocks, undivided


 Nenana Gravel

 Coal-bearing rocks

 Fluviatile sedimentary rocks and subordinate volcanic rocks

Igneous Rocks
Volcanic and Hypabyssal Rocks

 Tertiary volcanic rocks, undivided

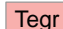
 Hypabyssal felsic and intermediate intrusions

 Hypabyssal mafic intrusions

Intrusive Rocks

 Granite and volcanic rocks, undivided

EOCENE

 Granite and granodiorite


PALEOCENE

 Granitic rocks

TERTIARY AND/OR CRETACEOUS

Igneous Rocks
Intrusive Rocks


 Granitic rocks

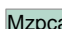
 Granodiorite, tonalite and monzonite dikes, and stocks

Metamorphic Rocks

 Gneissose granitic rocks


UNDIVIDED MESOZOIC ROCKS
METAMORPHIC ROCKS

 Schist and amphibolite

 Phyllite, pelitic schist, calc-schist, and amphibolite of the McClaren metamorphic belt

CRETACEOUS


Melange

 Melanges of the Alaska Range

 Limestone blocks

Igneous Rocks

Volcanic and hypabyssal rocks

 Andesite subvolcanic rocks

Intrusive Rocks

 Granitic rocks


 Granitic rocks younger than 85 Ma


 Ultramafic rocks

CRETACEOUS AND/OR JURASSIC

Sedimentary Rocks

 Argillite, chert, sandstone, and limestone

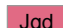
 Kahiltna flysch sequence

 Conglomerate, sandstone, siltstone, shale, and volcanic rocks

JURASSIC

Igneous Rocks

 Mafic and ultramafic rocks

 Alaska-Aleutian Range and Chitina Valley batholiths, undifferentiated

Metamorphic Rocks

 Uranatina metaplutonic complex


Sedimentary Rocks

 Limestone and marble

 Talkeetna Formation

TRIASSIC

Sedimentary Rocks

 Calcareous sedimentary rocks

 Kamishak limestone


Plutonic Rocks

 Gabbro, diabase, and metagabbro

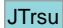
Volcanic Rocks

 Nikolai Greenstone and related similar rocks

Metamorphic Rocks


 Metavolcanics and associated metasedimentary rocks

MESOZOIC AND PALEOZOIC
Assemblages and Sequences

 Red and brown sedimentary rocks and basalt

 Crystal tuff, argillite, chert, graywacke, and limestone

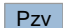
 Red beds

 Volcanic and sedimentary rocks

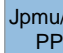
 Serpentinite, basalt, chert and gabbro

PALEOZOIC
Assemblages and Sequences
(Skolai Group)

 Eagle Creek Formation

 Station Creek and Slana Spur Fm., and equivalent rocks

 Teteina Volcanics

 Streina metamorphic complex

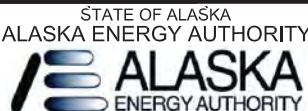
 Marble

- Stratigraphic contact
- Shoreline or riverbank
- Ice contact (glacier limit)
- Lineament
- Fault - certain
- Fault - approximate
- - - - Fault - inferred
- Fault - concealed
- ▲▲ Thrust fault - certain
- ▲▲ Thrust fault - approximate
- ▲▲ - Thrust fault - inferred
- ..▲..▲ Thrust fault - concealed

Geology from Wilson et al., 1998 (USGS Open-file Report 98-133)

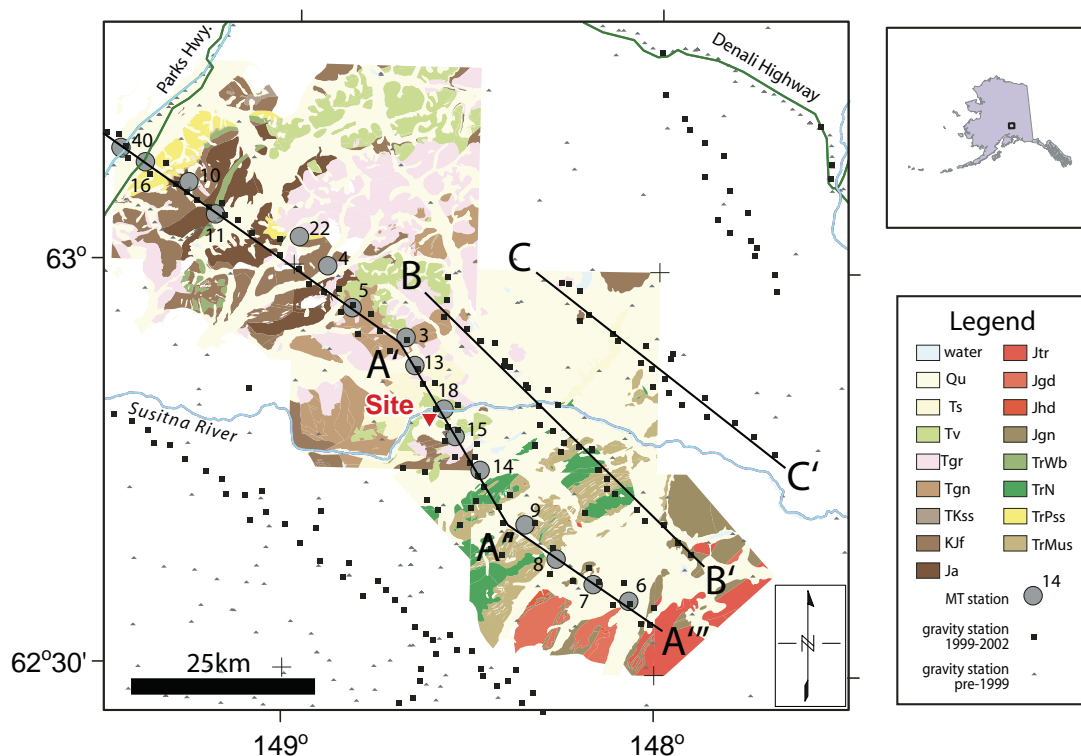
REV	DESCRIPTION	BY	DATE

Project No.	
Date	02/22/13
Designed	
Drawn	
Approved	

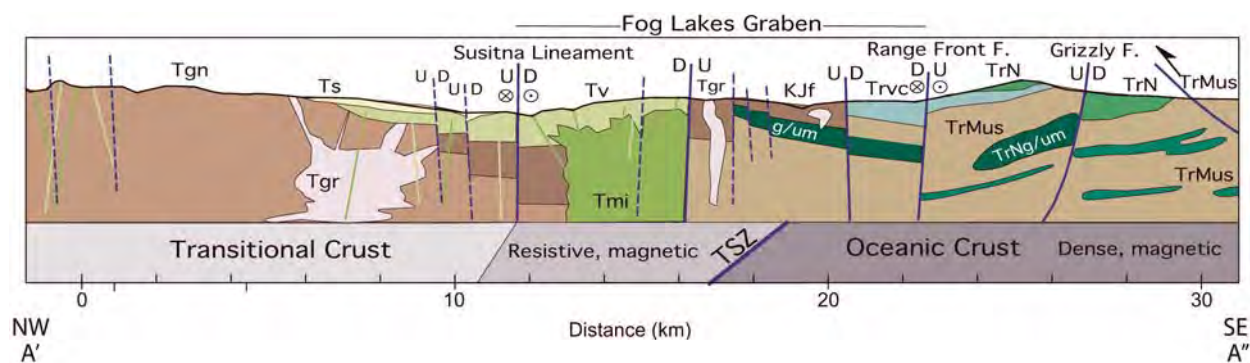


SUSITNA-WATANA HYDROELECTRIC PROJECT
SITE REGION
GEOLOGY LEGEND

FIGURE
FIGURE 8B



Gravity = squares (1999–2000) and triangles; MT stations and potential field profiles = black lines A–A', B–B', and C–C'; Qu = Quaternary sediments, undifferentiated; Ts = Tertiary nonmarine clastic sedimentary rocks; Tv = Tertiary volcanic rocks; Tgr = Tertiary granitoid intrusive rocks; Tgn = Tertiary gneiss and granitoid intrusive rocks, undifferentiated; TKss = Tertiary or Cretaceous sandstone; KJf = Jurassic to Cretaceous flysch, shale, sandstone, and conglomerate; Ja = Jurassic(?) argillite; Jtr = Jurassic trondjemite; Jgd = Jurassic granodiorite; Jhd = Jurassic hornblende diorite; Jgn = Jurassic gneiss; Trwb = Triassic basalts of Whale Ridge; TrN = Triassic Nikolai Greenstone and gabbros; TrPss = Permian(?) to Triassic quartzose sedimentary rocks; TrMus = Mississippian to early Triassic siliceous and calcareous sedimentary rocks. Geology modified from Wilson et al., 1998, and unpublished U.S. Geological Survey mapping.



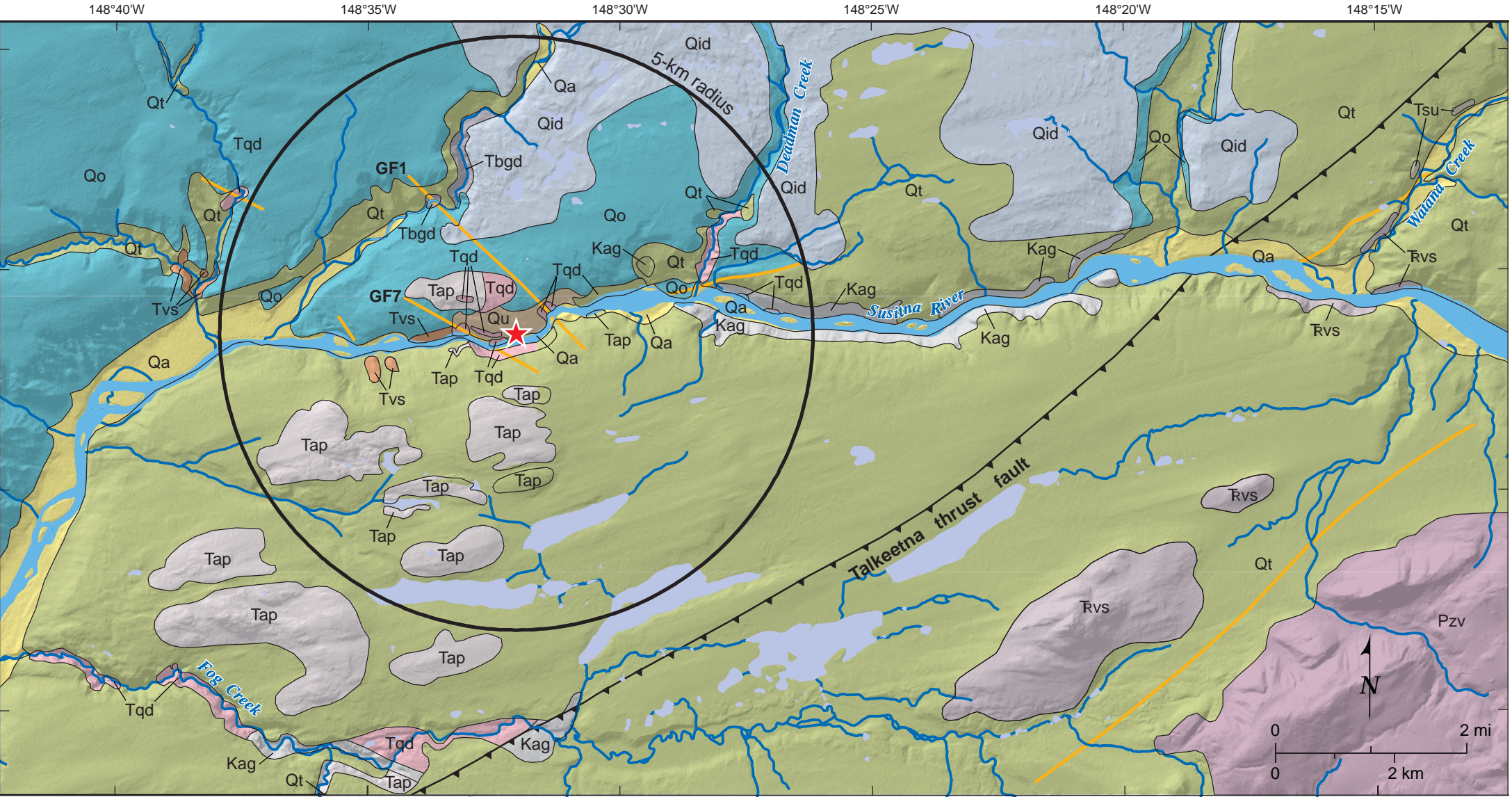
Simplified geologic map and cross section A'–A'' along a transect through the northern Talkeetna Mountains.

Modified from Figures 3 and 7 in Glen et al. (2007b)



SUSITNA-WATANA HYDROELECTRIC PROJECT

SIMPLIFIED GEOLOGIC MAP AND CROSS SECTION



Geology modified from Acres (1982)

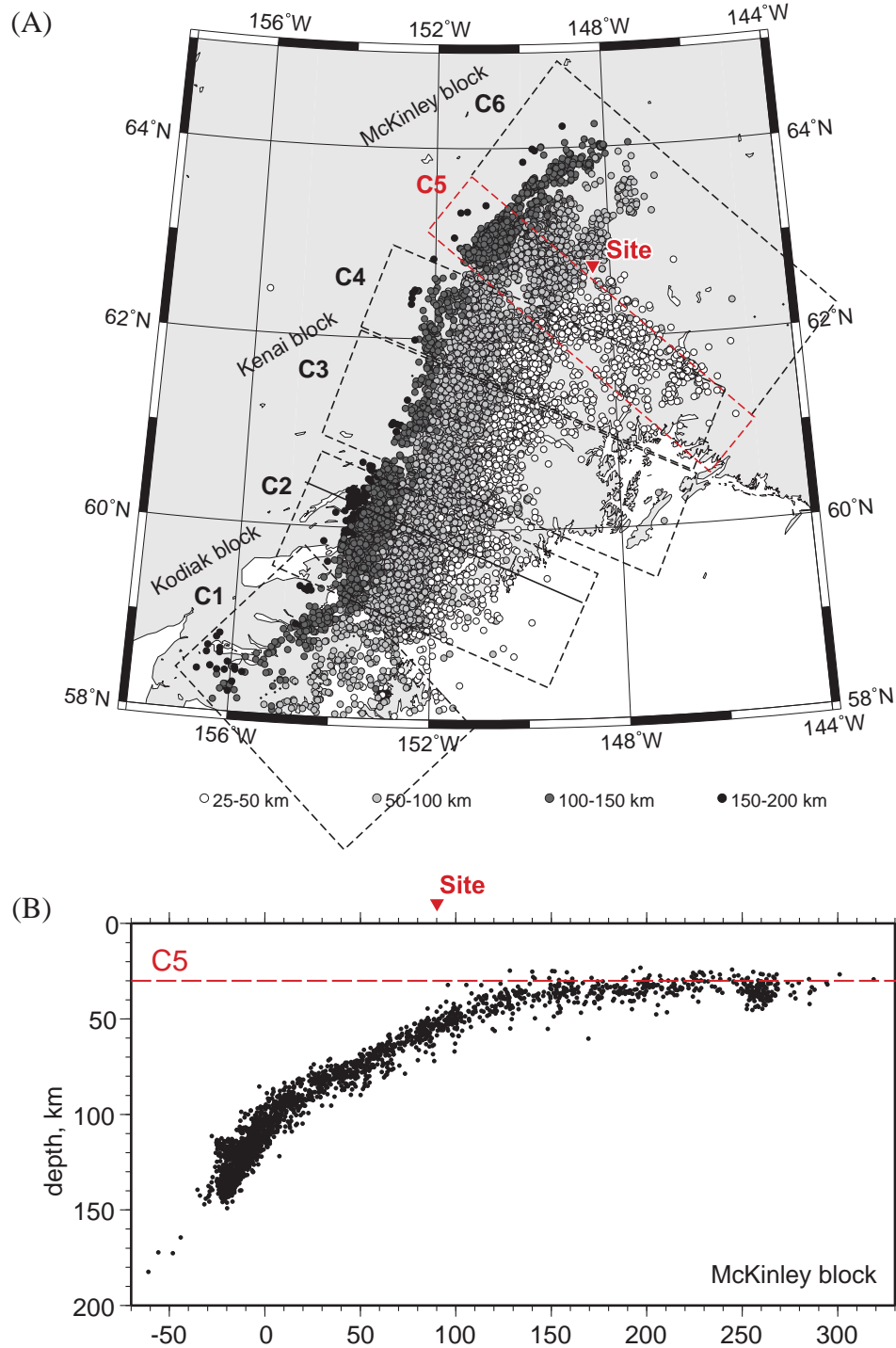
Explanation

- Proposed Watana site
- Contact
- Thrust fault
- Shear
- Water body
- Major River
- Stream

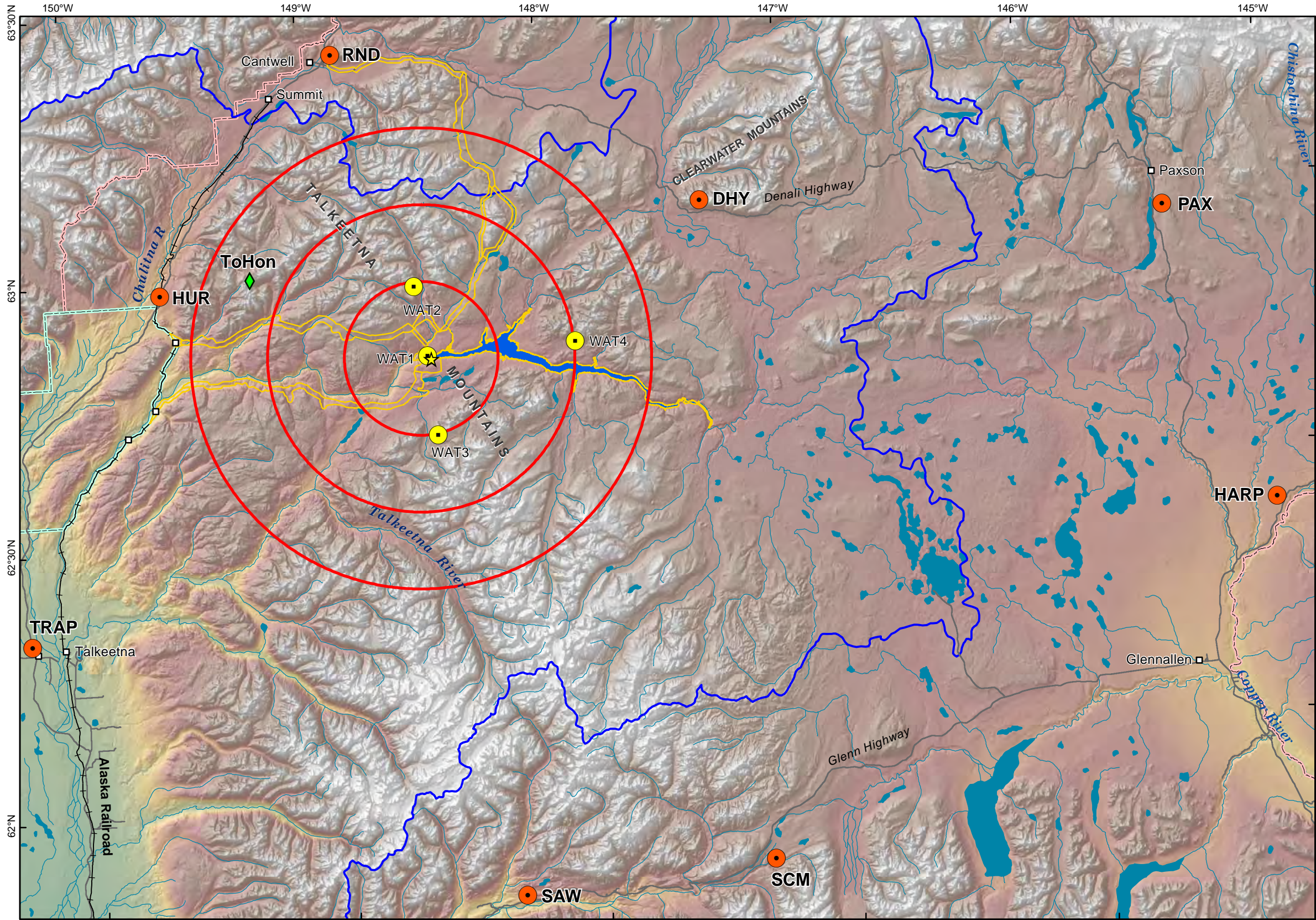
Geologic Units

QUATERNARY	Qa	Alluvium, alluvial terraces and fans
	Qid	Ice disintegration deposits
	Qt	Till
	Qo	Outwash
	Qu	Surficial deposits, undifferentiated, generally thin
TERTIARY	Tsu	Conglomerate, sandstone and claystone
	Tvs	Volcaniclastic sandstone, siltstone and shale
	Tap	Andesite porphyry, minor basalt
	Tqd	Diorite to quartz diorite, minor granodiorite
	Tbgd	Biotite granodiorite
MESOZOIC	CRETACEOUS	
	Kag	Argillite and graywacke
	TRIASSIC	
	Rvs	Basaltic metavolcanic rocks, metabasalt and slate
	PALEOZOIC	
	Pzv	Basaltic to andesitic metavolcanic rocks

Note: GF7 is equivalent to “Fingerbuster” and GF 1 is equivalent to “Fins” features of Acres (1981, 1982) and Harza Ebasco (1984).



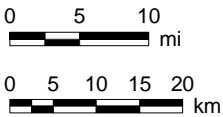
(A) Map of earthquakes showing location of cross section (dashed rectangle labeled C5) shown in (B), modified from Figure 5 of Ratchkovski and Hansen (2002). (B) Cross section (C5) of earthquakes, modified from Figure 6 of Ratchkovski and Hansen (2002). Triangle indicates approximate site location.



Legend

- AEIC Regional Seismographs
- Proposed Microseismic Station**
 - ◆ ToHon
 - WAT1
 - WAT2
 - WAT3
 - WAT4
- 10-mile buffer
- ▭ Preliminary project area
- ★ Proposed Watana dam site
- Proposed Watana Reservoir
- Susitna Drainage Basin
- ▭ National Park and Preserve
- ▭ Denali State Park (Special Land Use District)
- ▭ Susitna Flats State Game Refuge

Data Sources: See Map References



Projection: Alaska Albers NAD 1983
Date Created: 3/25/2013
Map Author: MWH - Eric Zimmerman
File: SuWa_Microseismic_Stations_11x17_Landsc_3_25_13.mxd

REV	DESCRIPTION	BY	DATE

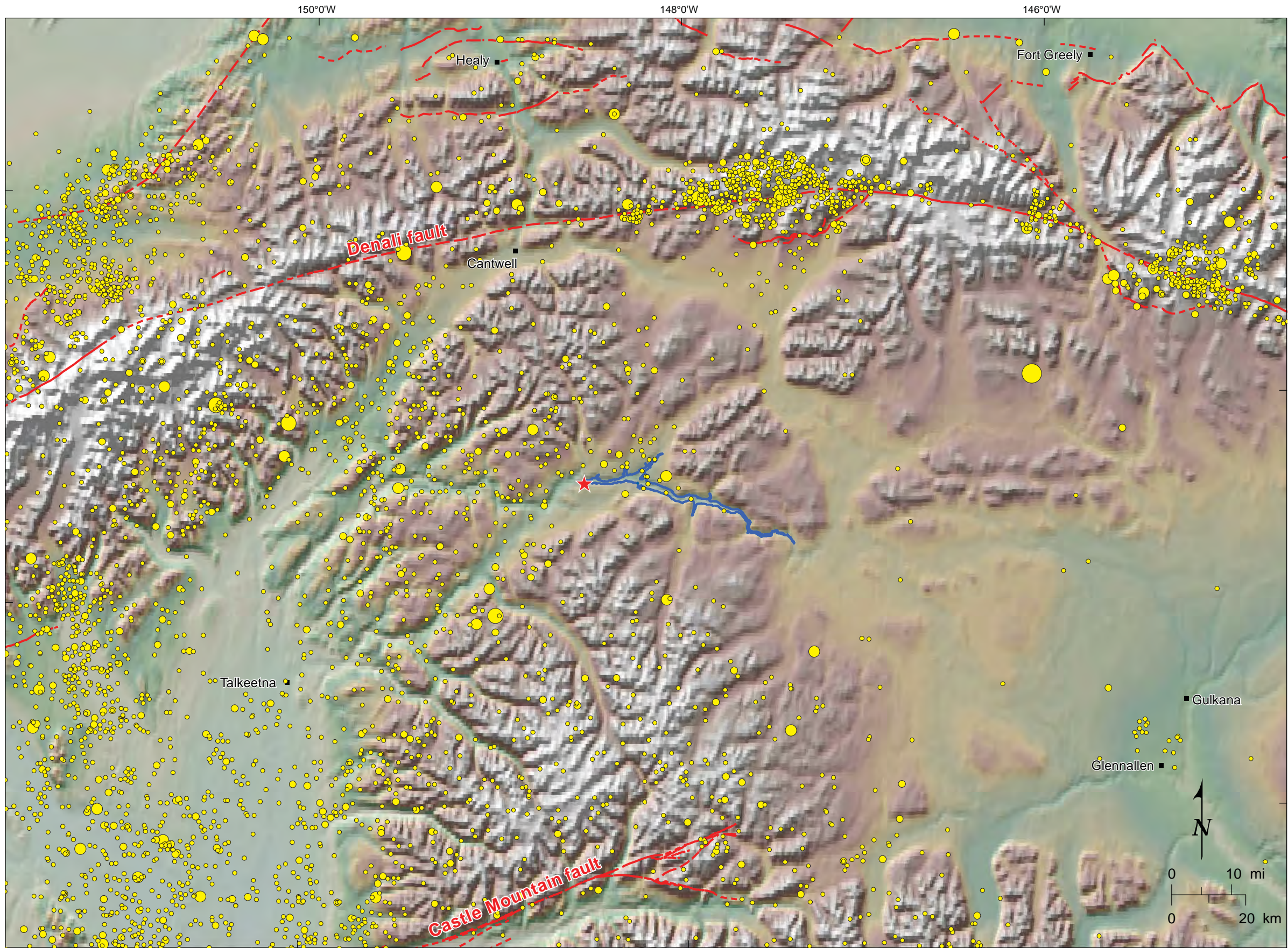
SCALE

Project No.	
Date	03/27/13
Designed	
Drawn	
Approved	



SUSITNA-WATANA HYDROELECTRIC PROJECT
WATANA SEISMIC NETWORK

FIGURE
FIGURE 12



Explanation

★ Proposed Watana site

*Seismicity by Magnitude
(AEIC, 1898-2010)*

- 3.0 - 3.9
- 4.0 - 4.9
- 5.0 - 5.9
- 6.0 - 6.9
- 7.0 - 7.9

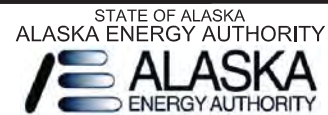
Faults from Alaska DGGS, 2012

- Fault, solid where certain, long dashed where approximate, short dash where inferred
- Reservoir extent (high level, 2,000 feet above sea level)

REV	DESCRIPTION	BY	DATE

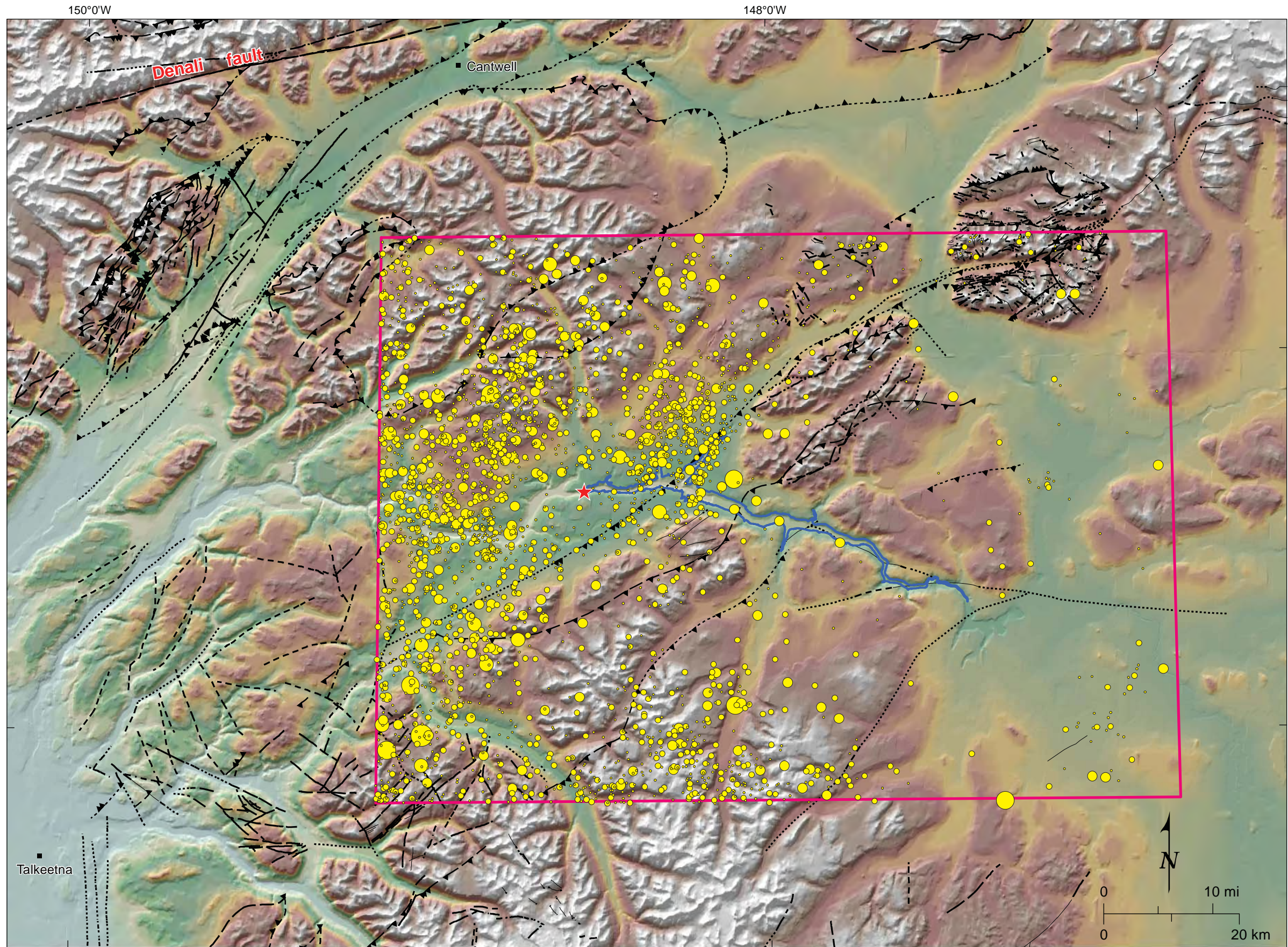
SCALE

Project No. _____
Date 03/26/13
Designed _____
Drawn _____
Approved _____



SUSITNA-WATANA HYDROELECTRIC PROJECT
SEISMICITY IN THE WATANA REGION

FIGURE
FIGURE 13



Explanation

- ★ Proposed Watana site
- Reservoir extent (high level, 2,000 feet above sea level)
- RTS zone

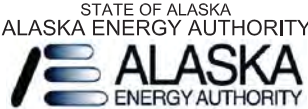
Seismicity by Magnitude (AEIC, 1898-2010)

- 1.0 - 1.9
- 2.0 - 2.9
- 3.0 - 3.9
- 4.0 - 4.9
- 5.0 - 5.9
- 6.0 - 7.0

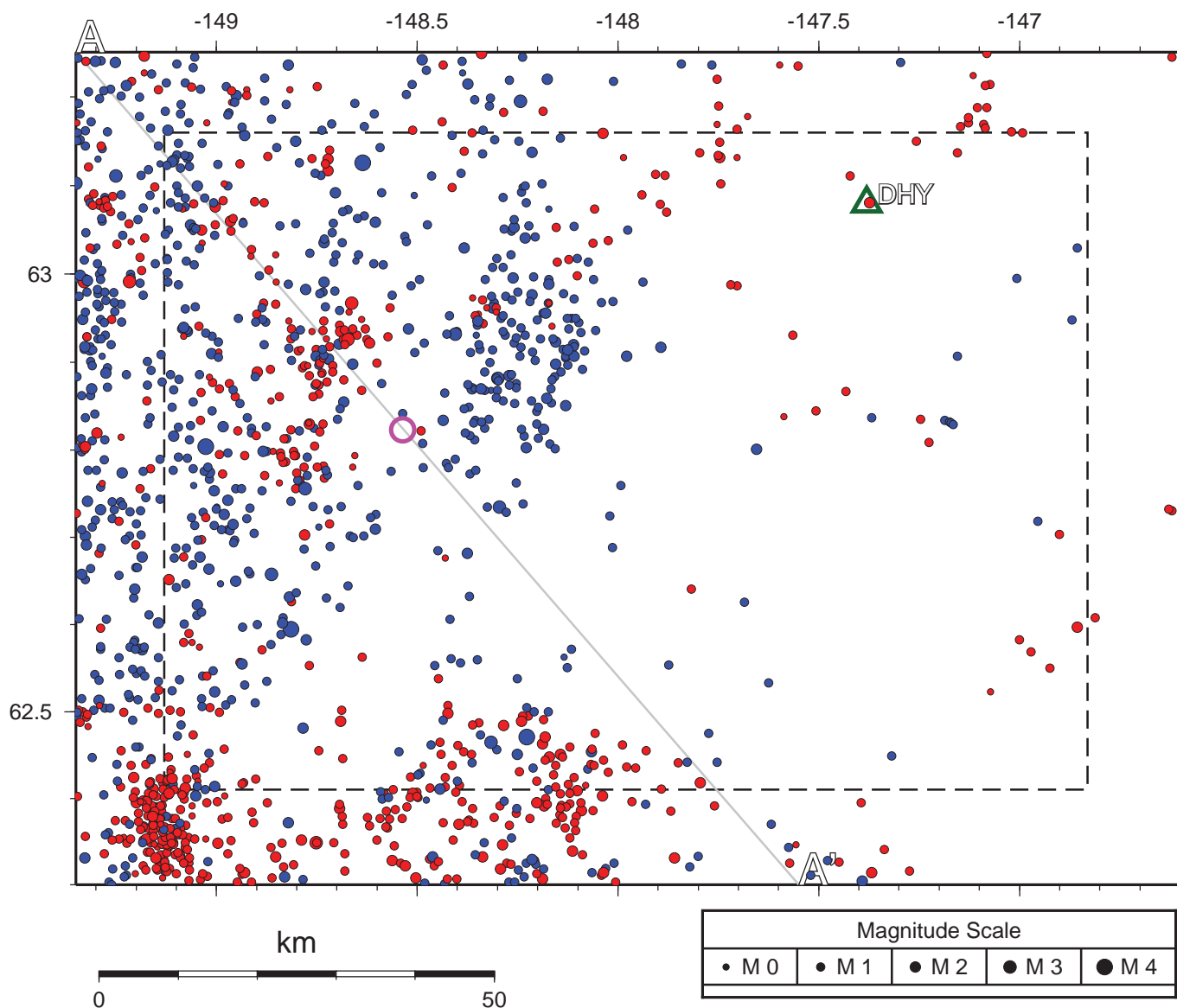
Faults

- — — — — Fault, solid where certain, long dash where approximate, short dash where inferred, dotted where concealed
- ▲ — — — — — Thrust fault, solid where certain, long dash where approximate, short dash where inferred, dotted where concealed

				SCALE		Project No. _____
						Date <u>03/27 /13</u>
						Designed _____
						Drawn _____
						Approved _____
REV	DESCRIPTION	BY	DATE			



2010 - Nov 15, 2012



Seismicity before WAT sub-network was operational, with stations operating in that period. Dam site is magenta circle. Blue epicenters signify a hypocentral depth below 30 km. Gray line is cross-section line shown in Figure 16. Dashed line is RTS zone.



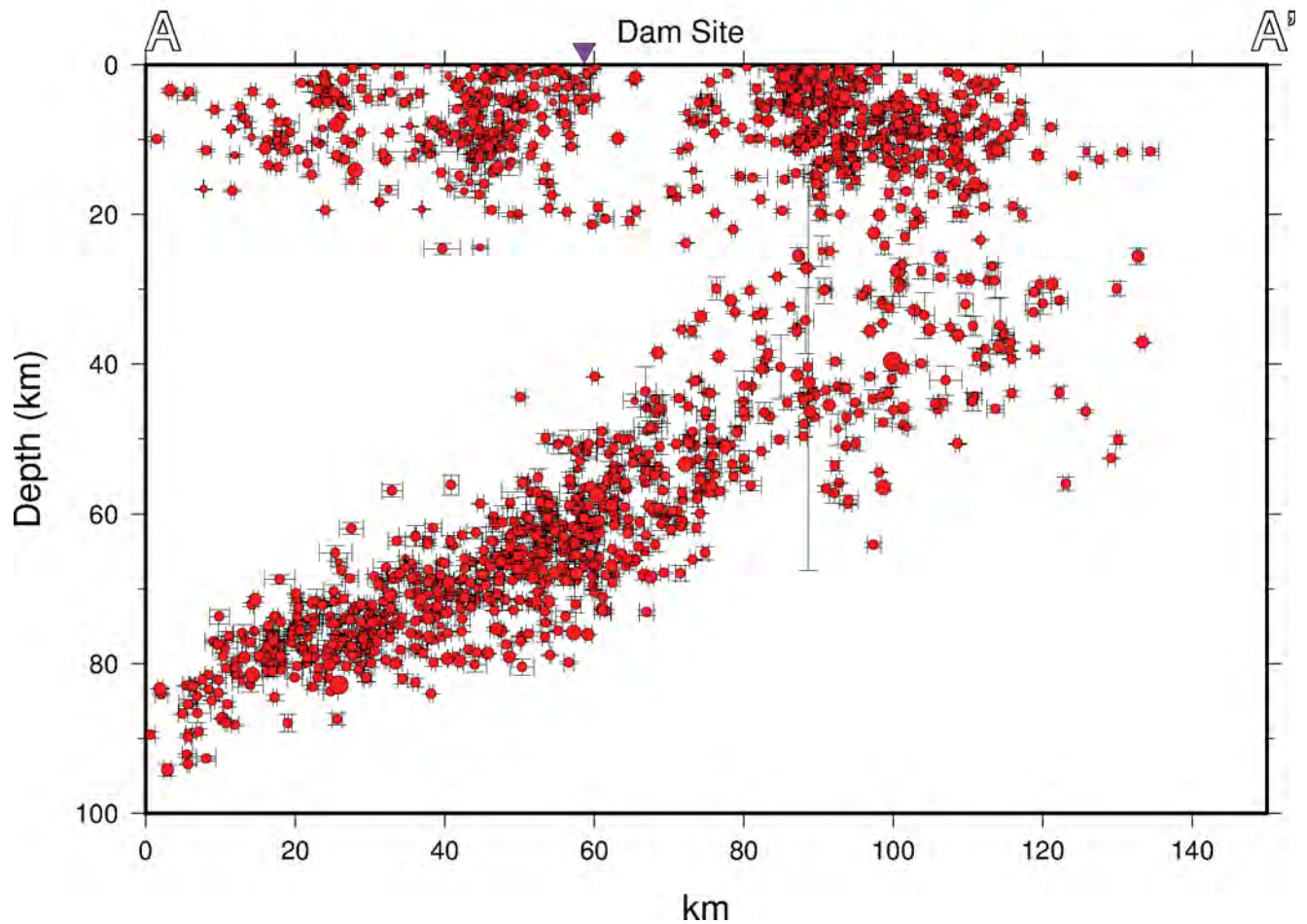
SUSITNA-WATANA HYDROELECTRIC PROJECT

SEISMICITY IN SITE AREA
2010 THROUGH
NOVEMBER 15, 2012

03/26/13

FIGURE 15

2010 - Nov 15, 2012



Cross section of seismicity shown in Figure 15. One standard deviation location errors are shown. No vertical exaggeration.



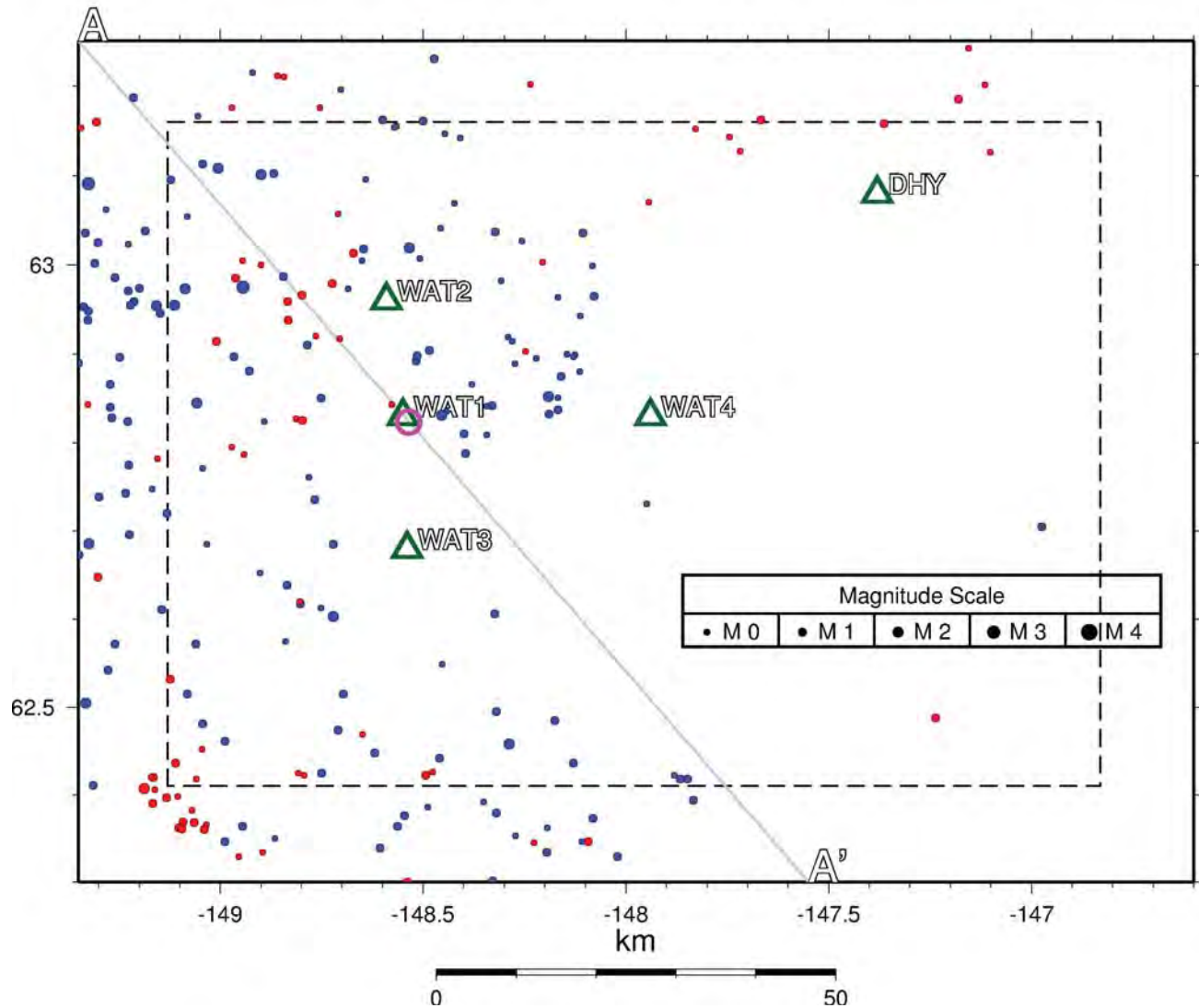
SUSITNA-WATANA HYDROELECTRIC PROJECT

NW-SE CROSS SECTION
SEISMICITY 2010 THROUGH
NOVEMBER 15, 2012

02/26/13

FIGURE 16

Nov 16, 2012 - January 31, 2013



Seismicity after WAT sub-network was operational, with stations operating in that period. Blue epicenters signify hypocentral depths below 30 km. Gray line is cross-section line shown in Figure 18. Dashed line is RTS zone.



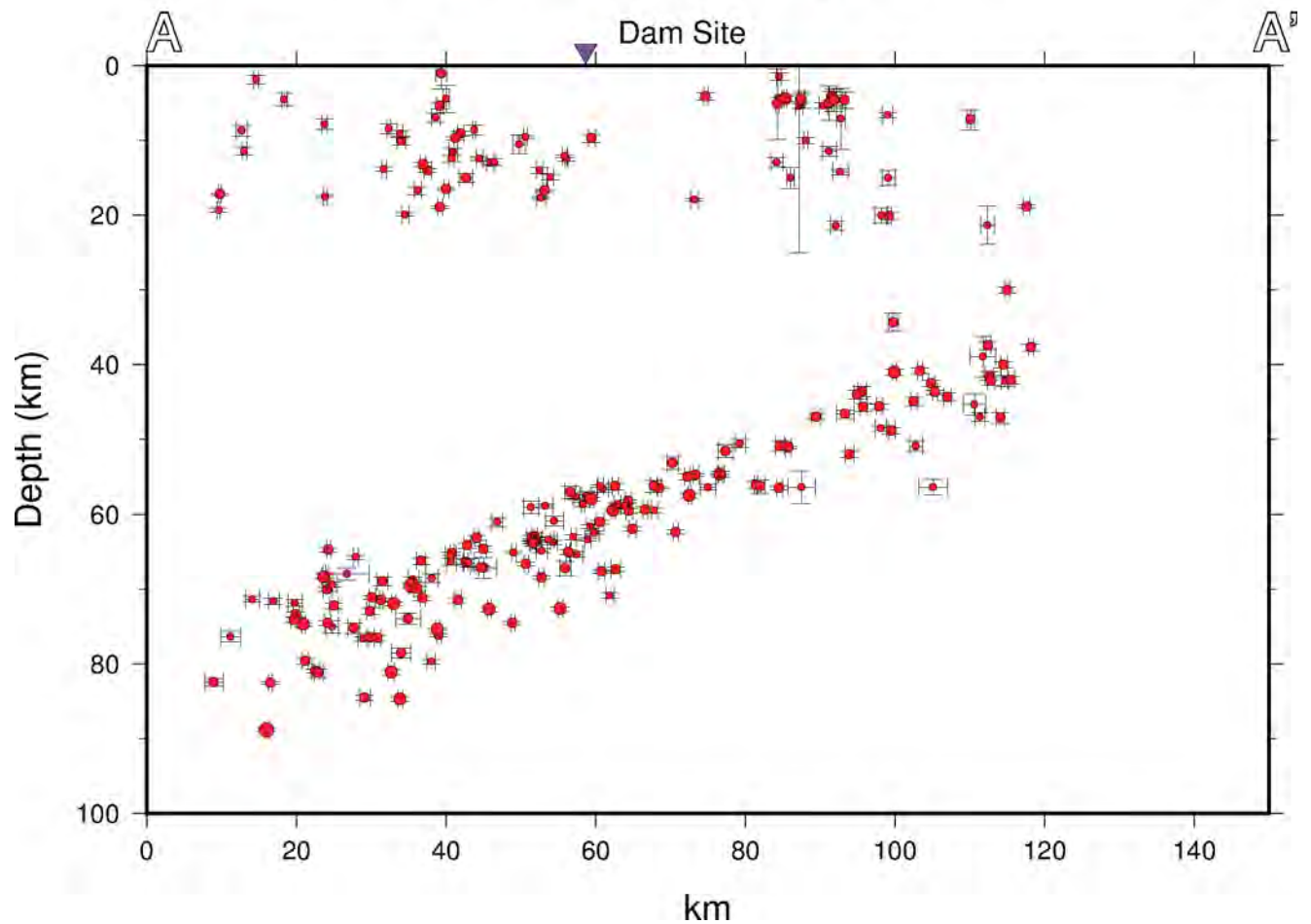
SUSITNA-WATANA HYDROELECTRIC PROJECT

SEISMICITY IN SITE AREA
NOVEMBER 16, 2012
THROUGH FEBRUARY 28, 2013

03/25/13

FIGURE 17

Nov 16, 2012 - January 31, 2013



Cross section of seismicity shown in Figure 17. One standard deviation location errors are shown. No vertical exaggeration.

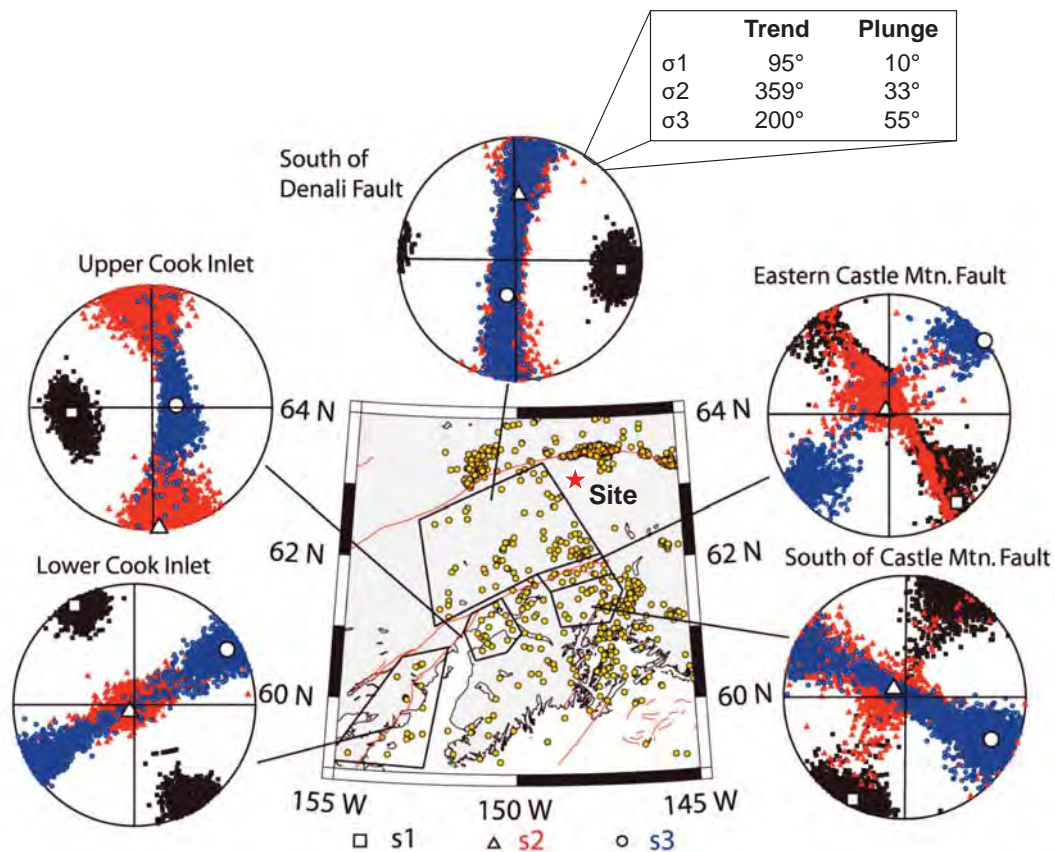


SUSITNA-WATANA HYDROELECTRIC PROJECT

NW-SE CROSS SECTION
NOVEMBER 16, 2012
THROUGH FEBRUARY 28, 2013

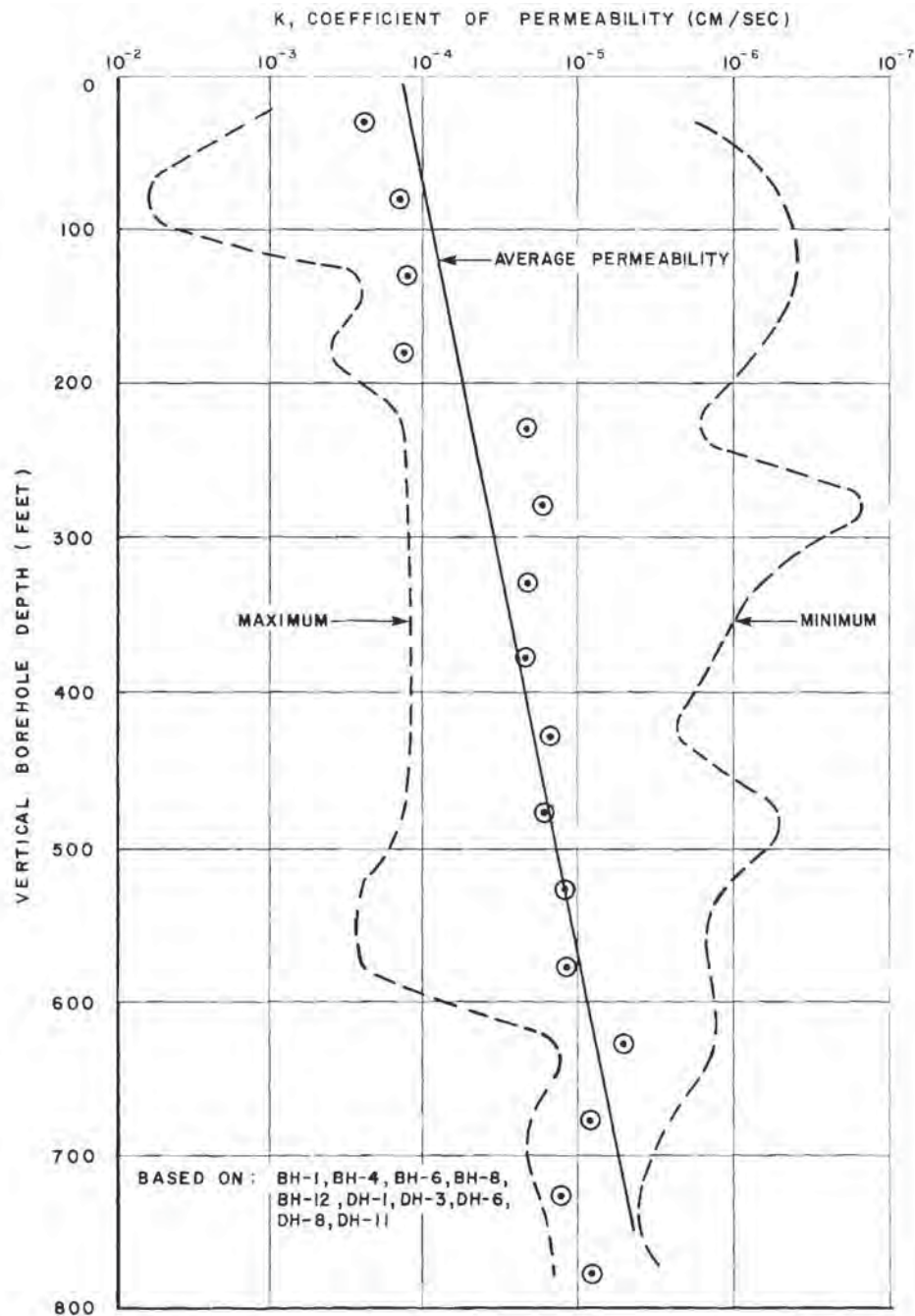
03/25/13

FIGURE 18



Larger symbols (square, triangle, and circle) show locations of the best-fitting maximum, intermediate, and least stress axis, respectively. Black, maximum stress s1; red, intermediate stress s2; blue, least stress s3. Yellow circles shown on map are locations of crustal earthquakes.

From Ruppert (2008)



WATANA ROCK PERMEABILITY

Summary of permeability values from Watana site boreholes. Figure 6.26 of Acres America (1981).

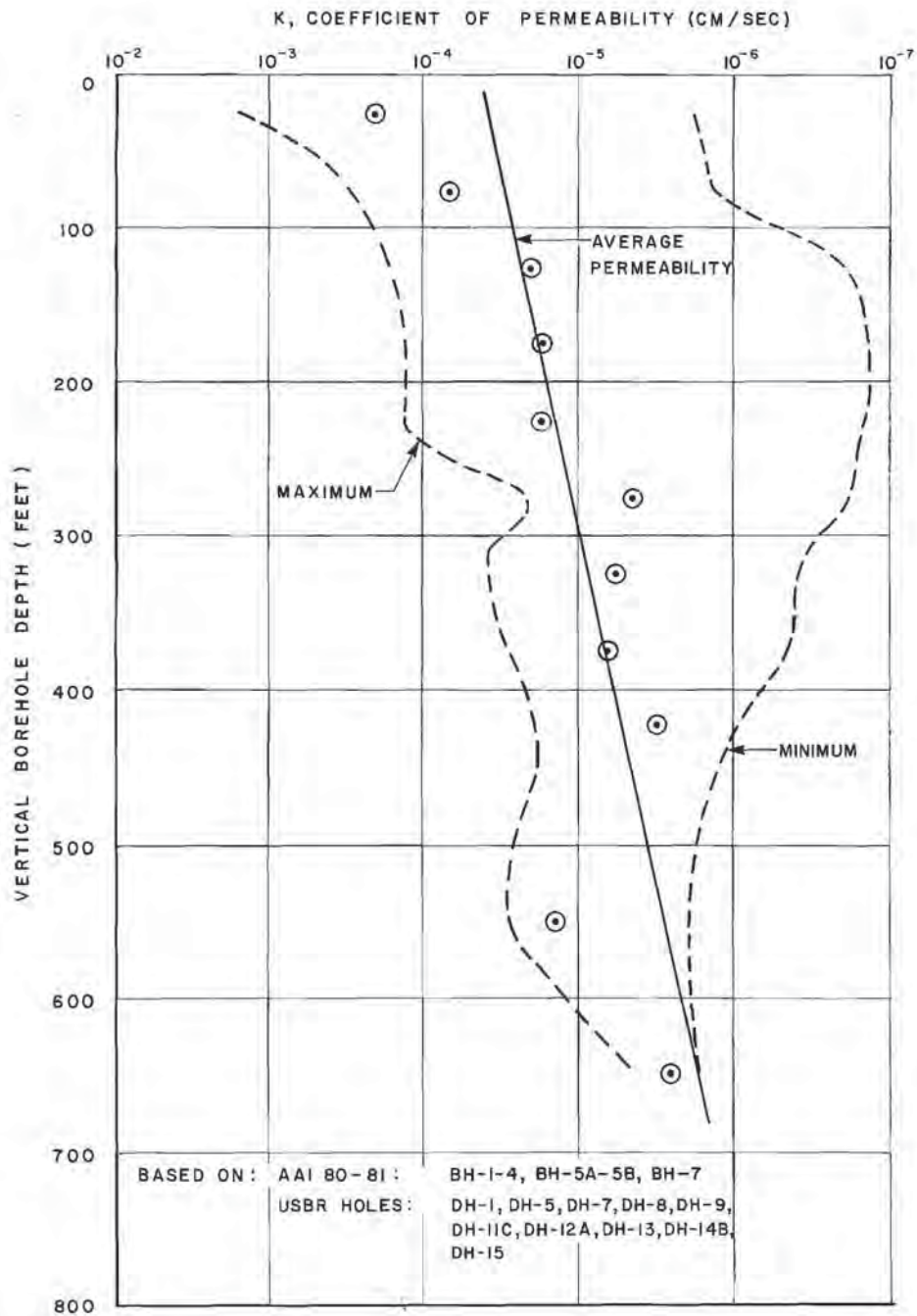


SUSITNA-WATANA HYDROELECTRIC PROJECT

SUMMARY OF PERMEABILITY VALUES FROM WATANA SITE BOREHOLES

02/22/13

FIGURE 20



DEVIL CANYON ROCK PERMEABILITY

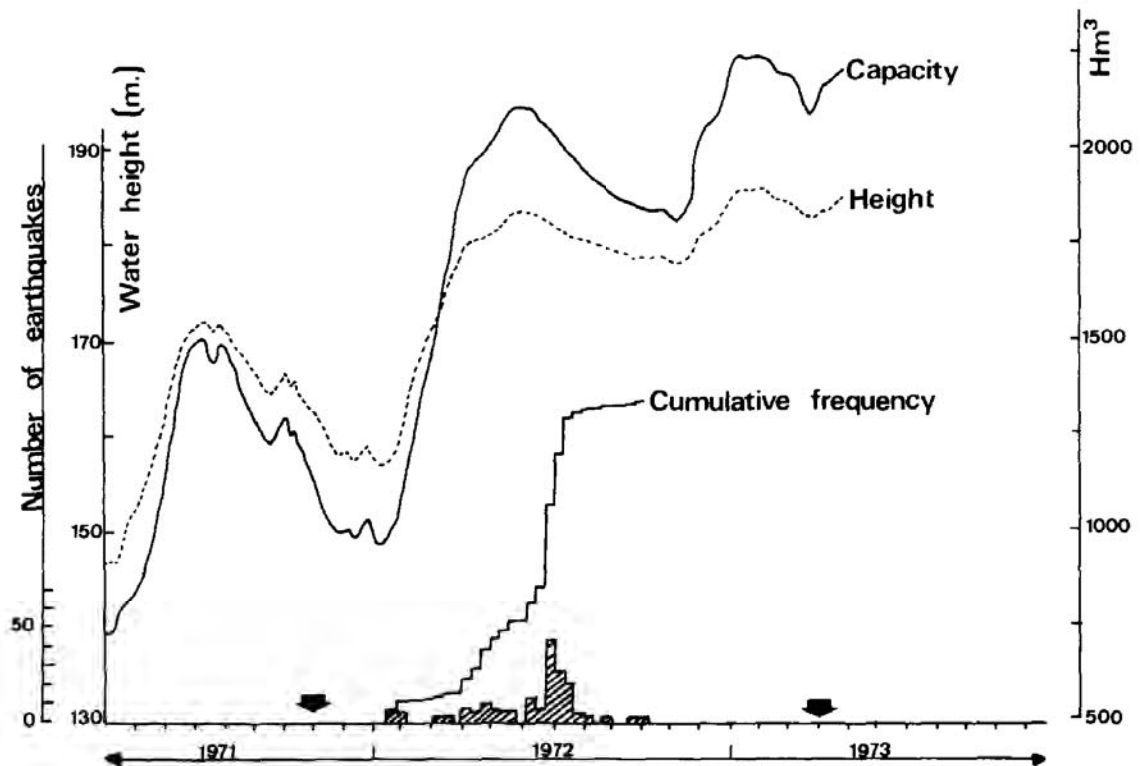


SUSITNA-WATANA HYDROELECTRIC PROJECT

**SUMMARY
OF PERMEABILITY VALUES
FROM DEVIL CANYON
SITE BOREHOLES**

02/22/13

FIGURE 21



From Bufo and Udias (1979). The large arrows mark the time of operation of the seismic instrumentation. Histogram shows the number of earthquakes recorded per week.

Appendix A

Case Number	Main Source	DAM NAME	RESERVOIR	RIVER	COUNTRY	LOCATION	DAM TYPE	LENGTH		HEIGHT		Calculation of Maximum Water depth (m)	VOLUME		DATE OF IMPOUNDMENT	BEDROCK	LARGEST MAGNITUDE	EVALUATION OF INDUCED SEISMICITY	
								feet	meters	feet	meters		acre-ft x10^3	m^3x10^6					
1 ICOLD-CIGB 2012	ABIQUIU DAM				United States	New Mexico	Earth	1801	549	354	108	103	1369	1689	1963 (dam completed)			No reported reservoir induced seismicity.	
2 ICOLD-CIGB 2012	ABITIBI CANYON				Canada	Cochrane, ONT	Gravity in Masonry or Concrete/Earth	1105	365	324	107	102	37	46	1933 (dam completed)			No reported reservoir induced seismicity.	
3 ICOLD-CIGB 2012	ACU (ENG. ARMANDO R.)				Brazil	Piranhas	Earth	8376	2553	135	41	37	1946	2400	1983 (dam completed)	Not Obtained	2.8	Questionable	
4 ICOLD-CIGB 2012	ADIGUZEL				Turkey	B. Menderes	Rock fill	1142	377	439	145	127	963	1188	1989 (dam completed)			No reported reservoir induced seismicity.	
5 ICOLD-CIGB 2012	ADOLFO RUIZ CORTINES				Mexico	Rio Mayo	Earth	2559	780	266	81	73	823	1015	1955 (dam completed)			No reported reservoir induced seismicity.	
6 ICOLD-CIGB 2012	AGIGAWA				Japan	Ena, Gifu	Rock fill	1302	430	309	102	84	39	48	1991 (dam completed)			No reported reservoir induced seismicity.	
7 ICOLD-CIGB 2012	AGUA DEL TORO				Argentina	Diamante	Arch	984	325	363	120	102	350	432	1976 (dam completed)			No reported reservoir induced seismicity.	
8 ICOLD-CIGB 2012	AGUAMILPA				Mexico	Santiago	Rock fill	1999	660	566	187	157	5634	6950	1994 (dam completed)			No reported reservoir induced seismicity.	
9 ICOLD-CIGB 2012	AGUZADERA, LA				Spain	AGUZADERA (BARRANCO AGUZADERA)	Rock fill	6568	2169	315	104	86	49	60	1999 (dam completed)			No reported reservoir induced seismicity.	
10 ICOLD-CIGB 2012	AKHANGARAN				Uzbekistan	Angren	Earth	4945	1633	303	100	90	211	260	1978 (dam completed)			No reported reservoir induced seismicity.	
11 Packer et al. 1979 & V	AKOSOMBO		Lake Volta		Ghana	Volta	Rock fill	2201	671	440	134	109	121607	150000	1965 (dam completed)	Sedimentary	MM V	Accepted case of reservoir induced macroearthquake activity.	
12 ICOLD-CIGB 2012	ALBERTO LLERAS C.		Guavio		Colombia	Guavio	Rock fill	1181	390	736	243	213	786	970	1989 (dam completed)			No reported reservoir induced seismicity.	
13 ICOLD-CIGB 2012	ALBIGNA				Switzerland	Albigna	Vicosoprano, Graubünden	Gravity in Masonry or Concrete	2298	759	348	115	97	58	71	1959 (dam completed)			No reported reservoir induced seismicity.
14 ICOLD-CIGB 2012	ALCANTARA II (SALTO JOSÉ MARÍA DE ORIOL)				Spain	TAJO	Buttress	1726	570	394	130	112	2563	3162	1969 (dam completed)			No reported reservoir induced seismicity.	
15 ICOLD-CIGB 2012	ALDEADAVILA				Spain	DUERO	Arch	757	250	424	140	122	93	114	1963 (dam completed)			No reported reservoir induced seismicity.	
16 ICOLD-CIGB 2012	ALDER				United States	NISQUALLY RIVER	Arch/Gravity in Masonry or Concrete	1372	453	306	101	83	241	298	1945 (dam completed)			No reported reservoir induced seismicity.	
17 ICOLD-CIGB 2012	ALICURA				Argentina	Limay	Earth	2665	880	394	130	124	2606	3215	1984 (dam completed)			No reported reservoir induced seismicity.	
18 Packer et al. 1979 & V	ALMENDRA		Tormes		Spain	Tormes	Concrete arch	1860	567	663	202	181	2146	2649	1970	Not Obtained	3.2	Accepted case of reservoir induced microearthquake activity.	
19 ICOLD-CIGB 2012	ALPE GERA				Italy	Cormor	Gravity in Masonry or Concrete	1599	528	527	174	144	55	68	1964 (dam completed)			No reported reservoir induced seismicity.	
20 ICOLD-CIGB 2012	ALTINKAYA				Turkey	Kizilirmak	Rock fill	1874	619	590	195	165	5	6	1988 (dam completed)			No reported reservoir induced seismicity.	
21 ICOLD-CIGB 2012	ALTO ANCHICAYA		Alto Anchicayá		Colombia	Anchicayá	Rock fill	727	240	424	140	122	36	45	1974 (dam completed)			No reported reservoir induced seismicity.	
22 ICOLD-CIGB 2012	ALTO LINDOSO				Portugal	Lima	Arch	899	297	333	110	92	307	379	1992 (dam completed)			No reported reservoir induced seismicity.	
23 ICOLD-CIGB 2012	ALVARO OBREGON*				Mexico	Tenasco	Gravity in Masonry or Concrete	266	88	787	260	230	11	13	1946 (dam completed)			No reported reservoir induced seismicity.	
24 ICOLD-CIGB 2012	AMBUKLAO				Philippines	Baguio	Rock fill	1290	426	397	131	113	254	313	1955 (dam completed)			No reported reservoir induced seismicity.	
25 ICOLD-CIGB 2012	AMIR-KABIR				I. Rep. Iran	KARADJ	Arch	1181	390	545	180	150	166	205	1963 (dam completed)			No reported reservoir induced seismicity.	
26 ICOLD-CIGB 2012	ANCIPIA				Italy	Troina	Buttress	766	253	339	112	94	25	30	1953 (dam completed)			No reported reservoir induced seismicity.	
27 ICOLD-CIGB 2012	ANDERSON RANCH				United States	SOUTH FORK BOISE RIVER	Earth/Rock fill	1245	411	421	139	132	503	621	1947 (dam completed)			No reported reservoir induced seismicity.	
28 ICOLD-CIGB 2012	ANDZHAN				Kirghizstan	Karadaria	Buttress	2786	920	348	115	97	1419	1750	1980 (dam completed)			No reported reservoir induced seismicity.	
29 ICOLD-CIGB 2012	ANGAT				Philippines	Angat	Rock fill	1720	568	397	131	113	689	850	1968 (dam completed)			No reported reservoir induced seismicity.	
30 ICOLD-CIGB 2012	ANKANG				China	Hanjiang	Gravity in Masonry or Concrete	1641	542	388	128	110	2092	2580	1998 (dam completed)			No reported reservoir induced seismicity.	
31 ICOLD-CIGB 2012	ANTONIVANOV TZI				Bulgaria	Vacha	Buttress/Gravity in Masonry or Concrete	1272	420	439	145	127	183	226	1975 (dam completed)			No reported reservoir induced seismicity.	
32 ICOLD-CIGB 2012	ARENOS				Spain	MUJARES	Rock fill	1296	428	318	105	87	111	137	1980 (dam completed)			No reported reservoir induced seismicity.	
33 ICOLD-CIGB 2012	ARIMINE				Japan	Wada	Gravity in Masonry or Concrete	1514	500	424	140	122	177	218	1961 (dam completed)			No reported reservoir induced seismicity.	
34 ICOLD-CIGB 2012	ARROWROCK				United States	BOISE RIVER	XX/Arch	1063	351	324	107	89	301	371	1915 (dam completed)			No reported reservoir induced seismicity.	
35 ICOLD-CIGB 2012	ASFALOU				Morocco	Asfalou	Arch	454	150	339	112	94	257	317	1999 (dam completed)			No reported reservoir induced seismicity.	
36 ICOLD-CIGB 2012	ATATURK				Turkey	Firat	Rock fill	5039	1664	512	169	139	39482	48700	1992 (dam completed)			No reported reservoir induced seismicity.	
37 ICOLD-CIGB 2012	ATAZAR, EL				Spain	LOZOYA	Arch	1466	484	406	134	116	345	425	1992 (dam completed)			No reported reservoir induced seismicity.	
38 ICOLD-CIGB 2012	BAD CREEK MAIN DAM				United States	BAD CR.WEST BAD CREEK	Earth/Rock fill	2398	792	333	110	105	34	42	1991 (dam completed)			No reported reservoir induced seismicity.	
39 ICOLD-CIGB 2012	BAELLS, LA				Spain	LLOBREGAT	Arch	1311	433	309	102	84	94	115	1976 (dam completed)			No reported reservoir induced seismicity.	
40 ICOLD-CIGB 2012	BAISHAN				China	Songhuajiang	Arch	2050	677	454	150	132	4313	5320	1986 (dam completed)			No reported reservoir induced seismicity.	
41 ICOLD-CIGB 2012	BAIXI(ZHEJIANG)				China	Baixi	Rock fill	1205	398	375	124	106	136	168	2001 (dam completed)			No reported reservoir induced seismicity.	
42 ICOLD-CIGB 2012	BAIYUN(HUNAN)				China	Wushui	Rock fill	606	200	363	120	102	292	360	1998 (dam completed)			No reported reservoir induced seismicity.	
43 Packer et al. 1979 & V	BAJINA BASTA		Bajina Basta		Yugoslavia	Drina	Hollow gravity concrete	1512	461	292	89	80	276	340	1966 (dam completed)	Sedimentary	3	Accepted case of reservoir induced microearthquake activity.	
44 ICOLD-CIGB 2012	BAO				Spain	BIBEY	Gravity in Masonry or Concrete	778	257	324	107	89	193	238	1960 (dam completed)			No reported reservoir induced seismicity.	
45 ICOLD-CIGB 2012	BAO				Dominican R.	Bao	Earth	1287	425	342	113	107	227	280	1985 (dam completed)			No reported reservoir induced seismicity.	
46 ICOLD-CIGB 2012	BAOZHUSI				China	Bailongjiang	Gravity in Masonry or Concrete	1590	525	400	132	114	2067	2550	1999 (dam completed)			No reported reservoir induced seismicity.	
47 ICOLD-CIGB 2012	BARCENA				Spain	SIL	Gravity in Masonry or Concrete	503	166	330	109	91	277	341	1960 (dam completed)			No reported reservoir induced seismicity.	
48 ICOLD-CIGB 2012	Bath Co. Pumped Stor				United States		Earth	0	0	351	116	110	36	44	1985 (dam completed)			No reported reservoir induced seismicity.	
49 ICOLD-CIGB 2012	BATH COUNTY P S UPPE				United States	LITTLE BACK CREEK	Earth/Rock fill	2032	671	424	140	133	38	46	1984 (dam completed)			No reported reservoir induced seismicity.	
50 ICOLD-CIGB 2012	BCI - TAILINGS				Philippines	Bayarong	Earth	3028	1000	348	115	109	49	60	1988 (dam completed)			No reported reservoir induced seismicity.	
51 ICOLD-CIGB 2012	BEAUREGARD				Italy	Dora Di Valgrisenche	Arch	1193	394	400	132	114	6	8	1960 (dam completed)			No reported reservoir induced seismicity.	
52 ICOLD-CIGB 2012	BELESAR				Spain	MIÑO	Arch	1514	500	400	132	114	530	654	1963 (dam completed)			No reported reservoir induced seismicity.	
53 ICOLD-CIGB 2012	BENAGEBER				Spain	TURIA	Gravity in Masonry or Concrete	672	222	333	110	92	179	221	1955 (dam completed)			No reported reservoir induced seismicity.	
54 Packer et al. 1979 & V	BENMORE		Lake Benmore		New Zealand	Waitaki	Earth fill	3140	957	387	118	86	1784	2200	1965 (dam completed)	Sedimentary	5	Accepted case of reservoir induced macroearthquake activity.	
55 Woodward-Clyde Con	BENNETT WAC		Not obtained.		Canada	Peace	Earth fill	6699	2042	600	183	173	60236	74300	1967 (dam completed)			No reported reservoir induced seismicity.	
56 ICOLD-CIGB 2012	BERKE				Turkey	Ceyhan	Arch	818	270	609	201	171	346	427	2001 (dam completed)			No reported reservoir induced seismicity.	
57 ICOLD-CIGB 2012	BEZNAR				Spain	IZBOR	Arch	1235	408	406	134	116	43	54	1986 (dam completed)			No reported reservoir induced seismicity.	
58 Woodward-Clyde Con	BHAKRA		Gobind Sagar		Indja	Sutlej	Concrete gravity	1699	518	741	226	158	7800	9621	1963			No reported reservoir induced seismicity.	
59 Gupta, 2002	BHATSA				India					289	88	79		947	1981	Not Obtained	4.9	Reported Case	
60 ICOLD-CIGB 2012	BHUMIBOL				Thailand	Ping	Gravity in Masonry or Concrete/Arch	1472	486	466	154	124	10914	13462	1964 (dam completed)			No reported reservoir induced seismicity.	
61 ICOLD-CIGB 2012	BIKOU				China	Bailongjiang	Rock fill	899	297	306	101	83	422	521	1978 (dam completed)			No reported reservoir induced seismicity.	
62 ICOLD-CIGB 2012	BINE EL OUIDANE				Morocco	El Abid	Arch	878	290	403	133	115	1122	1384	1953 (dam completed)			No reported reservoir induced seismicity.	
63 Packer et al. 1979 & V	BLOWERING		Lake Blowering		Australia	Tumut	Earth fill	2651	808	367	112	91	1320	1628	1968 (dam completed)	Igneous	3.5	Accepted case of reservoir induced macroearthquake activity.	
64 ICOLD-CIGB 2012	BLUE MESA				United States	GUNNISON RIVER	Earth	724	239	360	119	113	941	1160	1966 (dam completed)			No reported reservoir induced seismicity.	
65 ICOLD-CIGB 2012	BORT LES ORGUES				France	Dordogne	Gravity in Masonry or Concrete/Arch	1181	390	379	125	107	387	477	1951 (dam completed)			No reported reservoir induced seismicity.	
66 ICOLD-CIGB 2012	BOUNDARY				United States	PEND OREILLE	XX/Arch/Gravity in Masonry or Concrete	684	226	315	104	86	95	117	1967 (dam completed)			No reported reservoir induced seismicity.	
67 ICOLD-CIGB 2012	BOUROUMI				Algeria	Bouroumi	Earth	908	300	303	100	90	178	220	1986 (dam completed)			No reported reservoir induced seismicity.	
68 ICOLD-CIGB 2012	BRATSK				Russia	Angara	Gravity in Masonry or Concrete	4692	1430	410	125	107	137011	169000	1964 (dam completed)	Not Obtained	4.2	Reported Case	
69 ICOLD-CIGB 2012	BROWNEE				United States	Snake River	Rock fill/Gravity in Masonry or Concrete	1275	421	363	120	102	1420	1752	1958 (dam completed)			No reported reservoir induced seismicity.	
70 ICOLD-CIGB 2012	BUFFALO BILL				United States	SHOSHONE RIVER	XX/Arch	185	61	324	107	89	645	795	1910 (dam completed)			No reported reservoir induced seismicity.	
71 ICOLD-CIGB 2012	CA' SELVA				Italy	Silisia	Arch	733	242	336	111	93	34	42	1963 (dam completed)			No reported reservoir induced seismicity.	
72 Packer et al. 1979 & V	CABIN CREEK		Cabin Creek		U.S.A.	Clear Creek	Rock Fill	1490	454	161	49	46	15	18	1966	Not Obtained	--	Earthquake activity not related to reservoir impoundment.	
73 ICOLD-CIGB 2012	CABRA CORRAL	GRAL M. BELGRANO			Argentina	Juramento	Earth	1423	470	339	112	106	2513	3100	1973 (dam completed)			No reported reservoir induced seismicity.	
74 ICOLD-CIGB 2012	CABRIL				Portugal	Zêzere	Arch	878	290	412	136	118	583	719	1954 (dam completed)			No reported reservoir induced seismicity.	
75 ICOLD-CIGB 2012	CAHORA BASSA				Mocambique	Zambeze	Arch	972	321	518	171	141	42157	52000	1974 (dam completed)			No reported reservoir induced seismicity.	
76 Packer et al. 1979 & V	CAJIURU		Not Obtained		Brazil	Para	Concrete gravity	1119	341	75	23	20	156	92	1953 (dam completed)	Metamorphic	4	Questionable case of reservoir induced macroearthquake activity.	
77 ICOLD-CIGB 2012	CALIMA				Colombia	Calima	Rock fill	727	240	348	115	97	471	581	1964 (dam completed)			No reported reservoir induced seismicity.	
78 ICOLD-CIGB 20																			

94	ICOLD-CIGB 2012	CASITAS		COYOTE CREEK	United States	California	Earth	1847	610	309	102	97	287	354	1959 (dam completed)		No reported reservoir induced seismicity.		
95	ICOLD-CIGB 2012	CASTAGNARA METRAMO		Metramo	Italy	Reggio Calabria, Calabria	Rock fill	1802	595	306	101	83	22	27	1994 (dam completed)		No reported reservoir induced seismicity.		
96	ICOLD-CIGB 2012	CASTAIC		CASTAIC CREEK	United States	California	Earth	4800	1585	379	125	119	365	450	1973 (dam completed)		No reported reservoir induced seismicity.		
97	ICOLD-CIGB 2012	CASTELO DO BODE		Zézere	Portugal	Tomar, Santarém	Arch	1217	402	348	115	97	892	1100	1951 (dam completed)		No reported reservoir induced seismicity.		
98	ICOLD-CIGB 2012	CASTILLON		Verdon	France	Castellane, Alpes Haute Provence	Arch	606	200	303	100	90	121	149	1948 (dam completed)		No reported reservoir induced seismicity.		
99	ICOLD-CIGB 2012	CAVAGNOLI		Bavona	Switzerland	Bignasco, Ticino	Arch	969	320	336	111	93	24	29	1968 (dam completed)		No reported reservoir induced seismicity.		
100	ICOLD-CIGB 2012	CENAJO, EL		SEGURA	Spain	HELLIN, MORATALLA, ALBACETE/MURCIA	Gravity in Masonry or Concrete	609	201	309	102	84	354	436	1960 (dam completed)		No reported reservoir induced seismicity.		
101	ICOLD-CIGB 2012	CERNA PRINCIPAL		Cerna	Romania	Baile Herculane, Gorj	Rock fill	1036	342	333	110	92	101	124	1979 (dam completed)		No reported reservoir induced seismicity.		
102	ICOLD-CIGB 2012	CERRO PELADO		Grande	Argentina	Amboy, Cordoba	Earth	1242	410	315	104	99	300	370	1984 (dam completed)		No reported reservoir induced seismicity.		
103	ICOLD-CIGB 2012	CETHANA		0 Forth	Australia	DEVONPORT, Tasmania	Rock fill	645	213	333	110	92	88	109	1971 (dam completed)		No reported reservoir induced seismicity.		
104	ICOLD-CIGB 2012	CHAISHITAN		Nanpanjiang	China	Yiliang, YunnanProv.	Rock fill	957	316	312	103	85	354	437	1999 (dam completed)		No reported reservoir induced seismicity.		
105	ICOLD-CIGB 2012	CHAMBON (LE)		Romanche	France	Grenoble, Isère	Gravity in Masonry or Concrete	890	294	412	136	118	41	51	1934 (dam completed)		No reported reservoir induced seismicity.		
106	ICOLD-CIGB 2012	CHAMERA		Ravi	India	Banikhet, Himachal Pradesh	Earth	727	240	427	141	134	3172	3913	1994 (dam completed)		No reported reservoir induced seismicity.		
107	ICOLD-CIGB 2012	CHARVAK		Chirchik	Uzbekistan	Nearest town Tashkent, Uzbek.	Rock fill	2507	764	551	168	160	1621	2000	1977 (dam completed)	Not Obtained	5.3	Reported case.	
108	ICOLD-CIGB 2012	CHERUTHONI *		Cheruthoni	India	Idukki, Kerala	Gravity in Masonry or Concrete	1968	650	418	138	120	1618	1996	1976 (dam completed)		No reported reservoir induced seismicity.		
109	ICOLD-CIGB 2012	CHILATAN		Tepalcatepec	Mexico	Apatzingan, Jalisco	Earth	3482	1150	315	104	99	0	1	1986 (dam completed)		No reported reservoir induced seismicity.		
110	ICOLD-CIGB 2012	CHIOTAS		Bucera	Italy	Cuneo, Piemonte	Arch	696	230	394	130	112	24	30	1981 (dam completed)		No reported reservoir induced seismicity.		
111	Woodward-Clyde Con	CHIRKEY	Not obtained	Sulak	Russia	Nearest town Makhachkala, Daghest.	Concrete arch	1093	333	764	233	196	2254	2780	1975		No reported reservoir induced seismicity.		
112	Woodward-Clyde Con	CHIVOR	Not obtained	Bata	Colombia	Near Gateaque	Rock fill		310	778	237	215	661	815	1975		No reported reservoir induced seismicity.		
113	ICOLD-CIGB 2012	CIRATA		Citarum	Indonesia	Purwakarta, West Java	Rock fill	1372	453	379	125	107	2566	3165	1988 (dam completed)		No reported reservoir induced seismicity.		
114	Packer et al. 1979 & V	CLARK HILL	Clark Hill	Savannah	U.S.A.		Concrete gravity	5680	1731	172	52	47	2851	3517	1952 (dam completed)	Metamorphic	4.3	Accepted case of reservoir induced macroearthquake activity.	
115	ICOLD-CIGB 2012	COHILLA, LA		NANSA	Spain	TUDANCA, CANTABRIA	Arch	860	284	351	116	98	10	12	1950 (dam completed)		No reported reservoir induced seismicity.		
116	ICOLD-CIGB 2012	COLBUN		Maule	Chile	Linares, VII Región	Earth	1665	550	351	116	110	892	1100	1985 (dam completed)		No reported reservoir induced seismicity.		
117	ICOLD-CIGB 2012	CONDOROMA		Colca	Peru	Chivay, Arequipa	Rock fill	1556	514	306	101	83	231	285	1985 (dam completed)		No reported reservoir induced seismicity.		
118	Packer et al. 1979 & V	CONTRA	Vogorno	Verzasca	Switzerland		Concrete arch	1246	380	722	220	183	70	86	1964		Igneous	3	Accepted case of reservoir induced microearthquake activity.
119	ICOLD-CIGB 2012	CONTRERAS		CABRIEL	Spain	MINGLANILLA, VILLAGORDO DEL	Gravity in Masonry or Concrete	730	241	388	128	110	709	874	1974 (dam completed)		No reported reservoir induced seismicity.		
120	ICOLD-CIGB 2012	COPETON		0 Gwydir	Australia	INVERELL, New South West Australiales	Rock fill	4494	1484	342	113	95	1106	1364	1976 (dam completed)		No reported reservoir induced seismicity.		
121	ICOLD-CIGB 2012	CORTES II		JUCAR	Spain	CORTES DE PALLAS, VALENCIA	Arch	945	312	351	116	98	92	113	1988 (dam completed)		No reported reservoir induced seismicity.		
122	ICOLD-CIGB 2012	COUGAR		SOUTH FORK MCKENZIE RIVE	United States	Oregon	Rock fill	1478	488	478	158	128	219	270	1964 (dam completed)		No reported reservoir induced seismicity.		
123	Packer et al. 1979 & I	COYOTE VALLEY	LAKE MEDOCI	East Fork Russian River	United States	California	Earth		1070	164	50	22		151	1959		Metamorphic	5.2	Accepted case of reservoir induced macroearthquake activity.
124	ICOLD-CIGB 2012	CUEVAS DE ALMANZORA		ALMANZORA	Spain	CUEVAS DEL ALMANZORA, ALMERIA	Rock fill	2026	669	354	117	99	137	169	1986 (date of completion)		No reported reservoir induced seismicity.		
125	ICOLD-CIGB 2012	CURNERA		Rein da Curnera	Switzerland	Sedrun, Graubünden	Arch	1060	350	463	153	123	33	41	1966 (date of completion)		No reported reservoir induced seismicity.		
126	Gupta, 2002	Dahua			China					244	74.5	67		420	1982		Not Obtained	4.5	Reported case.
127	ICOLD-CIGB 2012	DALESICE		Jihlava	Czech Rep.	Trebic, South Moravia	Rock fill	908	300	303	100	90	103	127	1979 (dam completed)		No reported reservoir induced seismicity.		
128	Woodward-Clyde Con	DANIEL JOHNSON (MANIC 5)	Not obtained.	Manicouagan	Canada	Nearest town Baie Comeau, QUE	Concrete arch	4311	1314	702	214	154	115001	141851	1968 (dam completed)		No reported reservoir induced seismicity.		
129	ICOLD-CIGB 2012	DANIEL PALACIOS		Paute	Ecuador	Cuenca, Azuay	Arch	1272	420	515	170	140	97	120	1982 (dam completed)		No reported reservoir induced seismicity.		
130	ICOLD-CIGB 2012	DANJIANGKOU		Hanjiang	China	Nearest town Danjiang, HubeiProv.	Gravity in Masonry or Concrete	8182	2494	318	97	87	16936	20890	1973 (dam completed)	Not Obtained	4.7	Reported Case	
131	Woodward-Clyde Con	DARTMOUTH	Lake Dartmouth	Mitta-Mitta	Australia	Nearest town MITTA MITTA, Victoria	Rock fill	2198	670	591	180	158	3243	4000	1975		No reported reservoir induced seisnUcity.		
132	ICOLD-CIGB 2012	DCHAR EL OUED		Oum Er Rbia	Morocco	Zawiat Echeikh, Beni Mellal	Rock fill	1211	400	306	101	83	600	740	2001 (dam completed)		No reported reservoir induced seismicity.		
133	ICOLD-CIGB 2012	DEJI		Dajiaxi	China	Taizhong, TaiwanProv.	Arch	878	290	548	181	151	188	232	1974 (dam completed)		No reported reservoir induced seismicity.		
134	ICOLD-CIGB 2012	DERBENDIKHAN		Diyala	Iraq	Sulayma-Niya, Sulayma-Niya	Rock fill	1620	535	388	128	110	2432	3000	1961 (dam completed)		No reported reservoir induced seismicity.		
135	ICOLD-CIGB 2012	DETROIT		NORTH SANTIAM RIVER	United States	Oregon	Gravity in Masonry or Concrete	1460	482	427	141	123	455	561	1953 (dam completed)		No reported reservoir induced seismicity.		
136	ICOLD-CIGB 2012	DEZ		DEZ	I. Rep. Iran	DEZFUL, KHUZESTAN	Arch	642	212	615	203	173	2708	3340	1962 (dam completed)		No reported reservoir induced seismicity.		
137	Gupta, 2002	Dhamni			India					194	59	53		285	1983		Not Obtained		Reported Case
138	ICOLD-CIGB 2012	DIABLO		SKAGIT R	United States	Washington	XX/Arch/Gravity in Masonry or Concrete	1090	360	360	119	101	88	109	1930 (dam completed)		No reported reservoir induced seismicity.		
139	ICOLD-CIGB 2012	DOKAN		Lesser Zab	Iraq	Sulayma-Niya, Sulayma-Niya	Arch	1090	360	351	116	98	5513	6800	1959 (dam completed)		No reported reservoir induced seismicity.		
140	ICOLD-CIGB 2012	Don Pedro Main		Tuolumne River	United States	California	Earth/Rock fill	1753	579	539	178	169	2300	2837	1971 (dam completed)		No reported reservoir induced seismicity.		
141	ICOLD-CIGB 2012	DONGFENG(GUIZHOU,QINGZHEN)		Wujiang	China	Qingzhen, GuizhouProv.	Arch	769	254	491	162	132	831	1025	1997 (dam completed)		No reported reservoir induced seismicity.		
142	ICOLD-CIGB 2012	DONGGAODAO			China	Xianggang, Hongkong.	Rock fill	1384	457	309	102	84	230	284	1997 (dam completed)		No reported reservoir induced seismicity.		
143	ICOLD-CIGB 2012	DONGJIANG		Laishui	China	Nearest town Laiyang, HunanProv.	Concrete Arch	1437	438	515	157	127	7416	9148	1992 (dam completed)	Not Obtained	3.2	Reported Case	
144	ICOLD-CIGB 2012	DRAGAN		Dragan	Romania	Huedin, Cluj	Arch	1284	424	363	120	102	91	112	1987 (dam completed)		No reported reservoir induced seismicity.		
145	ICOLD-CIGB 2012	DROSSEN	Mooserboden	Kapruner Ache	Austria	Zell/See, Salzburg	Arch	1081	357	339	112	94	71	87	1955 (dam completed)		No reported reservoir induced seismicity.		
146	Woodward-Clyde Con	DWORSHAK	Not obtained	Cleanwater	U.S.A.		Concrete gravity			719	219	182	3453	4259	1974		No reported reservoir induced seismicity.		
147	ICOLD-CIGB 2012	EGREKKAYA		Sey	Turkey	Kizilcahamam, Ankara	Earth	1030	340	303	100	90	92	113	1992 (dam completed)		No reported reservoir induced seismicity.		
148	ICOLD-CIGB 2012	EL CAJON		Comayagua	Honduras	San Pedro Sula, Yoro, Cortès, Comayagua	Arch	1157	382	709	234	204	5744	7085	1984 (dam completed)		No reported reservoir induced seismicity.		
149	Packer et al. 1979 & V	EL GRADO	Not obtained	Cinca	Spain		Concrete gravity	1312	400	289	88	79	Not Obtain	Not obtained	Not Obtained	--	Earthquake activity not related to reservoir impoundment.		
150	ICOLD-CIGB 2012	EL INFIERNILLO		Balsas	Mexico	Apatzingan, Michoacán	Earth	1060	350	448	148	141	7572	9340	1963 (dam completed)	Not Obtained	--	No reported reservoir induced seismicity.	
151	ICOLD-CIGB 2012	EMBORÇAÇÃO		Paranaíba	Brazil	Nearest town Araguari, Minas Gerais /Goias	Rock fill Earth	4987	1520	518	158	150	14259	17588	1982 (dam completed)	Not Obtained	2	Reported Case	
152	Packer et al. 1979 & V	EMOSSON	Lake Emosson	Barbarine	Switzerland	Near Martigny	Concrete arch	1736	529	590	180	170	182	225	1973		Igneous	3	Accepted case of reservoir induced microearthquake activity.
153	ICOLD-CIGB 2012	ESCALES		NOGUERA RIBAGORZANA	Spain	SOPEIRA Y TREMP, HUESCA	Gravity in Masonry or Concrete	606	200	379	125	107	125	154	1955 (dam completed)		No reported reservoir induced seismicity.		
154	Packer et al. 1979 & V	EUCUMBENE	Lake Eucumbene	Eucumbene	Australia	Nearest town COOMA, New South West Australiales	Earth fill	1900	579	381	116	106	3890	4798	1958 (dam completed)	Not Obtained	5	Accepted case of reservoir induced macroearthquake activity.	
155	ICOLD-CIGB 2012	EUME		EUME	Spain	CAPELA, A, MONFERO, CORUÑA, A	Arch	860	284	312	103	85	100	123	1960 (dam completed)		No reported reservoir induced seismicity.		
156	ICOLD-CIGB 2012	EVINOS	Evinos	Merced River	Greece	Nafpaktos, Sterea Hellas	Earth	1938	640	375	124	118	92	113	2001 (dam completed)		No reported reservoir induced seismicity.		
157	ICOLD-CIGB 2012	Exchequer Main		Merced River	United States	California	Rock fill/Earth	1293	427	451	149	142	1200	1480	1966 (dam completed)		No reported reservoir induced seismicity.		
158	Packer et al. 1979	Fairfield	Lake Monticello		United States	South Carolina	Earth			0		48		500	1977		Igneous	2.5	Accepted case of reservoir induced microearthquake activity.
159	ICOLD-CIGB 2012	FEICUI		Beishihé	China	Taipei, TaiwanProv.	Arch	1544	510	372	123	105	329	406	1987 (dam completed)		No reported reservoir induced seismicity.		
160	ICOLD-CIGB 2012	FENG TAN(HUNAN)		Yushui	China	Yualing, HunanProv.	Arch	1478	488	342	113	95	1411	1740	1979 (dam completed)		No reported reservoir induced seismicity.		
161	ICOLD-CIGB 2012	FIERZE		Drin	Albania	Nearest town B.Curri, Tropoje	Rock fill	1312	400	548	167	159	2189	2700	1978 (dam completed)	Not Obtained	2.6	Reported Case	
162	ICOLD-CIGB 2012	FINSTERTAL		Finstertalbach	Austria	Oetz, Tyrol	Rock fill	1986	656	454	150	132	50	62	1980 (dam completed)		No reported reservoir induced seismicity.		
163	ICOLD-CIGB 2012	FLAMING GORGE		GREEN RIVER	United States	Utah	XX/Arch	1187	392	463	153	123	4003	4938	1964 (dam completed)		No reported reservoir induced seismicity.		
164	ICOLD-CIGB 2012	FLORENTINO AMEGHINO		Chubut	Argentina	Gaiman, Chubut	Buttress	772	255	342	113	95	1504	1855	1963 (dam completed)		No reported reservoir induced seismicity.		
165	ICOLD-CIGB 2012	FOLSOM		AMERICAN RIVER	United States	California	XX/Gravity in Masonry or Concrete	1293	427	315	104	86	1120	1382	1956 (dam completed)		No reported reservoir induced seismicity.		
166	ICOLD-CIGB 2012	Fontana		Little Tennessee River	United States	North Carolina	XX/Gravity in Masonry or Concrete	2183	721	442	146	128	1443	1780	1944 (dam completed)		No reported reservoir induced seismicity.		
167	ICOLD-CIGB 2012	FORTE BUSO		Travignolo	Italy	Trento, Trentino Alto Adige	Arch	972	321	333	110	92	26	32	1952 (dam completed)		No reported reservoir induced seismicity.		
168	ICOLD-CIGB 2012	FORTUNA		Rio Chiriqui	Panama		Rock fill	0	0	303	100	90	130	160	1993 (dam completed)		No reported reservoir induced seismicity.		
169	ICOLD-CIGB 2012	FOZ DO AREIA		Iguaçu	Brazil	Bituruna, Parana	Rock fill/Gravity in Masonry or Concrete	2574	850	484	160	130	4945	6100	1980 (dam completed)		No reported reservoir induced seismicity.		
170	Gupta, 2002	Foziling			China					243	74	67		470	1954		Not Obtained	4.5	Reported case.
171	ICOLD-CIGB 2012	FRERA		Belviso	Italy	Sondrio, Lombardia	Arch	957	316	418	138	120	41	50	1959 (dam completed)		No reported reservoir induced seismicity.		
172	ICOLD-CIGB 2012	FURNAS		Grande	Brazil	Alpinopolis, Minas Gerais	Rock fill/Gravity in Masonry or Concrete	1678	554	385	127	109	18606	22950	1963 (dam completed)		No reported reservoir induced seismicity.		

192 ICOLD-CIGB 2012	GRAND COULEE		COLUMBIA RIVER	United States	Washington	XX/Gravity in Masonry or Concrete	5236	1729	509	168	138	9562	11795	1942 (dam completed)		No reported reservoir induced seismicity.
193 Woodward-Clyde Con	GRAND DIXENCE	Not obtained	Dixence	Switzerland	Near Heremence	Concrete gravity		695	935	285	248	324	400	1962		No reported reservoir induced seismicity.
194 ICOLD-CIGB 2012	GRAND/MAISON		Eau D'Olle	France	Grenoble, Isère	Rock fill/Earth	1665	550	484	160	152	111	137	1984 (dam completed)		No reported reservoir induced seismicity.
195 Packer et al. 1979 & V	GRANDVAL	Not obtained	Truyere	France		Concrete multiple	1312	400	262	80	78	237	292	1959	Not Obtained	V Accepted case of reservoir induced macroearthquake activity.
196 ICOLD-CIGB 2012	GREEN PETER		MIDDLE SANTIAM RIVER	United States	Oregon	Gravity in Masonry or Concrete	1399	462	348	115	97	430	530	1967 (dam completed)		No reported reservoir induced seismicity.
197 ICOLD-CIGB 2012	GROSS		SOUTH BOULDER CREEK	United States	Colorado	XX/Gravity in Masonry or Concrete	1005	332	315	104	86	47	59	1955 (dam completed)		No reported reservoir induced seismicity.
198 ICOLD-CIGB 2012	GUDONGKOU		Gufuhe	China	Xinshan, HubeiProv.	Rock fill	584	193	357	118	100	112	138	2001 (dam completed)		No reported reservoir induced seismicity.
199 ICOLD-CIGB 2012	GURI		Caroni	Venezuela	Nearest town Ciudad Guayana, Bolivar	Gravity in Masonry or Concrete Earth	24364	7426	531	162	132	109446	135000	1986 (dam completed)		No reported reservoir induced seismicity.
200 ICOLD-CIGB 2012	GUXIAN		Luohe	China	Luonin, HenanProv.	Gravity in Masonry or Concrete	954	315	379	125	107	953	1175	1995 (dam completed)		No reported reservoir induced seismicity.
201 ICOLD-CIGB 2012	HASAN UGURLU		Yesilirmak	Turkey	Carsamba, Samsun	Rock fill	1226	405	542	179	149	871	1074	1981 (dam completed)		No reported reservoir induced seismicity.
202 ICOLD-CIGB 2012	HASE		Omi	Japan	Himeji, Hyogo	Gravity in Masonry or Concrete	769	254	309	102	84	8	10	1992 (dam completed)		No reported reservoir induced seismicity.
203 ICOLD-CIGB 2012	HASSAN 1er		Lakhdar	Morocco	Demate, Azilal	Earth/Rock fill	1151	380	439	145	138	213	263	1986 (dam completed)		No reported reservoir induced seismicity.
204 ICOLD-CIGB 2012	HATANAGI NO1		Oi	Japan	Shizuoka, Shizuoka	Buttress	815	269	379	125	107	87	107	1962 (dam completed)		No reported reservoir induced seismicity.
205 ICOLD-CIGB 2012	HEIQUAN		Baokuhe	China	Datong, QinghaiProv.	Rock fill	1311	433	375	124	106	148	182	2001 (dam completed)		No reported reservoir induced seismicity.
206 ICOLD-CIGB 2012	Hell Hole		Rubicon River	United States	California	Rock fill	1450	479	379	125	107	208	257	1966 (dam completed)		No reported reservoir induced seismicity.
207 ICOLD-CIGB 2012	HELLS CANYON		Snake River	United States	Idaho	Gravity in Masonry or Concrete/XX	839	277	306	101	83	188	232	1967 (dam completed)		No reported reservoir induced seismicity.
208 Packer et al. 1979 & V	HENDRIK VERVOERD	Hendrik Verwo	Orange	South Africa		Concrete double arch	1968	600	217	66	45	4053	5000	1970	Sedimentary	2 Accepted case of reservoir induced microearthquake activity.
209 ICOLD-CIGB 2012	HIGH ASWAN DAM	Nasser	Nile	Egypt	Nearest town Aswan, Aswan	Rock fill	11811	3600	364	111	111	131336	162000	1972 (dam completed)	Sedimentary	5.4 Accepted case of the induced seismicity.
210 ICOLD-CIGB 2012	HILLS CREEK		MIDDLE FORK WILLAMETTE R	United States	Oregon	Earth	2062	681	315	104	99	356	439	1962 (dam completed)		No reported reservoir induced seismicity.
211 ICOLD-CIGB 2012	HITOTSUSE		Hitotsuse	Japan	Saito, Miyazaki	Arch	1260	416	394	130	112	212	261	1963 (dam completed)		No reported reservoir induced seismicity.
212 ICOLD-CIGB 2012	HOA BINH		Da	Viet Nam	Nearest town Hoa Binh, Hoa Binh	Rock fill	2165	660	420	128	122	7661	9450	1994 (dam completed)	Not Obtained	4.9 Reported Case
213 ICOLD-CIGB 2012	HOHEIKYO		Niikappu	Japan	Tomakomai, Hokkaido	Rock fill	987	326	312	103	85	118	145	1974 (dam completed)		No reported reservoir induced seismicity.
214 ICOLD-CIGB 2012	HONGRIN NORD	Hongrin	Hongrin	Switzerland	Aigle, Vaud	Arch	984	325	379	125	107	43	53	1969 (dam completed)		No reported reservoir induced seismicity.
215 Packer et al. 1979 & V	HOOVER	Lake Mead	Colorado	U.S.A.		Concrete arch - gravity	1243	379	732	223	166	30237	37297	1936 (dam completed)	Igneous	5 Accepted case of reservoir induced macroearthquake activity.
216 ICOLD-CIGB 2012	HUANGLONGTAN(HUBEI,SHIYAN)		Duhe	China	Shiyan, HubeiProv.	Gravity in Masonry or Concrete	1123	371	324	107	89	942	1163	1978 (dam completed)		No reported reservoir induced seismicity.
217 ICOLD-CIGB 2012	HUITES *		Fuerte	Mexico	El Fuerte, Sinaloa	Gravity in Masonry or Concrete/Arch	1302	430	460	152	122	3703	4568	1995 (dam completed)		No reported reservoir induced seismicity.
218 ICOLD-CIGB 2012	HUNANZHEN		Lanjiang	China	Nearest town Qluxian, ZhejiangProv.	Buttress	1444	440	423	129	123	1670	2060	1979 (dam completed)	Not Obtained	2.8 Reported Case
219 ICOLD-CIGB 2012	HUNGRY HORSE		SOUTH FORK FLATHEAD RIVE	United States	Montana	XX/Arch	1953	645	521	172	142	3588	4426	1953 (dam completed)		No reported reservoir induced seismicity.
220 Gupta, 2002	Hungshi			India					131	40	36		610	1970	Not Obtained	Reported Case
221 ICOLD-CIGB 2012	HWANGSUWON		Hwangsuwon	Korea N (RDK)	Pungsan , Ryanggangdo	Gravity in Masonry or Concrete	1787	590	306	101	83	470	580	1959 (dam completed)		No reported reservoir induced seismicity.
222 ICOLD-CIGB 2012	IDAMALAYAR *	Not obtained	Idamalayar	India	K/Mangalam, Kerala	Gravity in Masonry or Concrete	1136	375	303	100	90	935	1153	1985 (dam completed)		No reported reservoir induced seismicity.
223 Woodward-Clyde Con	IDUKKI		Periyar	India		Concrete arch			551	168	158	1182	1460	1974	Not Obtained	3.5 Reported Case
224 ICOLD-CIGB 2012	IKARI		Sagae	Japan	Sagae, Yamagata	Rock fill	1544	510	339	112	94	88	109	1990 (dam completed)		No reported reservoir induced seismicity.
225 ICOLD-CIGB 2012	IKAWA		Oi	Japan	Shizuoka, Shizuoka	Buttress	736	243	315	104	86	122	150	1957 (dam completed)		No reported reservoir induced seismicity.
226 ICOLD-CIGB 2012	IKEHARA		Kitayama	Japan	Kumano, Nara	Arch	1393	460	336	111	93	274	338	1964 (dam completed)		No reported reservoir induced seismicity.
227 ICOLD-CIGB 2012	INGURI		Inguri	Georgia	Zugdidi, Georgia	Arch	2059	680	824	272	242	892	1100	1980 (dam completed)		No reported reservoir induced seismicity.
228 ICOLD-CIGB 2012	Isacheon		Isa	Korea	Sunchon, Chonnam	Rock fill	1705	563	303	100	90	170	210	1992 (dam completed)		No reported reservoir induced seismicity.
229 ICOLD-CIGB 2012	ITA		Uruguai	Brazil	Nova Ita / Arativa, Santa Catarina	Rock fill	2665	880	379	125	107	4135	5100	2000 (dam completed)		No reported reservoir induced seismicity.
230 ICOLD-CIGB 2012	ITAIPU	Itaipu	Parana	Paraguay	Hemandarias, Parana	Gravity in Masonry or Concrete/Rock fill /Earth/Buttress	24225	8000	594	196	186	23511	29000	1983 (dam completed)		No reported reservoir induced seismicity.
231 ICOLD-CIGB 2012	ITAPARICA		Sao Francisco	Brazil	Petrolandia, Pernambuco	Rock fill	14326	4731	318	105	87	8739	10780	1988 (dam completed)		No reported reservoir induced seismicity.
232 Packer et al. 1979	Itezहितzhi		Kafue	Zambia		Rock fill			213	65	62		5000	1976	Igneous	4 Accepted case of reservoir induced macroearthquake activity.
233 ICOLD-CIGB 2012	ITUMBIARA		Paranaiba	Brazil	Itumbiara, Goias	Earth/Gravity in Masonry or Concrete	20591	6800	333	110	105	13782	17000	1980 (dam completed)		No reported reservoir induced seismicity.
234 ICOLD-CIGB 2012	IWAYA		Mase	Japan	Minokamo, Gifu	Rock fill	1108	366	388	128	110	141	174	1976 (dam completed)		No reported reservoir induced seismicity.
235 ICOLD-CIGB 2012	IZNAJAR		GENIL	Spain	RUTE, CUEVAS SAN MARCOS, CORDOBA	Gravity in Masonry or Concrete	1232	407	369	122	104	865	1067	1969 (dam completed)		No reported reservoir induced seismicity.
236 ICOLD-CIGB 2012	IZVORUL MUNTELUI		Bistrita	Romania	Piatra Neamt, Neamt	Gravity in Masonry or Concrete	1317	435	385	127	109	997	1230	1961 (dam completed)		No reported reservoir induced seismicity.
237 ICOLD-CIGB 2012	JAMRANI		Gola	India	Kathgodam, Uttaranchal	Earth	2316	765	424	140	133	167	207	1990 (dam completed)		No reported reservoir induced seismicity.
238 ICOLD-CIGB 2012	JATILUHUR		Citarum	Indonesia	Purwakarta, West Java	Rock fill	3694	1220	318	105	87	2072	2556	1967 (dam completed)		No reported reservoir induced seismicity.
239 ICOLD-CIGB 2012	JIANGYA		Luoshui	China	Cili, HunanProv.	Gravity in Masonry or Concrete	1017	336	388	128	110	1419	1750	1999 (dam completed)		No reported reservoir induced seismicity.
240 ICOLD-CIGB 2012	JIGUEY		Nizao	Dominican R.	Palo de Caja, Peravia	Arch	951	314	333	110	92	136	168	1992 (dam completed)		No reported reservoir induced seismicity.
241 ICOLD-CIGB 2012	JILINTAI		Keshihe	China	Nileke, XinjiangReg.	Rock fill	1187	392	460	152	122	1978	2440	2001 (dam completed)		No reported reservoir induced seismicity.
242 ICOLD-CIGB 2012	JINSHUITAN		Longqianxi	China	Yunhe, ZhejiangProv.	Arch	1063	351	309	102	84	1129	1393	1986 (dam completed)		No reported reservoir induced seismicity.
243 ICOLD-CIGB 2012	JIROFT		HALIL ROOD	I. Rep. Iran	JIROFT, KERMAN	Arch	757	250	406	134	116	349	430	1991 (dam completed)		No reported reservoir induced seismicity.
244 Packer et al. 1979 & V	JOCASSEE	Lake Jocassee	Keowee	U.S.A.	South Carolina	Earth and rock fill	1948	594	436	133	111	1288	1588	1973 (dam completed)	Metamorphic	3.2 Accepted case of reservoir induced macroearthquake activity.
245 ICOLD-CIGB 2012	JOZANKEI		Otarunai	Japan	Sapporo, Hokkaido	Gravity in Masonry or Concrete	1242	410	357	118	100	67	82	1990 (dam completed)		No reported reservoir induced seismicity.
246 ICOLD-CIGB 2012	JUAMJOJOL	Sangsaho	Isa	Korea	Yochon, Jeonnam	Rock fill	1705	563	303	100	90	203	250	1992 (dam completed)		No reported reservoir induced seismicity.
247 ICOLD-CIGB 2012	KAJIGAWA		Kaji	Japan	Shibata, Nigata	Gravity in Masonry or Concrete	866	286	324	107	89	18	23	1974 (dam completed)		No reported reservoir induced seismicity.
248 ICOLD-CIGB 2012	KAKKI *	Not obtained	Kakki	India	Vandiperiyar, Kerala	Rock fill	1017	336	345	114	96	369	455	1966 (dam completed)		No reported reservoir induced seismicity.
249 Packer et al. 1979 & V	KAMAFUSA		Goishi	Japan	20 km west of Sendai	Concrete gravity	581	177	155	47	42	36	45	1970 (dam completed)	Not Obtained	2.5 Accepted case of reservoir induced microearthquake activity.
250 ICOLD-CIGB 2012	KAMISHIBA		Mimi	Japan	Hyuga, Miyazaki	Arch	1033	341	333	110	92	74	92	1955 (dam completed)		No reported reservoir induced seismicity.
251 ICOLD-CIGB 2012	KAORE		Itatori	Japan	Gifu, Gifu	Arch	1033	341	327	108	90	14	17	1994 (dam completed)		No reported reservoir induced seismicity.
252 ICOLD-CIGB 2012	KARAKAYA		Firat	Turkey	Cungus, Diyarbakir	Arch	1399	462	524	173	143	7767	9580	1987 (dam completed)		No reported reservoir induced seismicity.
253 ICOLD-CIGB 2012	KARDGALI		Arda	Bulgaria	Kardgali, Haskovo	Arch/Gravity in Masonry or Concrete	1220	403	315	104	86	432	533	1976 (dam completed)		No reported reservoir induced seismicity.
254 Packer et al. 1979 & V	KARIBA	Lake Kariba	Zambezi	Zimbabwe	Nearest town Harare, Mashonaland	Double curvature concrete arch	1900	579	420	128	122	146415	180600	1959	Metamorphic	6.25 Accepted case of reservoir induced macroearthquake activity.
255 ICOLD-CIGB 2012	KARKHEH		KARKHEH	I. Rep. Iran	ANDIMESHK, KHUZESTAN	Earth	9175	3030	385	127	121	4517	5572	2001 (dam completed)		No reported reservoir induced seismicity.
256 ICOLD-CIGB 2012	KAROUN - 4 (MONJ)		KAROUN	I. Rep. Iran	IZEH, CHAHAR MAHAL &	Gravity in Masonry or Concrete/Arch	1732	572	672	222	192	1775	2190	Not Obtained		No reported reservoir induced seismicity.
257 ICOLD-CIGB 2012	KATSE		Malibamatso	Lesotho	Nearest town Katse, Lesotho	Concrete Arch	2329	710	607	185	155	1581	1950	1998 (dam completed)	Not Obtained	3.1 Reported Case
258 ICOLD-CIGB 2012	KAWAJI		Kinu	Japan	Imaichi, Tochigi	Arch	1090	360	424	140	122	67	83	1981 (dam completed)		No reported reservoir induced seismicity.
259 ICOLD-CIGB 2012	KAWAMATA		Kinu	Japan	Nikko, Tochigi	Arch	415	137	354	117	99	71	88	1966 (dam completed)		No reported reservoir induced seismicity.
260 ICOLD-CIGB 2012	KAZAYA	Not obtained	Totsu	Japan	Gojo, Nara	Gravity in Masonry or Concrete	999	330	306	101	83	105	130	1960 (dam completed)		No reported reservoir induced seismicity.
261 Packer et al. 1979 & V	KEBAN		Firat (Euphrates)	Turkey		Concrete gravity	3598	1097	535	163	153	25120	31000	1973	Igneous	3 Accepted case of reservoir induced microearthquake activity.
262 ICOLD-CIGB 2012	KEDDARA		Keddara	Algeria	Boudouaou, Boumerdes	Rock fill	1696	560	327	108	90	118	146	1987 (dam completed)		No reported reservoir induced seismicity.
263 ICOLD-CIGB 2012	KEMER		Akcay	Turkey	Bozdogan, Aydin	Gravity in Masonry or Concrete	905	299	345	114	96	302	373	1958 (dam completed)		No reported reservoir induced seismicity.
264 ICOLD-CIGB 2012	KENNEY		Nechako	Canada	Prince George, BC	Rock fill	1384	457	315	104	86	19295	23800	1952 (dam completed)		No reported reservoir induced seismicity.
265 ICOLD-CIGB 2012	KENYIR		Terengganu	Malaysia	Kuala Brang, Terengganu	Rock fill	2422	800	469	155	125	11026	13600	1985 (dam completed)		No reported reservoir induced seismicity.
266 Packer et al. 1979 & V	KERR	Flathead Lake	Flathead	U.S.A.		Concrete Concrete Arch	676	206	194	59	51	1791	2209	1958 (dam completed)	Igneous	4.9 Accepted case of reservoir induced macroearthquake activity.
267 ICOLD-CIGB 2012	KIAMBERE		Tana	Kenya	Embu, Eastern	Rock fill	2544	840	339	112	94	474	585	1987 (dam completed)		No reported reservoir induced seismicity.
268 ICOLD-CIGB 2012	KILICKAYA		Kelkit	Turkey	Susehri, Sivas	Rock fill	1226	405	406	134	116	1135	1400	1989 (dam completed)		No reported reservoir induced seismicity.
269 Packer et al. 1979 & V	KINARSANI	Kinarsani	Kinarsani	India		Not obtained	Not obtained		0		0	Not Obtain	Not obtained	Not Obtained	--	Questionable case of reservoir induced earthquake activity. Magnitude not obtained.
270 ICOLD-CIGB 2012	KIRAZDERE		Kirazdere	Turkey	Izmit, Izmit	Earth/Rock fill	1208	399	330	109	104	49	60	1999 (dam completed)		No reported reservoir induced seismicity.
271 ICOLD-CIGB 2012	KOELNBREIN		Malta	Austria	Gmuend, Carinthia	Arch	1896	626	606	200	170	166	205	1977 (dam completed)		No reported reservoir induced seismicity.
272 ICOLD-CIGB 2012	KOLYMA		Kolyma	Russia	Magadan, Magadan	Rock fill	2298	759	394	130	112	1184	1460	1991 (dam completed)		No

290 ICOLD-CIGB 2012	KYURAGI	Kyuragi	Japan	Taku, Saga	Gravity in Masonry or Concrete	1181	390	354	117	99	11	14	1987 (dam completed)		No reported reservoir induced seismicity.	
291 ICOLD-CIGB 2012	LA ANGOSTURA	Grijalva	Mexico	Tuxtla Gutierrez, Chiapas	Earth	978	323	442	146	139	7459	9200	1974 (dam completed)		No reported reservoir induced seismicity.	
292 ICOLD-CIGB 2012	LA ESMERALDA (CHIVOR)	Batá	Colombia	Santa María, Boyacá	Rock fill	939	310	718	237	207	616	760	1976 (dam completed)		No reported reservoir induced seismicity.	
293 ICOLD-CIGB 2012	LA HONDA	Uribante	Venezuela	San Cristobal, Tachira	Earth	421	139	421	139	132	628	775	1983 (dam completed)		No reported reservoir induced seismicity.	
294 ICOLD-CIGB 2012	LA VIÑA	Los Sauces	Argentina	Las Rosas, Córdoba	Arch	960	317	321	106	88	186	230	1944 (dam completed)		No reported reservoir induced seismicity.	
295 ICOLD-CIGB 2012	LA VUELTOSA	Caparo	Venezuela	San Cristobal, Tachira	Earth	1817	600	409	135	128	4621	5700	1994 (dam completed)		No reported reservoir induced seismicity.	
296 Gupta, 2002	Lake Baikal		Russia					0		0			Not Obtained	4.8	Reported Case	
297 ICOLD-CIGB 2012	LAPARAN	Aston	France	Tarascon, Ariège	Arch	848	280	321	106	88	13	16	1985 (dam completed)		No reported reservoir induced seismicity.	
298 ICOLD-CIGB 2012	LAR	LAR	I. Rep. Iran	TEHRAN, MAZANDARAN	Earth	3543	1170	318	105	100	778	960	1980 (dam completed)		No reported reservoir induced seismicity.	
299 ICOLD-CIGB 2012	LATIAN	JAUROOD	I. Rep. Iran	TEHRAN, TEHRAN	Buttress	1363	450	324	107	89	77	95	1967 (dam completed)		No reported reservoir induced seismicity.	
300 ICOLD-CIGB 2012	LAZICI	Beli Rzav	Yugoslavia	Bajina Basta, Serbia Zlatiborski	Rock fill	1620	535	397	131	113	138	170	1983 (dam completed)		No reported reservoir induced seismicity.	
301 ICOLD-CIGB 2012	LG DEUX PRINCIPAL CD-00	La Grande	Canada	Radisson, QUE	Rock fill	8557	2826	509	168	138	50033	61715	1978 (dam completed)		No reported reservoir induced seismicity.	
302 ICOLD-CIGB 2012	LG QUATRE - QA-00 PRINCIPAL	La Grande	Canada	Radisson, QUE	Rock fill/Earth	11355	3750	388	128	122	15833	19530	1981 (dam completed)		No reported reservoir induced seismicity.	
303 ICOLD-CIGB 2012	LG TROIS DIGUE FREGATE (LG3)	Sakami/La Grande	Canada	Nearest town Radisson, QUE	Earth	705	215	52	16	80	48659	60020	1981	Igneous	3.7	Questionable
304 ICOLD-CIGB 2012	LIBBY	KOOTENAI RIVER	United States	, Montana	Gravity in Masonry or Concrete	2668	881	391	129	111	6027	7434	1973 (dam completed)		No reported reservoir induced seismicity.	
305 ICOLD-CIGB 2012	LIJIAZIA	Yellow River	China	Hualong, QinghaiProv.	Arch	1157	382	469	155	125	1338	1650	1997 (dam completed)		No reported reservoir induced seismicity.	
306 ICOLD-CIGB 2012	LIMBERG	Wasserfallbode Kapruner Ache	Austria	Zell/See, Salzburg	Arch	1081	357	363	120	102	70	86	1951 (dam completed)		No reported reservoir induced seismicity.	
307 ICOLD-CIGB 2012	LIMMERN	Limmernbach	Switzerland	Linthal, Glarus	Arch	1136	375	442	146	128	75	93	1963 (dam completed)		No reported reservoir induced seismicity.	
308 ICOLD-CIGB 2012	LIUJIAZIA	Yellow River	China	Yongjin, GansuProv.	Gravity in Masonry or Concrete	2544	840	445	147	129	4962	6120	1974 (dam completed)		No reported reservoir induced seismicity.	
309 ICOLD-CIGB 2012	LLOSA DEL CAVALL	CARDONER	Spain	NAVES, LLEIDA	Arch	999	330	369	122	104	65	80	1999 (dam completed)		No reported reservoir induced seismicity.	
310 ICOLD-CIGB 2012	LONGYANGXIA	Huanghe	China	Gonghe, QinghaiProv.	Gravity in Masonry or Concrete	3712	1226	539	178	148	22400	27630	1997 (dam completed)		No reported reservoir induced seismicity.	
311 ICOLD-CIGB 2012	LOS LEONES - Final stage	Los Leones	Chile	Los Andes, V Región	Earth	1514	500	484	160	152	113	140	1998 (dam completed)		No reported reservoir induced seismicity.	
312 ICOLD-CIGB 2012	LOS REYUNOS	Diamante	Argentina	25 De Mayo, Mendoza	Earth	893	295	412	136	129	211	260	1980 (dam completed)		No reported reservoir induced seismicity.	
313 ICOLD-CIGB 2012	LOWER NOTCH MAIN GORGE D.RD	Montreal	Canada	North Bay, ONT	Rock fill	2123	701	400	132	114	139	171	1971 (dam completed)		No reported reservoir induced seismicity.	
314 ICOLD-CIGB 2012	LUBUGE	Huangnihe	China	Nearest town Luoping, YunnanProv.	Rock fill	709	216	331	101	96	900	1110	1990 (dam completed)	Not Obtained	3.4	Reported Case
315 ICOLD-CIGB 2012	LUCKY PEAK	BOISE RIVER	United States	Idaho	Rock fill	2159	713	315	104	86	307	379	1955 (dam completed)		No reported reservoir induced seismicity.	
316 ICOLD-CIGB 2012	LUMIEI	Lumiei	Italy	Udine, Friuli Venezia Giulia	Arch	460	152	412	136	118	64	79	1947 (dam completed)		No reported reservoir induced seismicity.	
317 Woodward-Clyde Con	LUZZONE	Not obtained	Switzerland	Brenno di Luzzone	Concrete arch		600	738	225	171	71	87	1963		No reported reservoir induced seismicity.	
318 ICOLD-CIGB 2012	MACHADINHO	Pelotas	Brazil	PIRATUBA/INHANDABA,	Rock fill	0	0	382	126	108	2756	3400	2002 (dam completed)		No reported reservoir induced seismicity.	
319 ICOLD-CIGB 2012	MAGAT	Magat	Philippines	San José, Isabela	Rock fill	12415	4100	318	105	87	1013	1250	1983 (dam completed)		No reported reservoir induced seismicity.	
320 ICOLD-CIGB 2012	MAGUGA	Komati	Swaziland	Pigg's Peak,	Rock fill	2634	870	348	115	97	269	332	2001 (dam completed)		No reported reservoir induced seismicity.	
321 Gupta, 2002	Makio		Russia					344	105	100		75	1961	Not Obtained		Reported Case
322 ICOLD-CIGB 2012	Mammoth Pool	San Joaquin River	United States	California	Earth/Rock fill	757	250	379	125	119	123	152	1959 (dam completed)		No reported reservoir induced seismicity.	
323 ICOLD-CIGB 2012	MANAGAWA	Mana	Japan	Ono, Fukui	Arch	1081	357	388	128	110	93	115	1977 (dam completed)		No reported reservoir induced seismicity.	
324 Packer et al. 1979 & V	MANGALAM	Not obtained.	India		Earth fill	3489	1063	62	19	17	21	26	1962 (dam completed)	Not Obtained	--	Questionable case of reservoir induced earthquake activity. Magnitude not obtained.
325 Packer et al. 1979 & V	MANGLA	Mangla	Pakistan	Jhelum	Earth fill	8402	2561	453	138	94	5878	7250	1967	Not Obtained	3.6	Earthquake activity not related to reservoir impoundment.
326 ICOLD-CIGB 2012	MANIC 3, PRINCIPAL BARRAGE	Manicouagan	Canada	Nearest town Baie Comeau, QUE	Rock fill	1280	390	354	108	205	8496	10480	1976 (dam completed)	Metamorphic	4.1	Questionable
327 Packer et al. 1979 & V	MANICOUGAN 3	Not obtained	Canada		Earth fill	1201	366	354	108	98	8450	10423	1975	Metamorphic	4.1	Accepted case of reservoir induced macroearthquake activity.
328 ICOLD-CIGB 2012	MANUEL M. DIEGUEZ *		Mexico	Guadalajara, Jalisco	Arch	454	150	345	114	96	324	400	1964 (dam completed)		No reported reservoir induced seismicity.	
329 ICOLD-CIGB 2012	MANUEL M. TORRES *		Mexico	Tuxtla Gutiérrez, Chiapas	Earth	1469	485	790	261	248	1308	1613	1980 (dam completed)		No reported reservoir induced seismicity.	
330 ICOLD-CIGB 2012	MANWAN	Lancanjiang	China	Yunxian, YunnanProv.	Gravity in Masonry or Concrete	1266	418	400	132	114	746	920	1995 (dam completed)		No reported reservoir induced seismicity.	
331 ICOLD-CIGB 2012	MAPYONG	Daeryonggang	Korea N (RDK)	Taecheon, Pyongbukdo	Gravity in Masonry or Concrete	1696	560	312	103	85	2351	2900	0 (dam completed)		No reported reservoir induced seismicity.	
332 Packer et al. 1979 & V	MARATHON	Lake Marathon	Greece		Concrete gravity	935	285	220	67	60	33	41	1929	Metamorphic/Ign	5.75	Accepted case of reservoir induced macroearthquake activity.
333 ICOLD-CIGB 2012	MARIMBONDO	Grande	Brazil	Nearest town Fronteira /Icem, Minas Gerais /Sao Pe	Gravity in Masonry or Concrete Earth	11811	3600	295	90	81	4986	6150	1975 (dam completed)	Not Obtained	IV	Reported Case
334 ICOLD-CIGB 2012	MAROUN	MAROUN	I. Rep. Iran	BEHBAHAN, KHUZESTAN	Earth	1045	345	515	170	162	973	1200	1999 (dam completed)		No reported reservoir induced seismicity.	
335 ICOLD-CIGB 2012	MASJED SOLEYMAN	KAROUN	I. Rep. Iran	MASJED SOLEYMAN, KHUZESTAN	Rock fill	1575	520	536	177	147	166	205	2001 (dam completed)		No reported reservoir induced seismicity.	
336 ICOLD-CIGB 2012	MATALAVILLA	VALSECO	Spain	PARAMO DEL SIL, LEON	Arch	651	215	348	115	97	53	65	1967 (dam completed)		No reported reservoir induced seismicity.	
337 ICOLD-CIGB 2012	MATTMARK	Saaser Vispa	Switzerland	Valais	Earth	2362	780	363	120	114	82	101	1967 (dam completed)		No reported reservoir induced seismicity.	
338 Woodward-Clyde Con	MAUVOISIN	Not obtained	Switzerland	Near Fionnay, alsornear Luzzone	Concrete arch		520	820	250	200	146	180	1958		No reported induced seismicity.	
339 ICOLD-CIGB 2012	MEDO	Malaya Almaatinka	Kazakhstan	Alma-Ata, Kazakhstan	Rock fill	1605	530	436	144	126	0	0	1977 (dam completed)		No reported reservoir induced seismicity.	
340 ICOLD-CIGB 2012	MENZELET	Ceyhan	Turkey	K.Maras, K.Maras	Rock fill	1287	425	457	151	121	1693	2088	1989 (dam completed)		No reported reservoir induced seismicity.	
341 ICOLD-CIGB 2012	MESSAURE	Luleålvén	Sweden	Jokkmokk, Norrbotten	Gravity in Masonry or Concrete/Earth	6192	2045	306	101	96	44	54	1963 (dam completed)		No reported reservoir induced seismicity.	
342 ICOLD-CIGB 2012	MESSOCHORA	Achelooos	Greece	Trikala, Thessalia	Rock fill	1030	340	454	150	132	185	228	1995 (dam completed)		No reported reservoir induced seismicity.	
343 ICOLD-CIGB 2012	MIANHUATAN	Dinjiang	China	Yong'ding, FujianProv.	Gravity in Masonry or Concrete	914	302	336	111	93	165	204	2001 (dam completed)		No reported reservoir induced seismicity.	
344 ICOLD-CIGB 2012	MIBORO	Sho	Japan	Gifu, Gifu	Rock fill	1226	405	397	131	113	300	370	1960 (dam completed)		No reported reservoir induced seismicity.	
345 Packer et al. 1979 & V	MICA	Not obtained	Canada		Rock fill	2598	792	797	243	188	20268	25000	1973	Not Obtained	--	Earthquake activity not related to reservoir impoundment.
346 ICOLD-CIGB 2012	MISAKUBO	Misakubo	Japan	Tenryu, Shizuoka	Rock fill	781	258	318	105	87	24	30	1969 (dam completed)		No reported reservoir induced seismicity.	
347 ICOLD-CIGB 2012	MİYAGASE	Nakatsu	Japan	Atsugi, Kanagawa	Gravity in Masonry or Concrete	1211	400	469	155	125	156	193	1995 (dam completed)		No reported reservoir induced seismicity.	
348 ICOLD-CIGB 2012	MOHALE	Senqunyane	Lesotho	Mohale, Lesotho	Rock fill	1877	620	439	145	127	768	947	2002 (dam completed)		No reported reservoir induced seismicity.	
349 Woodward-Clyde Con	MOHAMMED REZA SHAH PAHLAVI	Not obtained	Iran		Concrete arch			666	203	166	2705	3340	1963		No reported reservoir induced seismicity.	
350 ICOLD-CIGB 2012	MOIRY	Gougria	Switzerland	Grimentz, Valais	Arch	1847	610	448	148	130	63	78	1958 (dam completed)		No reported reservoir induced seismicity.	
351 ICOLD-CIGB 2012	MONT CENIS (LE)	Cenise	France	Modane, Savoie	Rock fill/Earth	4239	1400	363	120	114	256	315	1968 (dam completed)		No reported reservoir induced seismicity.	
352 Packer et al. 1979 & V	MONTEYNARD	Lake Monteyna	France		Concrete arch	689	210	443	135	125	223	275	1962	Sedimentary	4.9	Questionable case of reservoir induced macroearthquake activity.
353 ICOLD-CIGB 2012	MORNOS	Mornos	Greece	Lidhorkio, Sterea Hellas	Earth	2468	815	379	125	119	632	780	1976 (dam completed)		No reported reservoir induced seismicity.	
354 ICOLD-CIGB 2012	MORROW POINT	GUNNISON RIVER	United States	Colorado	XX/Arch	669	221	433	143	125	121	150	1968 (dam completed)		No reported reservoir induced seismicity.	
355 ICOLD-CIGB 2012	MOSSYROCK	COWLITZ RIVER	United States	Washington	Arch/Gravity in Masonry or Concrete	1520	502	560	185	155	1685	2078	1968 (dam completed)		No reported reservoir induced seismicity.	
356 ICOLD-CIGB 2012	MOSUL	Tigris	Iraq	Mosul, Nienava	Rock fill	10598	3500	397	131	113	10134	12500	1983 (dam completed)		No reported reservoir induced seismicity.	
357 ICOLD-CIGB 2012	MOULAY YOUSSEF	Tessout	Morocco	Marrakech, Marrakech	Earth	2195	725	303	100	90	142	175	1969 (dam completed)		No reported reservoir induced seismicity.	
358 Woodward-Clyde Con	MRATINJE	Not obtained	Yugoslavia		Concrete arch			722	220	180	1	2	1975	Sedimentary	4.1	Accepted case of reservoir induced macroearthquake activity.
359 ICOLD-CIGB 2012	MRICA	Serayu	Indonesia	Banjarnegara, Central Java	Rock fill	2519	832	333	110	92	157	194	1989 (dam completed)		No reported reservoir induced seismicity.	
360 ICOLD-CIGB 2012	MUD MOUNTAIN DAM	WHITE RIVER	United States	Washington	Rock fill	645	213	394	130	112	106	131	1948 (dam completed)		No reported reservoir induced seismicity.	
361 Packer et al. 1979 & V	MULA	Mula	India		Earth fill	9250	2819	184	56	50	824	1017	1972	Sedimentary	1	Accepted case of reservoir induced microearthquake activity.
362 ICOLD-CIGB 2012	NAGARJUNA SAGAR	Krishna	India	Hyderabad, Andhra Pradesh	Earth/Gravity in Masonry or Concrete	14732	4865	379	125	119	9373	11561	1960 (dam completed)		No reported reservoir induced seismicity.	
363 Gupta, 2002	Nagawdo		Japan					509	155	147		123	1969	Not Obtained		Reported Case
364 ICOLD-CIGB 2012	NALPS	Rein da Nalps	Switzerland	Sedrun, Graubünden	Arch	1453	480	385	127	109	36	45	1962 (dam completed)		No reported reservoir induced seismicity.	
365 ICOLD-CIGB 2012	NANAKURA	Takase	Japan	Omachi, Nagano	Rock fill	1030	340	379	125	107	26	33	1978 (dam completed)		No reported reservoir induced seismicity.	
366 Gupta, 2002	Nanchong		Japan					148	45	41		15	1969	Not Obtained		Reported Case
367 ICOLD-CIGB 2012	NANSHUI	Nanshui	China	Nearest town Rouyuan, GuangdongProv.	Rock fill	705	215	266	81	73	1008	1243	1971 (dam completed)	Not Obtained	2.3	Reported Case
368 ICOLD-CIGB 2012	NARAMATA		Japan	Numata, Gunma	Rock fill	1575	520	478	158	128	73	90	1990 (dam completed)		No reported reservoir induced seismicity.	
369 ICOLD-CIGB 2012	NAVAJO	SAN JUAN RIVER	United States	New Mexico	Earth	3367	1112	372	123	117	1987	2450	1963 (dam completed)		No reported reservoir induced seismicity.	
370 ICOLD-CIGB 2012	NETZAHUALCOYOTL	Grijalva	Mexico	Cárdenas, Chiapas	Earth	1447	478	418	138	131	6729	8300	1964 (dam completed)		No reported reservoir induced seismicity.	
371 Woodward-Clyde Con	NEW BULLARDS BAR	New Bullards B	U.S.A.		Concrete arch			646	197	174	1010	1246	1968		No reported reservoir induced seismicity.	
372 Woodward-Clyde Con	NEW DON PEDRO	New Don Pedr	U.S.A.		Earth and rock fill			568	173	163	2030	2505	1970		No reported reservoir induced seismicity.	
373 ICOLD-CIGB 2012	NEW MELONES	STANISLAUS RIVER	United States	California	Rock fill Earth	1558	475	627	191	181	2870	3540	1979 (dam completed)		No reported reservoir induced seismicity.	
374 ICOLD-CIGB 2012	NICHU	Oshikiri	Japan	Kitakata												

388 ICOLD-CIGB 2012	OUCHI	Ono	Japan	Aizuwaka -matsu, Fukushima	Rock fill	1030	340	309	102	84	15	19	1988 (dam completed)			No reported reservoir induced seismicity.
389 Packer et al. 1979 & V	Oued FODDA	Oued Fodda	Algeria		Concrete gravity	558	170	285	87	78	182	225	1932	Not Obtained	3	Accepted case of reservoir induced microearthquake activity.
390 ICOLD-CIGB 2012	OUTARDES 4 NO.1	Outardes	Canada	Baie Comeau, QUE	Rock fill	1941	641	369	122	104	1451	1790	1969 (dam completed)			No reported reservoir induced seismicity.
391 ICOLD-CIGB 2012	OWYHEE	OWYHEE RIVER	United States	Oregon	XX/Arch	769	254	385	127	109	1200	1480	1932 (dam completed)			No reported reservoir induced seismicity.
392 ICOLD-CIGB 2012	OYMAPINAR	Manavgat	Turkey	Manavgat, Antalya	Arch	1090	360	560	185	155	191	236	1984 (dam completed)			No reported reservoir induced seismicity.
393 ICOLD-CIGB 2012	OZLUCE	Peri	Turkey	Mazgirt, Bingol	Rock fill	1441	476	436	144	126	872	1075	1998 (dam completed)			No reported reservoir induced seismicity.
394 ICOLD-CIGB 2012	PACOIMA	PACOIMA CREEK	United States	California	Arch	590	195	336	111	93	9	11	1929 (dam completed)			No reported reservoir induced seismicity.
395 Packer et al. 1979 & V	PALISADES	Snake	U.S.A.		Earth fill	2100	640	269	82	67	1418	1749	1957 (dam completed)	Sedimentary	3.7	Accepted case of reservoir induced microearthquake activity.
396 ICOLD-CIGB 2012	PALTINU	Doftana	Romania	Campina, Prahova	Arch	1393	460	327	108	90	44	54	1971 (dam completed)			No reported reservoir induced seismicity.
397 ICOLD-CIGB 2012	PANGUE	Bio-Bio	Chile	Los Angeles, VIII Región	Gravity in Masonry or Concrete	1242	410	366	121	103	53	65	1996 (dam completed)			No reported reservoir induced seismicity.
398 ICOLD-CIGB 2012	PANJIAKOU	Luanghe	China	Qianxi, HebeiProv.	Gravity in Masonry or Concrete	3143	1038	321	106	88	2375	2930	1984 (dam completed)			No reported reservoir induced seismicity.
399 ICOLD-CIGB 2012	PANTABANGAN	Upper Papanga	Philippines	San José, Nueva Ecija	Earth	3028	1000	336	111	105	2429	2996	1974 (dam completed)			No reported reservoir induced seismicity.
400 ICOLD-CIGB 2012	PAPANSKAYA	Akbura	Kirghizstan	Osh, Kirghizstan	Earth	324	107	303	100	90	211	260	1985 (dam completed)			No reported reservoir induced seismicity.
401 ICOLD-CIGB 2012	PARADELA	Cávado	Portugal	Chaves, Vila Real	Rock fill	1635	540	333	110	92	133	165	1958 (dam completed)			No reported reservoir induced seismicity.
402 ICOLD-CIGB 2012	PARAIBUNA	Paraibuna	Brazil	Nearest town Paraibuna, Sao Paulo	Earth	4216	1285	276	84	76	1997	2463	1978 (dam completed)	Not Obtained	3	Reported Case
403 Packer et al. 1979 & V	PARAMBIKULAM	Parambikulam	India		Concrete gravity	1043	318	187	57	51	409	504	1967 (dam completed)	Not Obtained	--	Questionable case of reservoir induced earthquake activity. Magnitude not obtained.
404 ICOLD-CIGB 2012	Pardee	Mokelumne River	United States	California	XX/Gravity in Masonry or Concrete	1235	408	324	107	89	198	244	1929 (dam completed)			No reported reservoir induced seismicity.
405 ICOLD-CIGB 2012	PDTE. A. LOPEZ MATEOS*	Humaya	Mexico	Culiacán, Sinaloa	Earth	2483	820	324	107	102	2554	3150	1964 (dam completed)			No reported reservoir induced seismicity.
406 ICOLD-CIGB 2012	PDTE. GUSTAVO DIAZ *	Sinaloa	Mexico	Guamuchil, Sinaloa	Earth	2422	800	345	114	108	1459	1800	1982 (dam completed)			No reported reservoir induced seismicity.
407 ICOLD-CIGB 2012	PDTE. JOSE L. PORTILLO*	San Lorenzo	Mexico	Cosala, Sinaloa	Earth	1211	400	412	136	129	2311	2850	1981 (dam completed)			No reported reservoir induced seismicity.
408 ICOLD-CIGB 2012	PECINEAGU	Dambovita	Romania	Rucar, Dambovita	Rock fill	818	270	318	105	87	56	69	1984 (dam completed)			No reported reservoir induced seismicity.
409 ICOLD-CIGB 2012	PEDRA DO CAVALO	Paraguassu	Brazil	Cachoeira/Sao Felix, Bahia	Rock fill	1544	510	430	142	124	4321	5330	1986 (dam completed)			No reported reservoir induced seismicity.
410 ICOLD-CIGB 2012	PERTUSILLO	Agri	Italy	Potenza, Basilicata	Arch	1030	340	306	101	83	123	152	1963 (dam completed)			No reported reservoir induced seismicity.
411 Packer et al. 1979 & V	PIASTRA	Gesso	Italy		Concrete gravity	1411	430	305	93	84	10	13	1965 (dam completed)	Sedimentary	4.4	Accepted case of reservoir induced macroearthquake activity.
412 ICOLD-CIGB 2012	PICOTE	Douro	Portugal	Miranda do Douro, Bragança	Arch	421	139	303	100	90	52	64	1958 (dam completed)			No reported reservoir induced seismicity.
413 ICOLD-CIGB 2012	PIEDRA DEL AGUILA	Limay	Argentina	Piedra del Aguila, Neuquen / Río Negro	Gravity in Masonry or Concrete	2483	820	515	170	140	10053	12400	1993 (dam completed)			No reported reservoir induced seismicity.
414 Packer et al. 1979 & V	PIEVE DI CADORE	Pieve di Cadore	Italy		Concrete arch-gravity	1345	410	354	108	98	56	69	1949	Sedimentary	v	Accepted case of reservoir induced microearthquake activity.
415 ICOLD-CIGB 2012	PINE FLAT DAM	KINGS RIVER	United States	California	Gravity in Masonry or Concrete	1699	561	406	134	116	1000	1233	1954 (dam completed)			No reported reservoir induced seismicity.
416 ICOLD-CIGB 2012	PLACE MOULIN	Butthier	Italy	Aosta, Val D'Aosta	Arch	2053	678	469	155	125	86	105	1965 (dam completed)			No reported reservoir induced seismicity.
417 ICOLD-CIGB 2012	PLUTARCO ELIAS C.*	El Yaqui	Mexico	Hermosillo, Sonora	Arch	908	300	403	133	115	2456	3030	1964 (dam completed)			No reported reservoir induced seismicity.
418 ICOLD-CIGB 2012	POLYPHYTO	Aliakmon	Greece	Kozani, W. Macedonia	Rock fill	896	296	339	112	94	1572	1939	1974 (dam completed)			No reported reservoir induced seismicity.
419 ICOLD-CIGB 2012	PONG DAM	Beas	India	Mukerian, Himachal Pradesh	Earth	5923	1956	403	133	126	6948	8570	1974 (dam completed)			No reported reservoir induced seismicity.
420 ICOLD-CIGB 2012	PONTE COLA	Toscolano	Italy	Brescia, Lombardia	Arch	866	286	375	124	106	42	52	1962 (dam completed)			No reported reservoir induced seismicity.
421 ICOLD-CIGB 2012	PORTAS, LAS	CAMBA	Spain	VILARIÑO DE CONSO, OURENSE	Arch	1444	477	427	141	123	434	536	1974 (dam completed)			No reported reservoir induced seismicity.
422 Packer et al. 1979 & V	PORTO COLOMBIA	Porto Columbia Grande	Brazil	Nearest town Planura, Sao Paulo	Earth fill with concrete gravity section	7054	2150	131	40	48	1236	1524	1973 (dam completed)	Igneous	4.2	Accepted case of reservoir induced macroearthquake activity.
423 ICOLD-CIGB 2012	POURNARI	Arachthos	Greece	Arta, Epirus	Earth	1756	580	324	107	102	592	730	1981 (dam completed)			No reported reservoir induced seismicity.
424 ICOLD-CIGB 2012	PUEBLO VIEJO	Chixoy	Guatemala	San Cristobal Verapaz, Alta Verapaz	Rock fill	696	230	394	130	112	373	460	1983 (dam completed)			No reported reservoir induced seismicity.
425 ICOLD-CIGB 2012	PUNT DAL GALL	Lago di Livigno	Switzerland	Zernez, Graubünden / Italia	Arch	1635	540	394	130	112	133	165	1968 (dam completed)			No reported reservoir induced seismicity.
426 ICOLD-CIGB 2012	Pyramid	Pyramid	United States	California	Earth/Rock fill	1005	332	391	129	123	171	211	1974 (dam completed)			No reported reservoir induced seismicity.
427 Gupta, 2002	Qianjin	Qianjin	China					164	50	45		20	1971	Not Obtained		Reported Case
428 ICOLD-CIGB 2012	QINSHAN	Muyangxi	China	Zhouning, FujianProv.	Rock fill	787	260	369	122	104	215	265	2000 (dam completed)			No reported reservoir induced seismicity.
429 ICOLD-CIGB 2012	QUENTAR	AGUAS BLANCAS	Spain	QUENTAR, GRANADA	Arch	606	200	403	133	115	11	14	1975 (dam completed)			No reported reservoir induced seismicity.
430 ICOLD-CIGB 2012	QUNYING(HENAN)	Dashahe	China	Jiaozuo, HenanProv.	Arch	363	120	306	101	83	16	20	1971 (dam completed)			No reported reservoir induced seismicity.
431 ICOLD-CIGB 2012	RALCO	Bio-Bio	Chile	Los Angeles, VIII Región	Gravity in Masonry or Concrete	1120	370	469	155	125	649	800	2002 (dam completed)			No reported reservoir induced seismicity.
432 ICOLD-CIGB 2012	RAMA	Rama	Bosnia-Herz.	Prozor,	Rock fill	0	0	312	103	85	395	487	1969 (dam completed)			No reported reservoir induced seismicity.
433 ICOLD-CIGB 2012	RAMGANGA	Ramganga	India	Pauri Garhwal, Uttaranchal	Earth	2165	715	388	128	122	199	245	1974 (dam completed)			No reported reservoir induced seismicity.
434 ICOLD-CIGB 2012	RAPEL	Rapel	Chile	Melipilla, VI Región	Arch	1014	335	339	112	94	551	680	1968 (dam completed)			No reported reservoir induced seismicity.
435 ICOLD-CIGB 2012	RAPPBODE	Rappbode	Germany	Vernigerode, Sachsen - Anhalt	Gravity in Masonry or Concrete	1257	415	321	106	88	88	109	1959 (dam completed)			No reported reservoir induced seismicity.
436 ICOLD-CIGB 2012	RAUSOR	Raul Targului	Romania	Campulung, Arges	Rock fill	1151	380	363	120	102	49	60	1987 (dam completed)			No reported reservoir induced seismicity.
437 ICOLD-CIGB 2012	REECE	Pieman	Australia	QUEENSTOWN, Tasmania	Rock fill	1133	374	369	122	104	520	641	1986 (dam completed)			No reported reservoir induced seismicity.
438 ICOLD-CIGB 2012	REVELSTOKE	Columbia	Canada	Revelstoke, BC	Gravity in Masonry or Concrete/Rock fill	1423	470	530	175	145	4199	5180	1983 (dam completed)			No reported reservoir induced seismicity.
439 Woodward-Clyde Con	REZA SHAH KABIR	Karoun	Iran		Concrete arch			656	200	163	2531	2900	1975			No reported reservoir induced seismicity.
440 ICOLD-CIGB 2012	RIALB	SEGRE	Spain	BARONIA RIALB, TIURANA, LLEIDA	Gravity in Masonry or Concrete	1802	595	306	101	83	327	403	1999 (dam completed)			No reported reservoir induced seismicity.
441 ICOLD-CIGB 2012	RIANO	ESLA	Spain	CREMENES, LEON	Arch	1020	337	306	101	83	528	651	1988 (dam completed)			No reported reservoir induced seismicity.
442 ICOLD-CIGB 2012	RIDGWAY	UMCOMPAGHRE RIVER	United States	Colorado	Earth	2244	741	306	101	96	89	110	1987 (dam completed)			No reported reservoir induced seismicity.
443 ICOLD-CIGB 2012	RIDRACOLI	Bidente	Italy	Forli, Emilia Romagna	Arch	1311	433	315	104	86	27	33	1982 (dam completed)			No reported reservoir induced seismicity.
444 Gupta, 2002	Ridracoli	Ridracoli	Italy					338	103	98		33	1988	Not Obtained		Reported Case
445 ICOLD-CIGB 2012	RIO GRANDE	Córdoba	Argentina	Córdoba	Rock fill	11113	3670	1242	410	380	0	0	1986 (dam completed)			No reported reservoir induced seismicity.
446 ICOLD-CIGB 2012	Robert Moses - Niaga	Niagara River	United States	New York	XX/Gravity in Masonry or Concrete	1014	335	360	119	101	0	0	1963 (dam completed)			No reported reservoir induced seismicity.
447 Packer et al. 1979 & V	ROCKY REACH	Columbia	U.S.A.		Concrete gravity	2900	884	141	43	39	650	802	1962 (dam completed)	Not Obtained	--	Earthquake activity not related to reservoir impoundment.
448 Packer et al. 1979 & V	ROI CONSTANTINE	Achelooos	Greece		Earth fill	1692	516	315	96	86	1	1	1969 (dam completed)	Sedimentary	5.2	Accepted case of reservoir induced macroearthquake activity.
449 Packer et al. 1979 & V	ROI PAUL	Achelooos	Greece		Earth fill	6890	2100	492	150	120	3850	4750	1964	Sedimentary	6.3	Accepted case of reservoir induced macroearthquake activity.
450 ICOLD-CIGB 2012	ROSELEND	Doron De Beaufort	France	Albertville, Savoie	Arch/Buttress	2441	806	454	150	132	152	187	1961 (dam completed)			No reported reservoir induced seismicity.
451 ICOLD-CIGB 2012	ROSS	SKAGIT R	United States	Washington	XX/Arch	1199	396	500	165	135	1453	1792	1949 (dam completed)			No reported reservoir induced seismicity.
452 ICOLD-CIGB 2012	ROUND BUTTE	Deschutes	United States	Oregon	Rock fill	1338	442	406	134	116	535	660	1964 (dam completed)			No reported reservoir induced seismicity.
453 ICOLD-CIGB 2012	RUAKOHUA	Ruakokua Stream	New Zealand	Auckland	Earth	454	150	363	120	114	0	0	1984 (dam completed)			No reported reservoir induced seismicity.
454 ICOLD-CIGB 2012	RYONDUPYONG	Nunggwigang	Korea N (RDK)	Pungso, Ryanggangdo	Gravity in Masonry or Concrete	1393	460	318	105	87	407	503	1958 (dam completed)			No reported reservoir induced seismicity.
455 ICOLD-CIGB 2012	SABIGAWA	Kosabigawa	Japan	Kuroiso, Tochigi	Gravity in Masonry or Concrete	827	273	315	104	86	9	11	1994 (dam completed)			No reported reservoir induced seismicity.
456 ICOLD-CIGB 2012	SAGAE	Ojika	Japan	Nikko, Tochigi	Gravity in Masonry or Concrete	808	267	339	112	94	45	55	1956 (dam completed)			No reported reservoir induced seismicity.
457 ICOLD-CIGB 2012	SAGURIGAWA	Saguri	Japan	Tokamachi, Nigata	Rock fill	1272	420	363	120	102	22	28	1994 (dam completed)			No reported reservoir induced seismicity.
458 ICOLD-CIGB 2012	SAKAIGAWA	Sakai	Japan	Toba, Toyama	Gravity in Masonry or Concrete	902	298	348	115	97	49	60	1993 (dam completed)			No reported reservoir induced seismicity.
459 ICOLD-CIGB 2012	SAKAMOTO	Kitayama	Japan	Owase, Nara	Arch	778	257	312	103	85	71	87	1962 (dam completed)			No reported reservoir induced seismicity.
460 ICOLD-CIGB 2012	SAKUMA	Tenryu	Japan	Toyohashi, Aichi	Gravity in Masonry or Concrete	890	294	472	156	126	265	327	1956 (dam completed)			No reported reservoir induced seismicity.
461 ICOLD-CIGB 2012	SALAL (CONCRETE DAM)	Chinab	India	Jammu, Jammu & Kashmir	Earth	1475	487	342	113	107	231	285	1986 (dam completed)			No reported reservoir induced seismicity.
462 ICOLD-CIGB 2012	SALIME	NAVIA	Spain	GRANDAS DE SALIME, ASTURIAS	Gravity in Masonry or Concrete	757	250	379	125	107	216	266	1956 (dam completed)			No reported reservoir induced seismicity.
463 ICOLD-CIGB 2012	Salt Springs	North Fork Mokelumne Riv	United States	California	Rock fill	1160	383	303	100	90	143	176	1931 (dam completed)			No reported reservoir induced seismicity.
464 ICOLD-CIGB 2012	SALTO	Salto	Italy	Rieti, Lazio	Gravity in Masonry or Concrete	709	234	327	108	90	218	269	1940 (dam completed)			No reported reservoir induced seismicity.
465 ICOLD-CIGB 2012	SALVAJINA	Cauca	Colombia	Popayán, Cauca	Rock fill	1211	400	448	148	130	735	906	1985 (dam completed)			No reported reservoir induced seismicity.
466 ICOLD-CIGB 2012	SAMBUCO	Maggia	Switzerland	Fusio, Ticino	Arch	1099	363	394	130	112	51	63	1956 (dam completed)			No reported reservoir induced seismicity.
467 ICOLD-CIGB 2012	SAMEURA	Yoshino	Japan	Nankoku, Kochi	Gravity in Masonry or Concrete	1211	400	321	106	88	256	316	1974 (dam completed)			No reported reservoir induced seismicity.
468 ICOLD-CIGB 2012	SAN ESTEBAN	SIL	Spain	NOGUEIRA DE RAMUIN, OURENSE	Gravity in Masonry or Concrete	893	295	348	115	97	173	213	1955 (dam completed)			No reported reservoir induced seismicity.
469 ICOLD-CIGB 2012	San Gabriel	San Gabriel River	United States	California	Earth/Rock fill	1402	463	351	116	110	45	55	1937 (dam completed)			No reported reservoir induced seismicity.

486	Packer et al. 1979 & II	SEFID RUD	SEFID RUD	I. Rep. Iran	Nearest town MANJIL, GILAN	Buttress	1394	425	394	120	80	1459	1800	1961 (dam completed)	Igneous	4.7	Questionable case of reservoir induced macroseismic activity.
487	ICOLD-CIGB 2012	SEGREDO	Iguaçu	Brazil	Pinhao, Parana	Rock fill/Gravity in Masonry or Concrete	2120	700	439	145	127	2432	3000	1992 (dam completed)			No reported reservoir induced seismicity.
488	ICOLD-CIGB 2012	SEITEVARE	Blackälven	Sweden	Porjus, Norrbotten	Rock fill	6089	2011	321	106	88	1358	1675	1967 (dam completed)			No reported reservoir induced seismicity.
489	ICOLD-CIGB 2012	SERRA DA MESA	Tocantins	Brazil	Minaçu, Goias	Rock fill	4542	1500	466	154	124	44103	54400	1998 (dam completed)			No reported reservoir induced seismicity.
490	ICOLD-CIGB 2012	SERRE PONCON	Durance	France	Gap, Alpes (Haute)	Earth	1817	600	391	129	123	1030	1270	1960 (dam completed)			No reported reservoir induced seismicity.
491	ICOLD-CIGB 2012	SETO	Setodani	Japan	Gojo, Nara	Rock fill	1039	343	336	111	93	14	17	1978 (dam completed)			No reported reservoir induced seismicity.
492	ICOLD-CIGB 2012	SEVEN OAKS DAM	SANTA ANA RIVER	United States	California	Earth	2550	842	584	193	183	146	180	1999 (dam completed)			No reported reservoir induced seismicity.
493	ICOLD-CIGB 2012	SHAHID ABBAS-POUR	KAROON	I. Rep. Iran	MASJED-SOLAYMAN, KHUZESTAN	Arch	1151	380	606	200	170	2351	2900	1976 (dam completed)			No reported reservoir induced seismicity.
494	ICOLD-CIGB 2012	SHAHID RAJAI (TAJAN)	DODANGEH (TAJAN)	I. Rep. Iran	SARI, MAZANDARAN	Multiple Arch	1293	427	421	139	121	155	192	1997 (dam completed)			No reported reservoir induced seismicity.
495	ICOLD-CIGB 2012	SHANXI	Feiyunjiang	China	Wencheng, ZhejiangProv.	Rock fill	1357	448	403	133	115	1479	1824	2001 (dam completed)			No reported reservoir induced seismicity.
496	ICOLD-CIGB 2012	SHAPAI	Caopohe	China	Wenchuan, SichuanProv.	Arch	721	238	400	132	114	15	18	2001 (dam completed)			No reported reservoir induced seismicity.
497	Packer et al. 1979 & V	SHARAVATHI	Not obtained	India	Not obtained	Not obtained	Not obtained		0		0	Not Obtain	Not obtained		Not Obtained	--	Questionable case of reservoir induced earthquake activity. Magnitude not obtained.
498	Packer et al. 1979 & V	SHASTA	Lake Shasta	U.S.A.	Concrete gravity, arched		3461	1055	600	183	138	4662	5750	1945 (dam completed)	Sedimentary	3	Accepted case of reservoir induced microearthquake activity.
499	Gupta, 2002	Shengjiaxia		China					115	35	32		4	1984		Not Obtained	Reported Case
500	Gupta, 2002	Shenwo		China					164	50	45		540	1972		Not Obtained	Reported Case
501	ICOLD-CIGB 2012	SHIMEN	Dahanxi	China	Taoyuan, TaiwanProv.	Arch	1090	360	403	133	115	256	316	1964 (dam completed)			No reported reservoir induced seismicity.
502	ICOLD-CIGB 2012	SHIMENZI(XINJIANG)	Taxihe	China	Manasi, XinjiangReg.	Arch	566	187	333	110	92	65	80	2002 (dam completed)			No reported reservoir induced seismicity.
503	ICOLD-CIGB 2012	SHIMOKOTORI	Kotori	Japan	Takayama, Gifu	Rock fill	972	321	360	119	101	100	123	1973 (dam completed)			No reported reservoir induced seismicity.
504	ICOLD-CIGB 2012	SHIMOKUBO	Kanna	Japan	Fujioka, Saitama	Gravity in Masonry or Concrete	1896	626	391	129	111	105	130	1968 (dam completed)			No reported reservoir induced seismicity.
505	ICOLD-CIGB 2012	SHINNARIWAGAWA	Nariwa	Japan	Niimi, Okayama	Arch	875	289	312	103	85	104	128	1968 (dam completed)			No reported reservoir induced seismicity.
506	ICOLD-CIGB 2012	SHINTOYONE	Onyu	Japan	Toyohashi, Aichi	Arch	942	311	354	117	99	43	54	1978 (dam completed)			No reported reservoir induced seismicity.
507	ICOLD-CIGB 2012	SHIRORO	Kaduna , Dinya	Nigeria	Minna, Niger	Earth	2120	700	379	125	119	5675	7000	1984 (dam completed)			No reported reservoir induced seismicity.
508	ICOLD-CIGB 2012	SHITOUHE(SHAANXI)	Shitouhe	China	Meixian, ShaanxiProv.	Earth	1787	590	345	114	108	119	147	1989 (dam completed)			No reported reservoir induced seismicity.
509	Packer et al. 1979 & V	SHOLAYAR	Sholayar	India		Concrete gravity	1400	426	190	58	52	124	154	1965 (dam completed)	Not Obtained	--	Questionable case of reservoir induced earthquake activity. Magnitude not obtained.
510	ICOLD-CIGB 2012	SHUIFENG*(LIAONING)	Yalujiang	China	Kuandian, LiaoningProv.	Gravity in Masonry or Concrete	2725	900	321	106	88	1197	14700	1943 (dam completed)			No reported reservoir induced seismicity.
511	ICOLD-CIGB 2012	SHUIKOU(FUJIAN)	Minjiang	China	Nearest town Mingqing, FujianProv.	Gravity in Masonry or Concrete	2595	791	331	101	83	1897	2340	1995 (dam completed)	Not Obtained	3.2	Reported Case
512	ICOLD-CIGB 2012	SIDI SAID	Moulouya	Morocco	Midelt, Khenifra	Gravity in Masonry or Concrete	1817	600	363	120	102	324	400	Not Obtained			No reported reservoir induced seismicity.
513	ICOLD-CIGB 2012	SIR	Ceyhan	Turkey	Ceyhan, K.Maras	Arch	1036	342	351	116	98	908	1120	1991 (dam completed)			No reported reservoir induced seismicity.
514	ICOLD-CIGB 2012	SIRIKIT	Nan	Thailand	Uttaradit	Earth	2422	800	345	114	108	7710	9510	1974 (dam completed)			No reported reservoir induced seismicity.
515	ICOLD-CIGB 2012	SIRIU	Buzau	Romania	Nehoiu, Buzau	Rock fill	1726	570	369	122	104	126	155	1994 (dam completed)			No reported reservoir induced seismicity.
516	ICOLD-CIGB 2012	SMOKOVO	Sofaditis	Greece	Karditsa, Thessalia	Rock fill	1453	480	315	104	86	162	200	1994 (dam completed)			No reported reservoir induced seismicity.
517	ICOLD-CIGB 2012	SOBRADINHO	Sao Francisco	Brazil	Nearest town Petrolina /Juazeiro, Bahia /Pernambur	Rock fill	27992	8532	141	43	39	27645	34100	1979 (dam completed)	Not Obtained	2	Reported Case
518	ICOLD-CIGB 2012	SONGWON	Chungman gang	Korea N (RDK)	Songwon, Chagangdo	Gravity in Masonry or Concrete	1908	630	484	160	130	2594	3200	Not Obtained			No reported reservoir induced seismicity.
519	ICOLD-CIGB 2012	SORIA	SORIA	Spain	SAN BARTOLOME DE TIRAJANA, PALMAS, LAS	Arch	751	248	394	130	112	27	33	1972 (dam completed)			No reported reservoir induced seismicity.
520	ICOLD-CIGB 2012	SOYANGGANG	Soyang	Korea	Chuncheon, Gangwon	Rock fill	1605	530	372	123	105	1540	1900	1973 (dam completed)			No reported reservoir induced seismicity.
521	ICOLD-CIGB 2012	SPECCHERI	Leno Vallarsa	Italy	Trento, Trentino Alto Adige	Arch	575	190	445	147	129	8	10	1957 (dam completed)			No reported reservoir induced seismicity.
522	ICOLD-CIGB 2012	SPIIJE	Crni Drim	F.Y.R.O. Macedonia	Debar, F.Y.R.O. Macedonia	Rock fill	8173	2699	339	112	94	422	520	1969 (dam completed)			No reported reservoir induced seismicity.
523	ICOLD-CIGB 2012	SPITALLAMM	Aare	Switzerland	Innetkirchen, Bern	Arch	781	258	345	114	96	82	101	1932 (dam completed)			No reported reservoir induced seismicity.
524	ICOLD-CIGB 2012	SRINAGARIND	Quae Yai	Thailand	Kanchanaburi	Rock fill	2001	610	459	140	133	14386	17745	1978 (dam completed)	Not Obtained	5.9	Reported Case
525	ICOLD-CIGB 2012	SRISAILAM	Krishna	India	Nearest town Hyderabad, Andhra Pradesh	Gravity in Masonry or Concrete	1680	512	476	145	127	7071	8722	1984 (dam completed)	Not Obtained	3.2	Reported Case
526	ICOLD-CIGB 2012	STORGLOMVTN	Fykanaga	Norway	Bodo, Norland	Rock fill	2483	820	379	125	107	2812	3468	1997 (dam completed)			No reported reservoir induced seismicity.
527	ICOLD-CIGB 2012	SUMMERSVILLE DAM	GAULEY RIVER	United States	West Virginia	Rock fill	2105	695	360	119	101	413	510	1965 (dam completed)			No reported reservoir induced seismicity.
528	ICOLD-CIGB 2012	SUPA	Kalinadi	India	Dandeli, Karnataka	Earth	975	322	306	101	96	3387	4178	1987 (dam completed)			No reported reservoir induced seismicity.
529	ICOLD-CIGB 2012	SUPUNG	Amnokgang	Korea N (RDK)	Sakju, Pyongbukdo	Gravity in Masonry or Concrete	2725	900	321	106	88	11917	14700	1957 (dam completed)			No reported reservoir induced seismicity.
530	ICOLD-CIGB 2012	SUSQUEDA	TER	Spain	SUSQUEDA, GIRONA	Arch	1544	510	409	135	117	189	233	1968 (dam completed)			No reported reservoir induced seismicity.
531	ICOLD-CIGB 2012	SVARTEVATN DAM	Sira	Norway	Stavanger, Rogaland	Rock fill	1272	420	394	130	112	1133	1398	1976 (dam completed)			No reported reservoir induced seismicity.
532	ICOLD-CIGB 2012	SWIFT NO. 1	LEWIS R	United States	Washington	Earth	1938	640	382	126	120	756	932	1958 (dam completed)			No reported reservoir induced seismicity.
533	ICOLD-CIGB 2012	TAGOKURA	Tadami	Japan	Aizuwaka -matsu, Fukushima	Gravity in Masonry or Concrete	1399	462	439	145	127	400	494	1960 (dam completed)			No reported reservoir induced seismicity.
534	ICOLD-CIGB 2012	TAKAMI	Shizunai	Japan	Tomakomai, Hokkaido	Rock fill	1317	435	363	120	102	186	229	1994 (dam completed)			No reported reservoir induced seismicity.
535	ICOLD-CIGB 2012	TAKANE NO1	Hida	Japan	Takayama, Gifu	Arch	839	277	403	133	115	35	44	1969 (dam completed)			No reported reservoir induced seismicity.
536	ICOLD RTS 1996	Dra TAKASE	Takase		Japan	Earth and rockfill		362	577	176	167		76	Not Obtained	Not Obtained	3.6	Questionable
537	Packer et al. 1979 & V	TALBINGO	Tumut	Australia		Earth and rock fill	2296	700	502	153	143	758	935	1971	Igneous	3.5	Accepted case of reservoir induced macroearthquake activity.
538	ICOLD-CIGB 2012	TAMAGAWA	Tama	Japan	Omagari, Akita	Gravity in Masonry or Concrete	1338	442	303	100	90	206	254	1990 (dam completed)			No reported reservoir induced seismicity.
539	ICOLD-CIGB 2012	TAMAHARA	Hotchi	Japan	Numata, Gunma	Rock fill	1726	570	351	116	98	12	15	1982 (dam completed)			No reported reservoir induced seismicity.
540	ICOLD-CIGB 2012	TARBELA	Indus	Pakistan	Haripur, NWFP	Earth	8306	2743	433	143	136	11096	13687	1976 (dam completed)			No reported reservoir induced seismicity.
541	ICOLD-CIGB 2012	TEDORIGAWA	Tedori	Japan	Kanazawa, Ishikawa	Rock fill	1272	420	466	154	124	187	231	1979 (dam completed)			No reported reservoir induced seismicity.
542	ICOLD-CIGB 2012	TEMENGOR	Perak	Malaysia	Genik, Perak	Rock fill	1626	537	385	127	109	4905	6050	1978 (dam completed)			No reported reservoir induced seismicity.
543	ICOLD-CIGB 2012	THISSAVROS	Nestos	Greece	Drama, E. Macedonia	Rock fill	1453	480	515	170	140	572	705	1996 (dam completed)			No reported reservoir induced seismicity.
544	ICOLD-CIGB 2012	THOMSON	Thomson	Australia	Nearest town MOE, Victoria	Rock fill	1936	590	545	166	158	911	1123	1983 (dam completed)	Not Obtained	3	Reported Case
545	Woodward-Clyde Con	TIGNES	Iserre	France	Near Albertville	Concrete arch		375	591	180	150	186	230	1952			No reported reservoir induced seismicity.
546	ICOLD-CIGB 2012	TIKVES	Crna Reka	F.Y.R.O. Macedonia	Kavadarcy, F.Y.R.O. Macedonia	Rock fill	1023	338	345	114	96	385	475	1968 (dam completed)			No reported reservoir induced seismicity.
547	ICOLD-CIGB 2012	TOKTOGUL	Naryn	Kirghizstan	Nearest town Naryn, Kirghizstan	Gravity in Masonry or Concrete	961	293	705	215	185	15809	19500	1978 (dam completed)	Not Obtained	2.5	Reported Case
548	Gupta, 2002	Tongjiezi		China				243	74		67		30	1992	Not Obtained		Reported Case
549	ICOLD-CIGB 2012	TONKIN SPRINGS TAIL	OFF STREAM	United States	Nevada	Earth	3852	1272	382	126	120	0	0	Not Obtained			No reported reservoir induced seismicity.
550	ICOLD-CIGB 2012	TORI	Oyabe	Japan	Takaoka, Toyama	Arch	693	229	306	101	83	19	23	1966 (dam completed)			No reported reservoir induced seismicity.
551	ICOLD-CIGB 2012	TOUS (NUEVA PRESA)	JUCAR	Spain	TOUS, VALENCIA	Rock fill	3101	1024	412	136	118	307	379	1996 (dam completed)			No reported reservoir induced seismicity.
552	ICOLD-CIGB 2012	TRÄNGSLET KRV O DAMM	Österdalälven	Sweden	Mora, Dalarna	Gravity in Masonry or Concrete/Earth	2801	925	369	122	116	713	880	1974 (dam completed)			No reported reservoir induced seismicity.
553	ICOLD-CIGB 2012	TRIGOMIL	Ayuquila	Mexico	Unión de Tula, Jalisco	Gravity in Masonry or Concrete	757	250	324	107	89	263	324	1993 (dam completed)			No reported reservoir induced seismicity.
554	ICOLD-CIGB 2012	TRINITY	TRINITY RIVER	United States	California	Earth	2398	792	497	164	156	2761	3405	1962 (dam completed)			No reported reservoir induced seismicity.
555	ICOLD-CIGB 2012	TSURUTA	Sendai	Japan	Kagoshima, Kagoshima	Gravity in Masonry or Concrete	1357	448	357	118	100	100	123	1965 (dam completed)			No reported reservoir induced seismicity.
556	ICOLD-CIGB 2012	TUCURUI	Tocantins	Brazil	Nearest town Tucurui, Para	Earth Rock fill	30144	9188	312	95	86	36917	45536	1984 (dam completed)	Not Obtained	3.4	Reported Case
557	ICOLD-CIGB 2012	TURIMIQUIRE	Turimiquire	Venezuela	Barcelona, Sucre	Rock fill	1332	440	412	136	118	446	550	1982 (dam completed)			No reported reservoir induced seismicity.
558	ICOLD-CIGB 2012	TURKWEL	Suam	Kenya	Codwar	Arch	545	180	454	150	132	1297	1600	1990 (dam completed)			No reported reservoir induced seismicity.
559	Packer et al. 1979 & V	UKAI	Tapi	India	Nearest town Fort Songadh, Gujarat	Earth fill, rock fill, centRock fill concrete gravity	16165	4927	266	81	62	6900	8511	1973 (dam completed)	Not Obtained	--	Questionable case of reservoir induced earthquake activity. Magnitude not obtained.
560	ICOLD-CIGB 2012	UNDONG	Amnokgang	Korea N (RDK)	Chasong, Chagangdo	Gravity in Masonry or Concrete	2507	828	345	114	96	3170	3910	1966 (dam completed)			No reported reservoir induced seismicity.
561	ICOLD-CIGB 2012	Union Valley	Big Silver Creek	United States	California	Earth	1838	607	421	139	132	277	342	1962 (dam completed)			No reported reservoir induced seismicity.
562	ICOLD-CIGB 2012	UST-ILIM	Angara	Russia	Ust-Ilimsk, Irkutsk	Gravity in Masonry or Concrete	4472	1477	309	102	84	48075	59300	1977 (dam completed)			No reported reservoir induced seismicity.
563	ICOLD-CIGB 2012	UVAC	Uvac	Yugoslavia	Nova Varos, Serbia Zlatiborski	Rock fill	930	307	333	110	92	170	210	1979 (dam completed)			No reported reservoir induced seismicity.
564	Packer et al. 1979 & V	VAJ															

584 ICOLD-CIGB 2012	WILLIAM L. JESS	ROGUE RIVER	United States	Oregon	Rock fill	3322	1097	318	105	87	500	617	1976 (dam completed)			No reported reservoir induced seismicity.
585 ICOLD-CIGB 2012	WUJIANGDU	Wujiang	China	Nearest town Zunyi, GuizhouProv.	Gravity in Masonry or Concrete	1207	368	541	165	135	1865	2300	1985 (dam completed)	Not Obtained	2.8	Reported Case
586 ICOLD-CIGB 2012	WUSHE	Zhuoshuixi	China	Nantou, TaiwanProv.	Gravity in Masonry or Concrete	684	226	345	114	96	122	150	1959 (dam completed)			No reported reservoir induced seismicity.
587 ICOLD-CIGB 2012	XIAOLANGDI	Huanghe	China	Mengjin, HenanProv.	Rock fill	5048	1667	466	154	124	10256	12650	2001 (dam completed)			No reported reservoir induced seismicity.
588 ICOLD-CIGB 2012	XIN'ANJIANG	Xin'anjiang	China	Jiande, ZhejiangProv.	Gravity in Masonry or Concrete	1408	465	318	105	87	14479	17860	1965 (dam completed)			No reported reservoir induced seismicity.
589 Woodward-Clyde Con	XINFENGJIANG (HSINFENGKIANG)	Xinfeng jiang	China	Nearest town Heyuan, GuangdongProv.	Buttress	1444	440	344	105	100	11266	13896	1960 (dam completed)	Igneous	6	Accepted case of reservoir induced macroearthquake activity.
590 ICOLD-CIGB 2012	XINGO	Sao Francisco	Brazil	Caninde do Sao Francisco, Sergipe	Rock fill	2422	800	454	150	132	3081	3800	1994 (dam completed)			No reported reservoir induced seismicity.
591 ICOLD-CIGB 2012	YAGISAWA	Tone	Japan	Numata, Gunma	Arch	1217	402	397	131	113	165	204	1967 (dam completed)			No reported reservoir induced seismicity.
592 ICOLD-CIGB 2012	YAHAGI	Yahagi	Japan	Toyoda, Gifu	Arch	978	323	303	100	90	65	80	1971 (dam completed)			No reported reservoir induced seismicity.
593 ICOLD-CIGB 2012	YANASE	Nabari	Japan	Aki, Kochi	Rock fill	612	202	348	115	97	85	105	1965 (dam completed)			No reported reservoir induced seismicity.
594 ICOLD-CIGB 2012	YANTAN	Hongshuihe	China	Nearest town Dahua, GuangxiReg.	Gravity in Masonry or Concrete	1722	525	361	110	92	1970	2430	1995 (dam completed)	Not Obtained	3.5	Reported Case
595 ICOLD-CIGB 2012	YASAKA	Ose	Japan	Iwakuni, Yamaguchi	Gravity in Masonry or Concrete	1635	540	363	120	102	91	112	1990 (dam completed)			No reported reservoir induced seismicity.
596 ICOLD-CIGB 2012	YELLOWTAIL	BIGHORN RIVER	United States	Montana	XX/Arch	1366	451	484	160	130	1427	1761	1966 (dam completed)			No reported reservoir induced seismicity.
597 ICOLD-CIGB 2012	YULONGYAN	Gongxihe	China	Qianyang, HunanProv.	Gravity in Masonry or Concrete	1211	400	303	100	90	42	52	1997 (dam completed)			No reported reservoir induced seismicity.
598 ICOLD-CIGB 2012	YUNFENG	Yalujiang	China	Ji'an, JilinProv.	Gravity in Masonry or Concrete	2507	828	345	114	96	3006	3708	1967 (dam completed)			No reported reservoir induced seismicity.
599 ICOLD-CIGB 2012	ZAYANDEH-ROOD	ZAYANDEH-ROOD	I. Rep. Iran	SHAHR-KORD, ESFAHAN	Arch	1363	450	303	100	90	1176	1450	1970 (dam completed)			No reported reservoir induced seismicity.
600 ICOLD-CIGB 2012	ZENGWEN	Zengwenhe	China	Tainan, TaiwanProv.	Earth	1423	470	415	137	130	8046	9924	1973 (dam completed)			No reported reservoir induced seismicity.
601 ICOLD-CIGB 2012	ZERVREILA	Valserrhein	Switzerland	Vals, Graubünden	Arch	1526	504	457	151	121	81	101	1957 (dam completed)			No reported reservoir induced seismicity.
602 ICOLD-CIGB 2012	ZEUZIER	Lienne	Switzerland	Sion, Valais	Arch	775	256	472	156	126	41	51	1957 (dam completed)			No reported reservoir induced seismicity.
603 ICOLD-CIGB 2012	ZEYA	Zeya	Russia	Blagovesh - chensk, Amur	Buttress	2295	758	348	115	97	55453	68400	1978 (dam completed)			No reported reservoir induced seismicity.
604 ICOLD-CIGB 2012	ZHELIN	Xiuhe	China	Nearest town Yongxiu, JiangxiProv.	Earth	1939	591	210	64	58	6421	7920	1972 (dam completed)	Not Obtained	3.2	Reported Case
605 ICOLD-CIGB 2012	ZHEXI	Zishui	China	Anhua, HunanProv.	Buttress	999	330	315	104	86	2894	3570	1975 (dam completed)			No reported reservoir induced seismicity.
606 ICOLD-CIGB 2012	ZILLERGRUENDL	Ziller	Austria	Mayrhofen, Tyrol	Arch	1532	506	563	186	156	73	90	1986 (dam completed)			No reported reservoir induced seismicity.
607 ICOLD-CIGB 2012	ZIMAPAN	Moctezuma	Mexico	Tula, Hidalgo	Arch	348	115	627	207	177	807	996	1994 (dam completed)			No reported reservoir induced seismicity.
608 ICOLD-CIGB 2012	ZIPINGPU	Minjiang	China	Nearest town Dujiangyan, SichuanProv.	Rock fill	2093	638	512	156	148	876	1080	2000 (dam completed)	Not Obtained	7.9	Questionable